The delivery of pro-angiogenic growth factors from core-shell polymer particles

Laura Kelly

Department of Chemistry

University of Sheffield

April 2015

Acknowledgements

I would like to thank my supervisors, Stephen Rimmer, Sheila MacNeil and Paul Genever. I would also like to acknowledge the Tissue Engineering and Regenerative Medicine Doctoral Training Centre and Engineering and Physical Sciences Research Council for funding.

I am extremely grateful to Melanie Hannah, Claire Johnson and Jennifer Louth for technical assistance throughout my work. I would also like to thank Chris Hill and Svet Tsokov for their help with SEM and TEM imaging. A special thanks goes to Laura Platt for her assistance with emulsion polymerisation and to Amy Smith for her hard work during her summer placement.

Finally, I would like to thank my family for encouragement and advice (particularly Beth for her proof reading). I would especially like to thank Ryan for all his help and support both during my PhD and at home.

Contents

Abstract

Angiogenesis is the formation of new blood vessels from a pre-existing vascular network. Angiogenesis is stimulated by proteins called growth factors. Growth factors have been used to treat ischemic tissue for some time. When they were first used to induce angiogenesis, application of a single growth factor was used; this had limited success. Hence, there has been a move towards releasing two or more pro-angiogenic growth factors to induce blood vessel formation.

Three growth factors were investigated: vascular endothelial growth factor (VEGF); platelet derived growth factor (PDGF); and endothelial growth factor (EGF). These growth factors were chosen due to potential for binding and, to a lesser extent, for size variation.

Two sets of materials have been used to study the release of these proteins. The first set of materials contained oleyl phenyl hydrogen phosphate (OPHP) to bind to the protein. The second was materials containing poly (2-Acrylamido-2-methyl-1-propane sulfonic acid) (PAMPS) to bind the protein of interest. These systems mimic heparin through electrostatically binding to the growth factor peptide sequences containing arginine and lysine amino acids. These two systems showed differing release profiles for each protein over the course of 31 days.

OPHP and PAMPS variants containing a fluorescent label were also synthesised. Acryloxyethyl thiocarbamoyl rhodamine B was added during polymerisation and resulted in materials containing a fluorescent label. However, these showed signs of aggregation both during and after synthesis.

The OPHP materials and PAMPS materials were set into hydrogel sheets composed of poly (N-vinyl-2-pyrrolidone-co-diethylene glycol bis allyl carbonate). The release of VEGF, PDGF and EGF was studied and exhibited a different release profile than OPHP or PAMPS materials.

Two novel systems have been developed that can successfully bind and release various heparin binding proteins by electrostatic binding of the growth factors on to or within the outer layer of polymer particles. It has been concluded that the protein size and the shell architecture have the main effect upon the release profile of the proteins.

Abbreviations

CMC	Critical micelle concentration
CTA	Chain transfer agent
bFGF	Basic fibroblast growth factor
BMA	Butyl methacrylate
BSA	Bovine serum albumin
DCM	Dichloromethane
DEGBAC	Diethylene glycol bis allyl carbonate
DMEM	Dulbecco's modified Eagle's medium
DVB	Divinyl benzene
ECM	Extracellular matrix
EGDA	Ethylene glycol diacrylate
EGDMA	Ethylene glycol dimethacrylate
EGF	Epithelial growth factor
ELISA	Enzyme linked immunosorbent assay
FBS	Foetal bovine serum
FGF	Fibroblast growth factor
FGFR	Fibroblast growth factor receptor
GFP	Green fluorescent protein
GAG	Glycosaminoglycan
GMAC	Glycerol methacrylate acetonide
HB EGF	Heparin binding epidermal growth factor like protein
HS	Heparan sulfonate
HEMA	Hydroxyethyl methacrylate

HPMA	Hydroxypropyl methacrylate
HUVEC	Human umbilical vein endothelial cells
HIF	Hypoxia-inducible factor
IPA	Propan-2-ol
MES	2-(*N*-morpholino)ethanesulfonic acid
MMP	Matrix metalloproteinase
OPHP	Oleyl phenyl hydrogen phosphate
PAMPS	Poly(2-acrylamido-2-methyl-1-propane sulfonic acid)
PBMA	Poly(n-butyl methacrylate)
PBS	Phosphate buffered saline
PCL	Polycaprolactone
PDGF	Platelet derived growth factor
PDGFR	Platelet derived growth factor receptor
PEG	Polyethylene glycol
phVEGF	VEGF gene carrying plasmid
PLA	Poly lactic acid
PLGA	Poly (lactide-co-glycolic acid)
PlGF	Placental growth factor
PLLA	Poly (L-lactic acid)
PS	Polystyrene
PVP	Poly (N-vinyl-2-pyrrolidone)
RNS	Reactive nitrogen species
ROS	Reactive oxygen species
RAFT	Reversible addition-fragmentation chain transfer

SDS	Sodium dodecyl sulphate
TEM	Transmission electron microscopy
TGF	Transforming growth factor
VEGF	Vascular endothelial growth factor
VEGFR	Vascular endothelial growth factor receptor
4-(VPC)	4-vinylbenzyl-pyrrole carbodithioate

1.1 *Angiogenesis*

Angiogenesis is the formation of new blood vessels by branching from a pre-existing vascular network. Angiogenesis mainly occurs during embryogenesis and to some extent in adults, such as neovascularisation after wound healing, disease processes and in the female reproductive system. It is distinct from vasculogenesis, as angiogenesis relies on the migration of endothelial cells and remodelling of vasculature, rather than the differentiation of endothelial cells from angioblasts [1]. Both processes consist of similar regulatory mechanisms [2]. The cellular and molecular mechanisms of angiogenesis differ depending upon the tissue type, hence, the method of stimulating angiogenesis must be adjusted to the target tissue [3]. Angiogenesis can be induced by a variety of factors such as, the expression of angiopoietins, such as TIE receptors, members of growth factor families; for example, the vascular endothelial growth factor (VEGF) family, transforming growth factors (TGF), platelet derived growth factors (PDGF) and the fibroblast growth factor (FGF) family; along with tumour necrosis factor- α and interleukins [4].

Normal health and healing requires a balance between angiogenic inhibitors and angiogenic stimulators. For the process of angiogenesis to occur a number of coordinated events must take place. Angiogenic stimulants are released and diffuse across tissues. These bind to nearby pre-existing blood vessels, promoting vasodilation. This is followed by endothelial cell basement membrane degradation by protease, such as the matrix metalloproteinase (MMP) family, which removes the collagen and other extracellular matrix components. This allows the endothelial cells to migrate from pre-existing blood vessels to the source of the angiogenic stimuli, resulting in cell proliferation and the formation of new vasculature [5]. The initial blood vessel sprout begins to arrange into tubes containing a lumen. Lumen formation is dependent upon the cell-cell adhesion glycoprotein E-selectin [6]. Once these initial blood vessels are in place, remodelling must occur to produce a larger, mature vascular network. The crucial step in this is the recruitment of smooth muscle cell-like pericytes, which are differentiated from mesenchymal cells, and are known to stabilise newly formed vasculature [7].

1.2 *Wound healing*

Wounds are "a defect or a break in the skin, resulting from physical or thermal damage or as a result of the presence of an underlying medical or physiological condition" [8]. Wounds are categorised into acute or chronic wounds. Acute wounds result in minimum scarring and usually heal within 8-12 weeks [9]. Acute wounds are normally a result of physical trauma. Chronic wounds are often reoccurring wounds that result from underlying medical conditions. Chronic wounds do not heal within the normal time frame, i.e. healing time is greater than 12 weeks [9].

Wound healing is a specific biological process that occurs after injury. The purpose of wound healing is to seal the wound quickly to reduce the risk of bacterial infection, followed by the regeneration of damaged tissues. There are four main stages of wound healing (although these are occasionally described in five stages), see Figure 10.1.

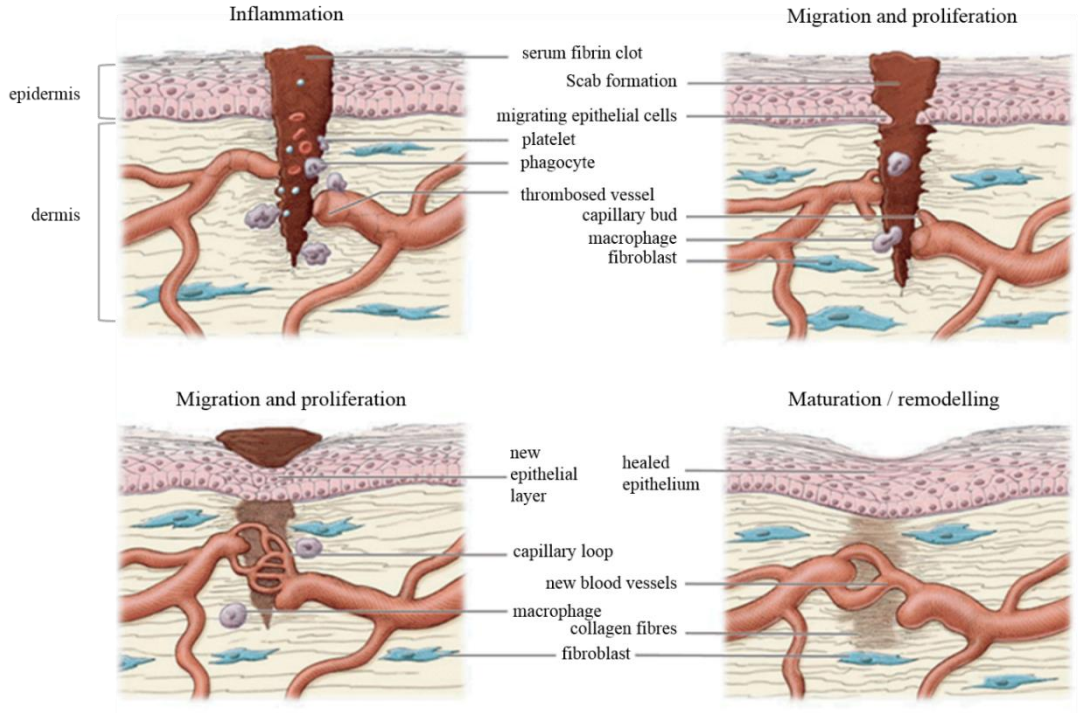

Figure 10.1 Schematic of wound healing within the epidermis and dermis of the skin. Image adapted from *[10]*.

Haemostasis

Haemostasis begins with bleeding from the wound. The aim of this process is to assist with the flushing out of bacteria, thereby, preventing an infection [11]. Fibronectin that is present in wound exudate begins the clotting process by promoting the release of clotting factors. This begins with the coagulation of the exudate (absence of blood cells or blood platelets). A fibrin network clot follows and finally scab formation occurs. This provides strength to the clot and protection from infection [8]. The fibrin clot also provides guidance for cell migration and proliferation at later stages of healing [12]. Platelet mediated vasoconstriction prevents excessive blood loss during scab formation [11].

Inflammation

Inflammation often occurs simultaneously with haemostasis, but, in some instances, can begin up to 24 hours after injury. Inflammation lasts between 1-3 days and involves a cellular and vascular response to the injury. Upon injury, exudate is released from the wound. This contains histamine and serotonin which causes vasodilation. The first immune cells to arrive at the site of injury are neutrophils. These remove any microorganisms that are present within the wound [11]. Unless infection occurs, neutrophils are the predominant immune cell present within the first few days after injury [13, 14]. Vasodilation allows phagocytes to enter the wound site and remove any potentially necrotic tissue. The clotting process is assisted by platelets, which are released from damaged blood vessels, becoming activated when in contact with collagen [8].

Migration and Proliferation

The aim of the migration and proliferation stages is to restore the wound surface, re-vascularise the tissue and structurally repair connective tissue [11]. Migration of cells to the wound site is essential for a wound to heal. In initial stages of wound healing, fibroblasts and epithelial cells separate themselves from the extracellular

matrix (ECM) and migrate to the site of injury. Fibroblasts migrate from the edges of the wound underneath the scab followed by epithelial cells that thicken the cell layers [8]. As migration across the wound bed occurs, the cells leave markers, allowing for ECM production [12].

Proliferation occurs from 3 days post injury and lasts for 2-3 days. Growth of capillaries and lymphatic vessels into the wound site produces granulation tissue. Granulation tissue replaces the fibrin/fibronectin matrix [12]. Granulation tissue is predominantly fibroblasts, is highly vascular and has a high metabolic rate. This is why healing wounds have a pink hue compared to non-injured tissue [11]. Collagen is synthesised to provide structure and strength to the tissue. Epithelial thickening occurs until collagen has fully filled the wound. High levels of fibroblast proliferation and collagen synthesis occurs for approximately 2 weeks. After this, blood vessels decrease in size and oedema is reduced [8]. Re-epithelisation has occurred when keratinocytes (the main epithelial cell in the skin) have completely covered the wound area [11].

Angiogenesis occurs during this stage. After injury the wound becomes hypoxic and the pH drops to 6.8 [11]. The relationship between hypoxia and angiogenesis will be discussed in detail later (page 5).

Maturation/ remodelling phase

Depending upon the type of injury, the maturation phase can last from a few months up to 2 years. This phase forms cellular connective tissue and strengthens the epithelium. It is in this phase that final scar formation is determined [8, 15]. Remodelling involves mainly macrophages and fibroblasts. Wound maturation and remodelling is identified by ECM formation/shaping, increased collagen production and apoptosis [12]. Although increased strength is a marker that the wound is undergoing maturation, the tissue will never gain more than 80% of its original strength [16, 17].

1.2.1 Hypoxia, oxidative stress and nitroxidative stress

The oxygen supply to a wound is determined by a number of factors, such as, pulmonic gas exchange, blood vessel density, haemoglobin levels, cardiac output and oxygen consumption of inflammatory cells within the wound [18, 19]. Healing wounds require a higher oxygen supply than normal tissue due to the increased oxygen consumption from proliferating cells, collagen synthesis, immune response and the presence of NADPH-linked oxygenase species [19].

Hypoxia is the reduction of normal oxygen level in tissues. There are three categories of hypoxic tissue. Chronic hypoxia is oxygen tension of 2-3%. Under the limited oxygen diffusion that occurs with chronic hypoxia, cells begin to uncontrollably proliferate [20]. Chronic hypoxia lasts for a relatively long time in comparison to other forms of hypoxia. Due to this, normal cells cannot survive but tumour cells with mutations that survive hypoxic conditions are able to proliferate. Acute hypoxia and hypoxia with reperfusion can also be described as intermittent hypoxia [21]. Even in these short periods of limited oxygen diffusion, irregular and new blood vessel growth can still occur. This leads to increased oxygen diffusion at that site and also an increase in free radical species leading to tissue damage [21]. During hypoxic conditions angiogenesis is regulated by hypoxia-inducible factors (HIF) [22]. Immune cells that are present in hypoxic tissue after a wound release a series of pro-angiogenic growth factors [23, 24].

Oxygen can be reduced in one, two or four electron transfers. These produce a superoxide ($O_2^{\bullet}$), a peroxide anion ($HO_2^{\bullet}$) and a hydroxyl ion ($HO^{\bullet}$). $O_2^{\bullet}$ and $HO_2^{\bullet}$ can cause oxidative cell damage if in high enough concentrations [25]. Redox homeostasis is the cell's ability to prevent build-up of excess reactive oxygen species [26]. Some reactive oxygen species are important for wound healing as they provide protection from microorganisms [27]. However, reactive oxygen species must be detoxified or scavenged to prevent damage to the healthy cells. If these are maintained in high concentrations oxidative stress occurs.

Reactive nitrogen species are also capable of causing cell damage but they play a major role in wound healing [28]. NO and peroxynitrite ($ONOO^{\bullet}$) are the main two nitrogen species present. Platelets, macrophages, keratinocytes, endothelial cells and fibroblasts are all present in wounds and are capable of producing NO during

wound healing [26]. This can lead to the rapid oxidation of NO, also known as nitroxidative stress.

In acute wounds oxidative and nitroxidative stress are not a problem as antioxidant defence mechanisms can cope with the gradual detoxification of harmful species. This means cells can be returned to redox homeostasis without much trouble [26]. However, chronic wounds show uncontrolled production of reactive oxygen species (ROS) and reactive nitrogen species (RNS). Therefore, the normal antioxidant defence mechanism is not effective [29]. This leads to chronic wounds becoming trapped in the inflammatory stages of wound healing meaning no granulation tissue can form, finally resulting in long healing times and poor wound closure [26].

ROS have been shown to promote angiogenesis by enhancing the affinity of fibroblast growth factor-2 (FGF-2) for its receptor (FGFR) and inducing increased expression of FGFR. Small quantities of ROS also promote the release of VEGF from keratinocytes during wound healing [27]. NO species have a more profound role in promoting angiogenesis. It has been shown that NO activates VEGF, basic fibroblast growth factor (bFGF) and transforming growth factor β (TGF-β). These promote endothelial cell migration and proliferation [26].

1.3 *Growth factors*

Growth factors have been used to treat ischemic tissue for some time. It has been shown that, during angiogenesis endothelial cells can proliferate and move along a chemotactic gradient via ECM tracts towards the source of pro-angiogenic growth factors [30-32]. The original course of treatment was bolus injection to the affected site. This led to poor results, often due to the short lifetime of growth factors in an aqueous environment. Hence, a more localised, controllable delivery system is needed.

There are several pro-angiogenic growth factors that can stimulate endothelial cell migration and proliferation. When growth factors were first used to induce angiogenesis, application of single growth factors was used [33]. This had limited success, with problems including: immature blood vessels[34], leaking of resultant

blood vessels[35], impeding lymphatic vessel functionality [36], and incomplete angiogenesis [3]. Hence, there has been a move towards releasing two or more pro-angiogenic growth factors to induce blood vessel formation. The release of several growth factors in sequence mimics the release after injury. By using a more natural release of protein, the resultant vessels can be shown to be more mature, have thicker walls, induce smooth muscle cell migration and have a greater blood vessel volume [37].

1.3.1 Vascular Endothelial Growth Factor

Vascular endothelial growth factor (VEGF) is essential for normal angiogenesis to occur. VEGF was discovered in 1989 by Ferrara et al [38]. The protein discovered in 1989 was found to be the same as that known as Vascular Permeability Factor (VPF), which had been discovered by another group in 1983 [39]. VEGF belongs to the cysteine knot superfamily and is a dimer consisting of two units of identical molecular weights (~23 KDa), giving an approximate molecular weight of 45 KDa [7, 40]. Members of the VEGF family of growth factors include: placental growth factor (PLGF), VEGF-B, VEGF-C, VEGF-D and VEGF-E.

VEGF is produced by many different cell types, including tumour cells, osteoblasts, keratinocytes, smooth muscle cells and some immune cells, such as macrophages and T-cells. VEGF is known to play a major role in the proliferation and migration of endothelial cells [41]. This is achieved by interaction through the N-terminal amino acid sequence APMAG. As well as interaction with cells, VEGF also stimulates the release of vascular permeability factors and hexose transport molecules [42]. However, the most essential role of VEGF is as a regulator of pathological angiogenesis [43].

VEGF exists as five different isoforms [7]. These variants of VEGF differ by amino acid length. The five isoforms are 121, 145, 165, 189 and 206 amino acids, with $VEGF_{121}$ and $VEGF_{165}$ being the most abundant within the body [42]. $VEGF_{121}$ is freely available by diffusion, whereas, $VEGF_{165}$ binds to heparin sulphate and becomes associated with extracellular matrix and cell surface proteoglycans [7]. All isoforms share a common amino-terminal binding domain which consists of 115

residues and is unaffected by the varying length in the carboxy-terminal end. Endothelial cells have two VEGF receptors on the cell surface. These receptors are VEGFR-1 (Flt-1), a fms-like tyrosine kinase and VEGFR-2 (KDR/Flk-1), a kinase domain region [44, 45].

1.3.2 Platelet Derived Growth Factor

In normal cells, PDGF is at almost undetectable levels and only gets released in response to platelet degranulation [30]. PDGF is composed of two homologous polypeptide chains: chain A and chain B [46]. Each chain is a similar size and conformationally shows no difference in biological activity [30]. The two chains of PDGF can assemble into 3 isoforms: AA, BB and AB. The response of each isoform is dependent upon what PDGF receptor is available for binding. PDGF receptors are composed of two subunits: α and β [47, 48]. Both forms of receptor belong to the tyrosine kinase receptor family. They have specificity, with receptor α binding PDGF A and PDGF B, while receptor β will only bind PDGF B [30]. The PDGF receptor is expressed on the surface of pericytes, smooth muscle cells and capillary endothelial cells [46, 49-51]. PDGF plays a role in increasing DNA synthesis, forming angiogenic chords and sprouts; and forming mature and stabilised blood vessels [49, 50, 52]. *In vivo* experiments demonstrated that PDGF is crucial in recruiting pericytes to the capillaries and thus increases the structural integrity of these vessels [34]. Studies have also shown that PDGF may be a source of endothelial cell proliferation by upregulating the release of VEGF from smooth muscle cells, thereby indirectly affecting the recruitment of endothelial cells [53]. However, it is important to note that PDGF is not essential in the early stages of angiogenesis and has a weaker angiogenic effect than VEGF [34].

Endothelial cells grown in culture have been shown to bind PDGF A and B, in contrast to isolated endothelial cells which bind significantly less PDGF B. However, endothelial cells that are organised into 3D tubular structures, as would be desired for tissue engineering purposes, do not bind PDGF B [49, 54].

1.4 *The role of heparin sulphate family*

Heparan sulphates (HS) are a family of glycosaminoglycans (GAGs) produced by cells. GAGs are polysaccharides that often contain a net charge. Figure 1.2 shows the structure of heparin, which is in the HS family. HS are the most structurally complex GAG [55] and are both synthesised as proteoglycans. Heparin is only produced by mast cells whereas heparan sulphate is produced by most cells [55]. HS is present on cell surfaces and in the ECM. There are several structural differences which have been reviewed at length between heparin and HS [55-58]. Only differences directly relating to the binding of proteins will be discussed.

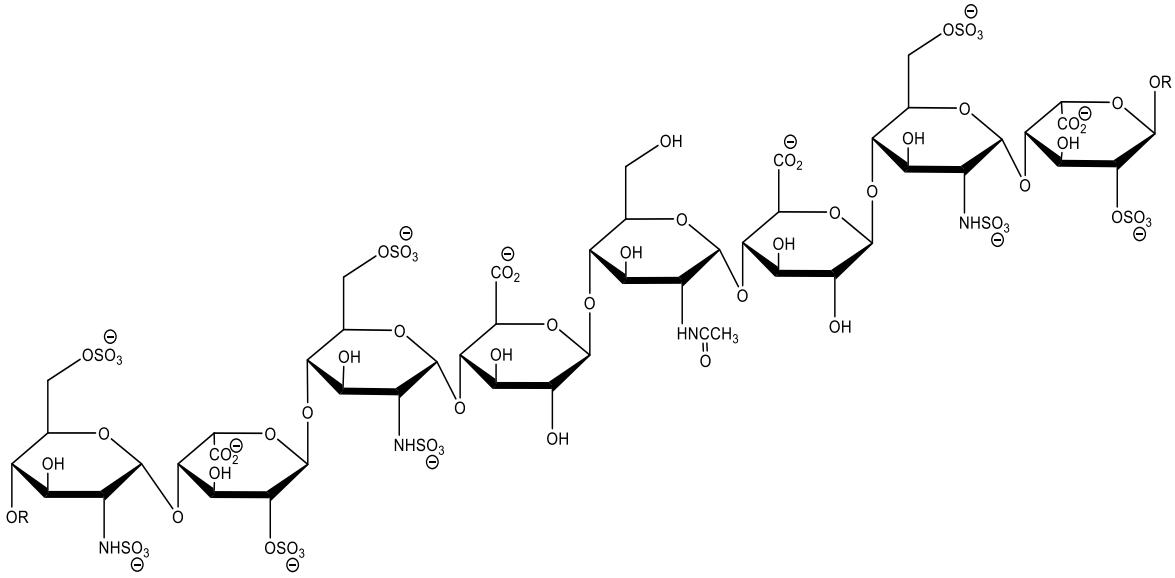

Figure 1.2 Structure of heparin. The large quantities of negatively charged groups give an overall net negative charge.

Heparin is a more sulfonated variant of HS. Heparin and HS have an affinity for binding to many proteins through non-covalent interactions. There are a variety of binding sites along the heparin/HS chain and many variants of heparin-protein binding sites [59]. Many proteins that can bind to heparin also show an interaction with HS, thereby making the distinction and characterisation of heparin/HS-protein binding difficult to determine. The majority of interactions between heparin/HS-proteins are ionic interactions [60]. This is due to the number of sulfo and carboxyl groups present. Heparin has stronger interactions (2.7 negative charges per

disaccharide) compared to HS (<2 negative charges per disaccharide) [59]. Due to this, heparin binding sites on proteins are often characterised by groups of positively charged basic amino acids. The most common basic amino acids found in heparin/HS-protein binding domains are arginine and lysine. They are both positively charged at physiological pH, however, arginine can bind approximately 2.5 times stronger than lysine [61]. Non-electrostatic interactions are also present in HS-proteins. Interactions with pro-angiogenic growth factors are reliant on electrostatic interactions. These will therefore be discussed in more detail.

Binding specificity and affinity is achieved by the orientation and patterning of the sulfo and carboxyl groups along the polysaccharide chain [59]. Many HS-protein interactions have been studied. It was found that a sequence consisting of [-X-B-B-X-B-X-] and [-X-B-B-X-X-B-X-] where B is a basic amino acid and X is a hydrophilic region shows a strong interaction with ECM [62]. Depending upon the orientation of the protein's secondary structure, it is not necessarily crucial to have a linear order of HS binding regions. This means that spatial arrangement can become more important than sequential arrangement in HS binding regions [63].

The binding of VEGF to HS is distinctly different from the VEGFR binding domain. The heparin-VEGF interaction is weak when compared to other HS-growth factor interactions but is comparable to the binding affinity of HS-PDGF [64]. However, unlike VEGF, PDGF bind more strongly through lysine rather than arginine [65]. Both VEGF and PDGF can bind to varying length polysaccharides. For both growth factors the minimum length chain is an oligosaccharide [66, 67]. It has been shown that this HS-VEGF interaction is crucial for the binding of VEGFR by stabilising VEGF from becoming inactivated [64]. It is not yet clear if the HS-PDGF interaction plays an important role in the binding of PDGFR [67].

1.5 *Treatment with VEGF and PDGF in wound healing*

Angiogenesis is essential in wound healing. Without the pro-angiogenic growth factors associated with blood vessel growth, wounds could not heal properly. In the general population this is not a problem. However, in certain cases this normal

healing process does not occur. Two cases will be briefly discussed; impaired healing due to diabetes mellitus and after burn injury.

In diabetic patients the production of VEGF is impaired [68]. It has been shown in diabetic mice fibroblasts that the production of VEGF and response to hypoxia are diminished compared to wild-type [69]. The inflammatory phase also differs in diabetic patients. Chronic moderate inflammation takes the place of the normal acute inflammatory phase. This results in a reduced number of macrophages and poor lymphatic vessel formation [69, 70]. Long term reduced VEGF production leads to impaired angiogenesis and poor formation of granulation tissue, resulting in reduced VEGF secretion in wounded tissue [68, 71]. Treatment with VEGF protein and VEGF gene-carrying plasmid ($phVEGF_{165}$) has been shown to slightly reduce the need for amputation in diabetic patients with critical limb ischemia [72]. Delivery of VEGF-C in a similar manner has shown improvement in angiogenesis and lymphomagenesis, resulting in wound closure in diabetic mouse models [73].

For complete healing of a wound, PDGF is needed to produce mature vasculature. During wound healing, PDGF is present in wound fluid. However, in diabetic animals the level of PDGF expression is reduced [74]. To improve diabetic wound healing PDGF may be used. The use of topical PDGF-BB gels have shown improved soft tissue healing in diabetic rats [75, 76]. A similar PDGF-BB gel has been used to show healing of full thickness wounds. Healthy volunteers were treated with either a conventional antibiotic ointment commonly used on wounds or a PDGF-BB gel. The study showed that the PDGF-BB gel improved wound healing faster than conventional treatment [77].

The assessment of the type and severity of a burn is essential to determine the type of treatment needed [78]. Full thickness burns take a long time to heal, are at high risk of bacterial colonisation and can result in significant skin contraction leading to scarring [79, 80]. If the wound is large or the vascular bed is heavily damaged or destroyed, re-vascularising the area can be difficult. VEGF has been used to re-establish a blood supply as a pre-treatment of burn wounds prior to grafting [81, 82]. The application of VEGF has been shown to reduce dermal necrosis and increase microvasculature before grafting [83]. PDGF has been shown to enhance tissue repair when applied to skin grafts. PDGF signals through macrophages which are

present in wounded tissue. This produces a positive autocrine feedback loop resulting in further expression of growth factors needed in wound healing [84]. Guinea pig models have shown that multiple applications of PDGF to healing tissue can result in faster granulation tissue formation, indirectly resulting in faster healing times [85].

1.6 *Release mechanisms*

Growth factors can be released via a number of techniques. The most notable of these are: directly loading the protein into the polymer matrix; covalently binding the growth factors to a peptide sequence; using the polymer to encapsulate the growth factors; and the growth factors binding to the polymer via electrostatic binding.

The main problem associated with release of growth factors from polymeric matrices or carriers is controlling the release kinetics of the protein. The typical burst release profile shows the majority of growth factor being released from the polymer within 24 hours of binding. The remainder of the growth factor will be released slowly over time. The type of binding and depth of binding can have a profound effect on the release profile of the protein from the matrix. In one study, pre-encapsulation and deeply embedding the bound growth factors in a polymeric matrix led to release being sustained for up to 21 days [86]. There have been efforts to control the release kinetics of growth factors from polymers by altering the molecular weight, porosity, polymer degradation and erosion, protein diffusion and growth factor loading concentrations [87-89].

Therapeutic application of pro-angiogenic growth factors can cause problems when applied in large doses to a non-localised area. Such problems include the development of new blood vessels and increase in vascular permeability in non-target tissue and tumour growths [90]. Therefore, the direct application of small doses of growth factor is preferential and has been shown to yield better results. Research into the therapeutic application of VEGF originally used intra-arterial bolus injection as the administration technique. To overcome problems associated

with non-localised delivery of growth factors, many research groups focus on synthetic or natural carriers of growth factors. The aim of this delivery system is to provide a small, consistent dose of growth factors, minimise side effects associated with application to non-target tissues and maintain the bioactivity of the protein to prolong the half-life of the growth factors [91-93].

As with all biomaterials, the delivery system for pro-angiogenic growth must be non-immunogenic, must not degrade to give toxic by-products and must be easily sterilised. It is also advantageous for the material to be easy to handle and be relatively simple and cheap to produce, as these are requirements for clinical application and commercialisation [91]. There have been many different materials and approaches investigated for the release of one or more growth factors and this area has been extensively reviewed [37, 94-96]. Figure 1.3 shows a schematic of the four main ways growth factors have been released.

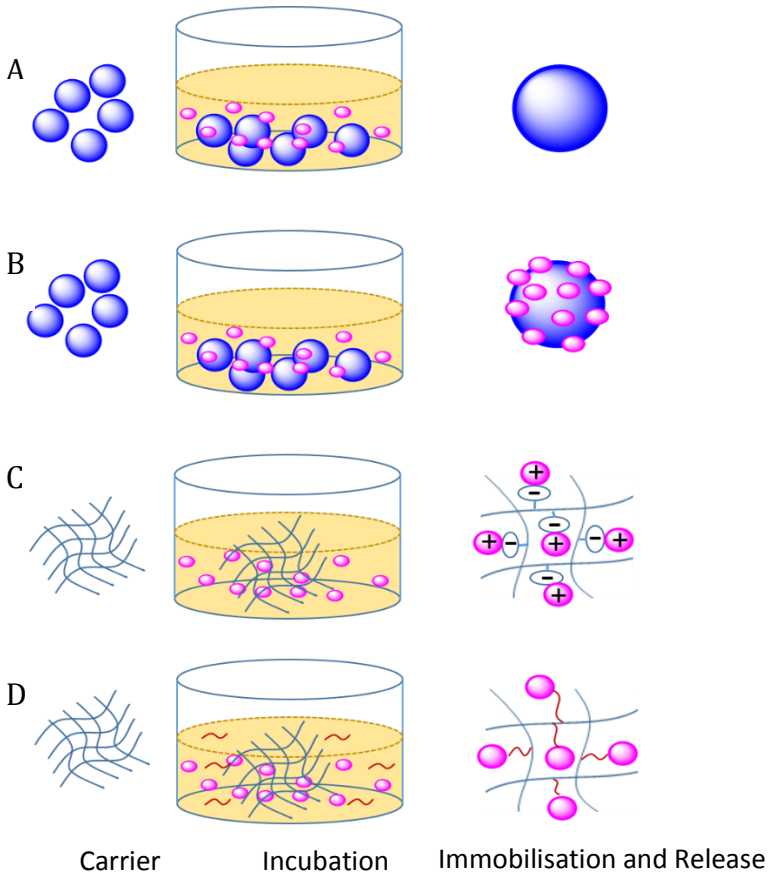

Figure 1.3 The four main ways in which proteins may be bound to a polymer surface. A) use of carrier system, B) directly loading onto the polymer surface, C) electrostatically binding the protein to the polymer and D) covalent bonds to the polymer backbone.

1.6.1 Direct Loading

The most simplified way to incorporate growth factors into a polymer is to directly load the protein into the material. This process is diffusion controlled, hence, the release profile of the growth factor is not consistent. It will show an initial burst release phase followed by a slow release of a small amount of protein that has become incorporated deeper in the polymeric matrix. Cross-linking of the polymer can be utilised to modify the release profile of growth factors and proteins that have been incorporated via direct loading [97]. However, the use of cross-linking can affect the efficiency of the protein release. If growth factors are added to the polymer prior to cross-linking, the growth factors may not still be functional after the polymer has been cross-linked. The distribution of protein evenly throughout the material cannot be ensured if growth factors are added after cross-linking [97].

1.6.2 Covalently binding

It is also possible to synthesise polymers with the ability to covalently bind to the amino acid sequence of growth factors, effectively tethering the amino acid sequence to the polymer [97]. Using these tethers, there is the potential to spatially arrange the growth factors within or on the surface of the polymer. The tethers can be made up of peptide sequences, synthetic polymers, natural polymers and whole proteins [98-100]. Along with allowing for growth factor release, growth factors covalently bound to a polymer surface by tethers can also increase cell adhesion, cell migration and extracellular matrix (ECM) production on the surface of the polymer [101-103]. Poly (ethylene glycol) (PEG) tethers have been used to bind VEGF and TGF-β1 to the surface of a polymeric growth factor carrier. PEG was used to tether cell adhesive peptide sequence RGD to the surface of a matrix metalloproteinase sensitive hydrogel [104]. This system allowed for VEGF to be retained on the polymer and only released upon cell demand. Alternatively, growth factors can be immobilised on the surface of a polymer using a 15-amino acid tag containing free sulfhydryl groups for specific conjugation to VEGF [99].

1.6.3 Carrier systems

Using a carrier system, such as drug release implants and microparticles, can reduce the rate of growth factor release over a longer period of time [97]. This technique has advantages when multiple growth factors are being applied as it allows for temporal and spatial arrangement of proteins within the polymer [94]. The growth factors of interest can either be spread throughout the polymer matrix or in the centre surrounded by a polymeric barrier to diffusion. Both of these techniques not only slow the release of growth factor to cells but also protect the delicate proteins from the biological environment [105, 106]. There are two main release systems that can be utilised in the release of growth factors from polymeric carrier systems: non degradable systems and degradable systems.

Non-degradable systems consist of an insoluble polymer matrix which contains the protein of interest. The movement of the growth factor out of the polymer is driven by concentration gradients and is only rate limited by mass transport. The polymer can be tuned to alter the release rate to give zero or first order release kinetics [106, 107].

Degradable systems have attracted great interest due to the number of degradable polymers with excellent biocompatibility. Along with diffusion of the growth factor out of the polymer, degradable systems can also be synthesised so the degradation of the polymer plays a major role in the release rate of the growth factors. This is of particular advantage in cases where more than one protein is released from the polymer. By tuning the release rate, each growth factor can have different release kinetics, depending upon the needs of the biological system [37, 106, 108].

1.6.4 Electrostatic interactions

Both VEGF and PDGF can bind to heparan sulphate whilst biologically active within the body [109]. This interaction can be utilised to prevent protein denaturing when the growth factor is bound to the polymeric matrix of the scaffold. Heparin binding domains are able to interact with the cell surface to promote adhesion of cells. However, their role of interest is their ability to bind to growth factors. Utilising HS binding domains can be used as a mechanism for controlled, precise release of growth factors *in vivo* [110, 111]. It is possible to include heparin-binding peptides

into a synthetic or natural hydrogel to promote adhesion of cells to the surface of the hydrogel and release growth factors [112-115]. The heparin spacer mimics the ECM, protecting the growth factor and spatially arranging the protein release from within the scaffold [98].

Heparin-growth factor binding occurs through a series of highly basic peptide sequences containing arginine and lysine amino acids. This makes it possible to use basic functional groups on the surface of the polymer to bind VEGF [116]. The use of specific groups to target electrostatic binding to VEGF and PDGF will be discussed later.

1.7 *Materials overview*

Although there are a wide array of signalling molecules important in the angiogenic response of endothelial cells, much of the research has been undertaken into controlled release of VEGF. The different materials and binding mechanisms have had varying success. However, a clear pattern can be seen when looking at release profiles. The first is a burst release phase, usually between 1-12 hours. This often follows with a region of slow release, eventually plateauing to a region in which little to no growth factor is released. Table 1-1 is an overview of the different materials that have previously been investigated.

Material	Author	Year
Polyethylene glycol (PEG) diacrylate hydrogel[117]	P.A. Netti	2012
Trimethylene carbonate, e-caprolactone and D,L lactide[118]	B.G. Amsden	2012
Polylactic-co-glycolic acid (PLGA) and PLGA polymer[119]	A.L. Daugherty	2011
Dextran (DEX) and poly(lactide-co-glycolide) (PLG)[120]	X. Jia	2011
Poly(lactic-co-glycolic acid) (PLGA)[121]	O. Karal-Yilmaz	2011
Poly(ether)urethane polydimethylsiloxane blend[122]	E. Briganti	2010
Polystyrene-co-divinyl benzene core oleyl phenyl hydrogen phosphate-co-ethylene glycol dimethacrylate shell[116]	L. Gilmore	2009
Alginate[93]	S.M. Jay	2009
Amino acid ester polyphosphazene (Pphos)[123]	O. Oredein-McCoy	2009
Gelatin[124]	Z. S. Patel	2008
Poly(DL-lactic) acid (PLA)[125]	J. M. Kanczler	2007
Poly(lactide-co-glycolide) (PLG)[86]	A.B.Ennett	2006
Poly (D,L-lactide-co-glycolide)[126]	J. Davda	2005
Poly(D,L-lactide-co-glycolide)[127]	A.Z. Faranesh	2004

Table 1-1 Brief overview of polymer materials used for release of VEGF since 2004.

Soon after researchers began looking at the effect that VEGF had on endothelial cells it became apparent that single growth factor release was not sufficient to produce useful vasculature. The focus shifted to looking at release of other pro-angiogenic growth factors. PDGF is important for stabilising angiogenic sprouts and forming strong vessels that are not prone to leaking. As with VEGF binding, a burst release phase is seen, followed by slow PDGF release. Table 1-2 is an overview of the materials used to bind and release PDGF.

Material	Author	Year
Hydroxyapatite, PLGA microspheres[128]	J.J. Delgado	2012
Cellulose acetate[129]	J.E. Tengood	2011
Alginate and poly lactide-co-glycolide (PLG)[130]	Q. H. Sun	2010
Polyurethane[131]	B. Li	2009
Kapp-carrageenan[132]	V.E. Santo	2009
poly(lactic-co-glycolic acid) (PLGA50) and poly(L-lactic acid) (PLLA) [133]	G.B. Wei	2006
Methylidene malonate[134]	L. Desire	2006
poly(epsilon-caprolactone)[135] (PCL)-chitosan	S.Y. Im	2003
Chrondroitin-4-sulfate (CS)-chitosan[136]	Y.J. Park	2000
Ethylene vinyl acetate copolymer (EVAc)[137]	W.R. Walsh	1995

Table 1-2 Overview of natural materials used for the release of PDGF.

1.8 *Determining bio-activity of proteins*

In vivo and *in vitro* assays are used to test the bioactivity of a biological molecule or drug. The use of bio-assays has been developed over many years and there are several commonly used experimental protocols that have been developed to assess the ability of a material or substance to promote angiogenesis [138-141]. Due to the large variety of assays available only a very brief summary will be included.

1.8.1 In vitro angiogenesis assays

In vitro assays are used to mimic the physiological environment but do not use living animals. In the case of angiogenesis assays, these are mostly focused on the use of endothelial cells. Only the most commonly used assays will be discussed in this thesis.

Endothelial cell proliferation assay

One of the markers of angiogenesis is the proliferation of endothelial cells. By quantifying this proliferation and the use of suitable controls, the ability of a substance to induce or inhibit angiogenesis can be determined. The presence of increased proliferation demonstrates that the molecule of choice (for example, growth factors or drugs) can bind to the cell receptors and induce a biological response. As with most cell culture based assays, a combination of detection methods is best. To determine the degree of endothelial cell proliferation MTT assay, DNA synthesis and DNA binding combined with flow cytometry have been used [139, 142-144].

Endothelial cell migration assay

Endothelial cell migration assays are one of the most commonly used *in vitro* angiogenesis assays. There are a variety of different techniques and different materials used for determining the migration of endothelial cells. The first is a transfilter based assay. This uses a modified Boyden chamber that allows cells to migrate through pores in the upper chamber along a chemotactic gradient present due to a pro-angiogenic source in the bottom chamber [145]. This technique has been of particular use in the study of tumour formation [146]. The phagokinetic track method is a high throughput technique for determining cell movement by looking at the movement of the overall population of cells. From there, it is possible to work backwards and determine the type of movement of individual cells. Although this technique is not only used for angiogenesis assays, it has been shown to be of use when determining the migration of endothelial cells [140, 147]. Finally, fibrin or collagen coated wells and Matrigel have been used to show endothelial cell migration [148, 149]. These mimic the ECM, as such, endothelial cells can move towards the source of pro-angiogenic factors. The use of Matrigel will be discussed further in following sections.

Endothelial cell differentiation assays

Endothelial cell differentiation assays are mainly focused on tubule formation. In angiogenesis, tubules are formed after proliferation and migration and just prior to lumen formation. Tubule formation assays are often performed in a 3D matrix such as ECM components, Matrigel or reduced growth factor Matrigel [139, 150, 151]. The use of Martigel must be undertaken with caution as it has been shown to induce tubule formation in non-lumen forming cells [148]. The degree of angiogenesis is assessed by measuring the average tubule length, the number of tubules formed, the average tubule area and the number of branching points [148]. Endothelial cell differentiation assays can be modified to include co-culture with different cell types.

Endothelial cell co-culture

Many different cell types play a role in angiogenesis and the influence of these varying cell types on endothelial cells is complex. Endothelial cell co-culture is useful for giving a more realistic physiological environment. Co-culture assays often look for the same angiogenic markers as described previously, but with the advantage of being able to study the interactions between different cell types. Various cytokines [152-154], the influence of adhesion molecules [155] and interactions with mesenchymal stem cells (MSCs) [156] have been studied. As with previously discussed assays, there are several different matrices in which to grow cells. Again, Matrigel is often the matrix of choice and is well studied. However, caution must be exercised, especially when working with non-lumen forming cell types [148].

Organ culture

Organ culture can bridge the gap between *in vitro* and *in vivo* experimentation. Whole sections of tissue are cultured and the micro vessel outgrowth is monitored [139]. Organ culture is the least used *in* vitro technique due to the technical difficulties and relatively high cost in comparison to other *in* vitro methods. The three most understood organ culture methods are the porcine carotid artery model [157], the aortic ring model [158-160] and the vena-cava aorta model [161].

1.8.2 In vivo angiogenesis assays

In vivo assays are performed in an animal model. By using a whole animal the immune response and inflammatory response can be studied along with the pro or anti angiogenic response of the material under investigation. The main *in vivo* angiogenesis assays will be looked at in greater detail.

Chick chorioallantoic membrane (CAM) assay

The chorioallantoic membrane (CAM) is a vascular membrane found in eggs and is formed by the chorion and allantois fusing during development. The CAM is analogous to the placenta in mammalian development. At this early stage in development the chick is relatively immunotollerant so can be used for studying cross species xenografts [139]. To perform a CAM assay the shell must be cut away. It is important to remove all shell dust as any remaining dust can lead to an inflammatory response [139]. Through this window in the shell, the materials of interest can be applied directly to the surface of the CAM [162, 163], implanted underneath the CAM or injected intravenously [164, 165]. Due to the flexibility and potential to test several materials using a single animal, the CAM assay is a popular choice for *in vivo* study.

Material implantation assay/ hindlimb ischemia model

It is possible to implant a material that can induce angiogenesis into a whole animal model. This is referred to as a hindlimb ischemia (HI) model. The HI model is used to investigate neovascularisation and angiogenesis in mice or rabbits. To begin with, ischemia must be induced by ligating the femoral artery in the hindlimb. Ischemia must be confirmed using laser Doppler imaging [166]. After ischemia has been induced, the material of interest can be implanted or injected subcutaneously. The restoration of blood perfusion and blood vessel outgrowth are measured. The HI model is widely used because it allows for study of the immune response to a material and the effect of hypoxia on the rate of angiogenesis. The HI model allows for injection of peptides and other angiogenic binders [167, 168], various polymer materials [169-172] and for cell and gene therapy [173-175].

Corneal angiogenesis assay

The corneal angiogenesis assay monitors vascular development in the cornea. The cornea is an avascular area so any vessel growth can be attributed to the material or pro-angiogenic factors under investigation. The assay is done by cutting a small pocket in the cornea. The material of interest can then be inserted. The material inserted includes polymers [176], pro-angiogenic factors [177] and stem cells [178]. The newly formed vasculature can be determined by measuring vessel penetration into the cornea and by using fluorescent dyes or ink to visualise the new blood vessels [139, 179].

Dorsal air sac model

The dorsal air sac model uses repeated subcutaneous injections of air resulting in the formation of an air pouch [180, 181]. After several days of repeated injection, the cells of the air pouch become translucent and the formation of new vessels on this surface can be studied [182]. The material of interest can then be implanted into this cavity. The vessel growth towards the implant can be monitored. This can be done by the injection of Evans Blue which will leak from newly formed vessels but does not leak from pre-existing vasculature [139].

Zebrafish angiogenesis assay

Zebrafish are used as a whole animal model for the study of blood vessel growth [183]. Despite being a non-mammalian species, zebrafish organs are a close match to humans [184]. They are a good candidate for laboratory experimentation as they can be housed in large numbers, have a relatively short generation time and are developed externally (within an egg sac). Their young are transparent allowing internal development to be viewed with a microscope and they can be genetically manipulated [185]. Zebrafish embryos have the ability to survive severe cardiovascular defects, allowing for study and manipulation of the developing vascular system [186, 187].

Transgenic zebrafish lines marked with green fluorescent protein (GFP) on their endothelial cells allow for the real time development of vasculature to be studied [188, 189]. Along with GFP transgenic fish, other fluorescent markers can be used to visualise how different cell types interact. An example of this is the double transgenic line Fli-eGFP GATA dsRED where the endothelial cells are green and red blood cells are red. This allows for vascular development and blood flow to be visualised [139].

Zebrafish have been used for fundamental understanding of vascular development for many years. More recently, zebrafish have been used to study the promotion or inhibition of angiogenesis. Zebrafish have been used as high throughput screening agents by the addition of pro- and anti-angiogenic molecules to their culture media [190, 191]. Microinjection techniques allow for controlled release systems to be tested using zebrafish models. These techniques are usually undertaken at the embryonic or larval stages of development. There have been several studies using microinjection of loaded micro or nano-particles into zebrafish to test the release profile, bioactivity and cytotoxicity of the payload [192-194].

1.9 *Emulsion polymerisation*

Particle systems are popular in the field of medical research and biomaterials. Reasons for this include: large surface area, ability to adsorb small molecules onto the surface or encapsulated within them, and the high mobility which particles have due to their small size. Polymer colloids for binding biological molecules can be synthesised in one of two ways. The first is a two-step process in which the desired polymer is first synthesised, followed by the formation of particles. The more favourable technique is the use of emulsion polymerisation to produce the polymer of the desired particle size in one step [195].

Emulsion polymerisation is a process in which radical chain polymerisation occurs in the form of a colloidal dispersion. This is distinct from suspension or dispersion polymerisation due to the size of the droplets, the type of initiation used and the resultant polymer (otherwise known as a latex) molecular weight and reaction

parameters [196]. Emulsion polymerisation holds some distinct advantages over other polymerisation techniques. Firstly, the colloidal system allows for easy control of the thermal and viscoelastic problems that are associated with bulk polymerisations. Secondly, the latex produced by emulsion polymerisation does not regularly need further separations. Finally, the kinetics of emulsion polymerisations allows the polymer molecular weight to be increased without decreasing the polymerisation rate. Emulsion polymerisation can produce latexes with high molecular weight and high reaction rates [196]. The size of latex particles can range between 50-300 nm.

Emulsion polymerisations are composed of monomer(s), a dispersal medium (usually water), surfactant and a water-soluble initiator. To maintain the colloidal dispersion, the emulsion system is kept well agitated (usually by stirring) throughout the polymerisation. Surfactants contain both hydrophobic and hydrophilic sections and when the concentration of surfactant exceeds the critical micelle concentration (CMC) the surfactants aggregate together to form micelles. This transforms the polymerisation mixture into a colloidal system. The free energy of the system is reduced by the formation of micelles and the surface tension also decreases. Micelles formed are typically 2-10 nm, however, by increasing the amount of surfactant, a larger number of smaller micelles can be formed [196]. By using a mixture of surfactants it is possible to control the size, and number of micelles, along with size of the resultant latex particles [197]. Water insoluble monomers are used for emulsion polymerisations. The majority of the monomer is located in large (1-100 μm) monomer droplets. The size of these droplets is controlled by the stirring rate of the reaction. However, a small proportion of monomer is located within micelles. These micelles containing monomer have a surface area more than two orders of magnitude bigger than monomer droplets. The micelles act as an inbetween point for the water-soluble initiator and the hydrophobic monomer. It is within the micelles that polymerisation occurs. As polymerisation occurs, monomer concentrations are replenished by the release of monomer from monomer droplets into the aqueous phase. There is some debate as to the mechanism by which initiation occurs in emulsion polymerisation. The first suggested mechanism for the formation of polymer particles is by micellar particle nucleation. This is when radicals (primary or oligomeric) from the aqueous phase

enter the micelles [198, 199]. This mechanism has suggested that it is the dominant nucleation process when the surfactant concentration is well above the CMC. At, or below the CMC, it has been suggested that homogenous nucleation plays a minor, but significant, role in the formation of polymer particles. The homogenous particle nucleation mechanism involves radicals polymerising in solution to give oligomeric radical species. These then become insoluble and precipitate out of the aqueous phase. This precipitate is stabilised by the surfactant present in the aqueous phase, allowing absorption of monomer into the droplet [196].

1.10 *Phosphate functionalised core-shell particles*

Core shell particles can be used to control the properties of a material. The outer shell and inner core can be synthesised with different properties and functionalities to alter how the material interacts and degrades [200]. Core-shell particles have many uses, including, surface coatings, printing, catalysts, sensors, biomedical applications and drug delivery [201]. Core-shell particles are usually spherical with the core and shell made from different materials. Crosslinking density can be altered to change the particle morphology and to change the properties of the material [202]. Core-shell particles can be classified as hydrogel-like or non-hydrogel-like. Hydrogel-like particles have a water swollen shell surrounding a collapsed hydrophobic core. Alternatively, both the core and shell can be hydrogels [203]. Hydrogel-like particles are formed with pores or holes throughout the structure. The density of porosity, size of pores and pore interconnection can be determined by the crosslinking density and the composition of the monomers used for polymerisation [204].

Core-shell particles are usually produced in a multi-step process. The core is first synthesised, followed by addition of the shell [205-207]. Multi-step syntheses can be time consuming and costly to produce on large scales. Single step methods can also be used to produce core shell particles.

There are three standard methods for producing core-shell polymer particles: dispersion, precipitation and emulsion polymerisations [208-210]. These are shown in Figure 1.4. Emulsion polymerisation is the most commercially viable process to produce core-shell particles. Industrially, a semi-batch emulsion process is used. However, in academic research batch emulsions are favoured due to the simplification of reaction kinetics and the possibility of avoiding problems associated with using large reactors [211, 212].

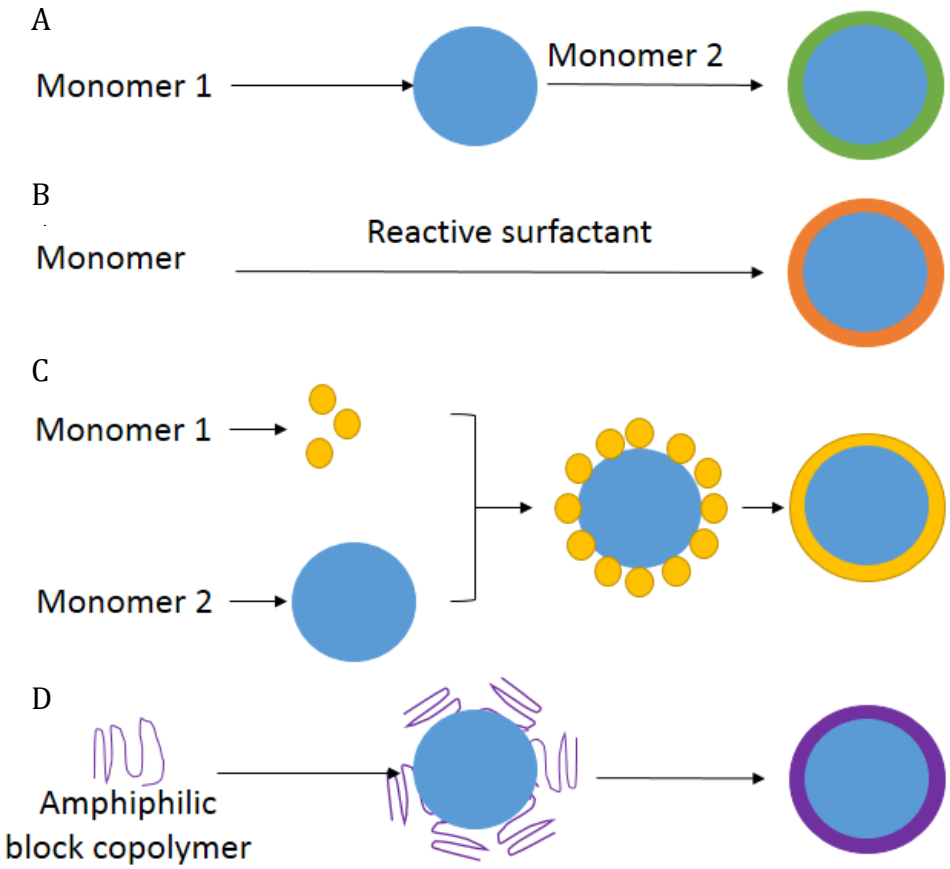

Figure 1.4 (A) Synthesis of core-shell particles in a two-step process. This can be done via emulsion, dispersion or precipitation. (B) Core-shell particle synthesis using a reactive surface. (C) Step wise coagulation of smaller particles on to larger particles followed by heat treatment can also produce core-shell particles. (D) Core-shell particle formation using block copolymers.

Core-shell polymer latexes consisting of a poly(styrene-co-divinyl benzene) core and oleyl phenyl hydrogen phosphate (OPHP) shell have been used to study the

release of vascular endothelial growth factor [213]. The study was based on molecularly imprinted particles to bind and release VEGF over time. Molecularly imprinted particles have been shown by Carter et al. [214-216] to recognise molecules through hydrogen bonding and electrostatic interaction of the phosphate group along with hydrophobic interactions. Short peptide sequences were used in an epitope approach to selectively bind to VEGF. However, the study showed that the performance was not markedly better than the non-imprinted poly (styrene-co-divinyl benzene) core OPHP shell latexes. This led to the conclusion that it was the electrostatic binding of the phosphate groups to VEGF that allowed for release. This mimics the binding of growth factors to heparin. The net negatively charged heparin can bind to VEGF via its basic peptide sequence containing arginine and lysine amino acids.

OPHP was originally synthesised by Takagi *et. Al.* in 1996 [217]. The position of the double bond on the long alkyl chain means that OPHP is relatively unreactive. Rather than copolymerising into the particle shell, OPHP is incorporated by radical transfer via hydrogen abstraction [216]. The same basic latex constituents were maintained but the ratio of ethylene glycol dimethacrylate (EGDMA) crosslinker was varied to change the properties of the particle shell. The decrease in crosslinker changes the openness of the particle, producing a material that can bind VEGF deep within the shell. An increase in crosslinker produces a shell with a higher barrier to diffusion, meaning any VEGF that is within the shell will take longer to diffuse out. The addition of glycerol methacrylate acetonide (GMAC) produced an open particle shell allowing VEGF to bind deeper within the shell. The ratios of EGDMA and GMAC crosslinkers can be altered to produce a size exclusion effect as well as electrostatically binding to VEGF, PDGF and EGF.

1.11 *Poly (2-acrylamido-2-methyl-1-propane sulfonic acid) stabilised particles*

Poly (2-acrylamindo-2-methyl-1-propane sulfonic acid) (PAMPS) was used as a negatively charged polymer shell for binding of VEGF, PDGF and EGF. Previous work

by Liekens et al. and García-Fernández et al. put forward the hypothesis that PAMPS acts as an anti-angiogenic unit when in culture with human umbilical vein endothelial cells (HUVECs) [218, 219]. It was concluded that this was due to pro-angiogenic growth factors binding to the sulfonic acid units on the PAMPS chains. This led to cell death as the cell became starved of nutrients as the PAMPS removed growth factors from solution.

PAMPS was synthesised via reversible addition-fragmentation chain-transfer polymerisation (RAFT). RAFT was first reported in 1998 and showed that controlled molecular weights, with narrow polydispersities could be achieved using a wide range of monomers and reaction conditions [220]. The synthesis of polymers using a RAFT agent or chain transfer agent (CTA) allows synthesis with control over molecular weight. A typical RAFT polymerisation reaction contains the following units: initiator, monomer, chain transfer agent (RAFT agent), and solvent. The termination steps have been removed resulting in the polymer chains growing at a constant rate until very high monomer conversion. The mechanism of RAFT polymerisation involves a reversible addition fragmentation sequence in which transfer of the S=C(Z)S- moiety between active and dormant chains serves to maintain the continuous character of the polymerisation. The RAFT agent can be varied, giving functionality to the capping group at the chain end. A variety of capping molecules can be used. This gives control of the polymer end groups allowing for a variety of different polymer architectures.

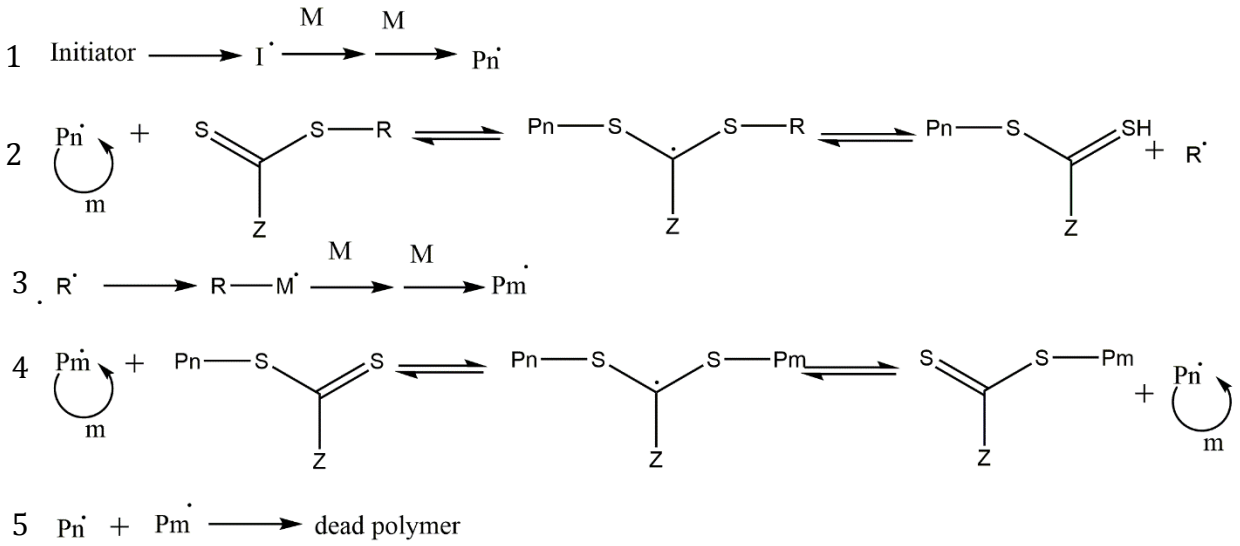

Figure 1.5 Generalised mechanism of RAFT polymerisation. In stages 1 -2 of the polymerisation the reagents [S=C(Z)S-R] are rapidly transformed into a polymeric thiocarbonylthio [S=C(Z)S-Pn] by reaction with propagating radical (Pn.). In stages 3 and 4, the radical liberated (R·) reacts with a monomer to form a new propagating radical (Pm·). Chain extension of the polymeric thiocarbonylthio compound [S=C(Z)S-Pm] occurs. The reversible addition-fragmentation sequence in which the S=C(Z)S- moiety is transferred between dormant and active chains maintains the living character of the polymerisation. Termination occurs when Pn and Pm radicals combine

RAFT polymerisation methods have been used for many years to provide polymers with a variety of end groups. The RAFT agent 4-vinylbenzyl-pyrrole carbodithioate (4-(VPC)) has been used to synthesise branched poly(2-Acrylamido-2-methyl-1-propane sulfonic acid) (PAMPS) [221]. The linear equivalent of 4-(VPC) has been used to produce linear poly (2-Acrylamido-2-methyl-1-propane sulfonic acid) (PAMPS).

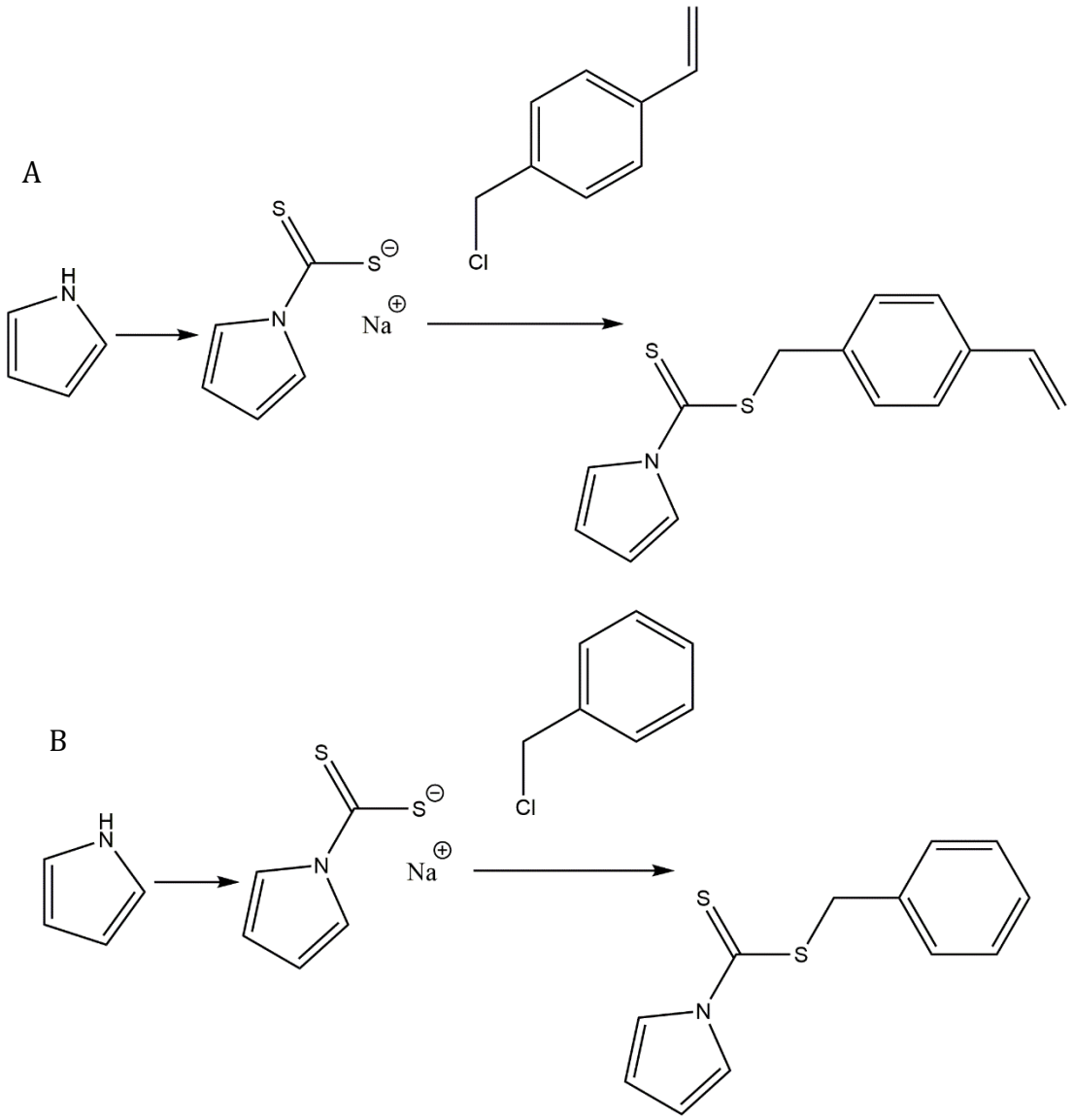

Figure 1.6 (A) Reaction scheme of the synthesis of branching RAFT agent 4-vinylbenzyl-pyrrole carbodithioate, 4-(VPC) (B) Reaction scheme of synthesis of branching RAFT agent 4-benzyl-pyrrole carbodithioate.

The presence or absence of a vinyl group on the RAFT agent allows for synthesis of branched or linear polymers. Branched polymers can contain more functionality in comparison to linear polymers, but they have a broad molecular weight distribution and can have irregular branching and distribution of functionality [222].

The linear and branched polymers synthesised by RAFT can be thought of as macro-RAFT agents. Using them as such, allows for further polymerisations. RAFT has been used in emulsion polymerisations to produce polymer particles with controlled molecular weights [223, 224]. The behaviour, including kinetics of RAFT agents in emulsion polymerisations is similar to that in homogeneous polymerisation [196].

Macro-RAFT agents have also been used as stabilisers in surfactant-free emulsion polymerisation. Surfactant-free emulsion polymerisations have some advantages over traditional emulsion reactions. These include, eliminating the need to remove surfactant after synthesis and allowing for a better understanding of how different monomers behave in emulsion polymerisations [225]. Trithiocarbonate and dithiocarbonate based RAFT agents have been used to form macro-RAFT agents capable of producing block copolymer structures that rearrange to form core-shell particles [226-229]. Hydrophobic units organise themselves in the centre of the particle with hydrophilic (often charged) units acting as stabilisers by organising themselves around the outside. Due to this behaviour, a surfactant is no longer needed to stabilise the water immiscible monomer.

Linear PAMPS (L-PAMPS) and branched PAMPS (B-PAMPS) were used as macro-RAFT agents in the emulsion polymerisation of n-butyl methacrylate (BMA). This produced core-shell particles with a poly (butyl methacrylate) (PBMA) core and PAMPS shell. The sulfonic acid group gives the particles a net negative charge within the shell. This can mimic a net negative charge similar to heparin. Since VEGF and PDGF are both heparin binding pro-angiogenic growth factors, the PAMPS shell can be used as a heparin mimic for the stabilisation and release of VEGF and PDGF. The design of the shell produces a material that can bind different sized growth factors with a size exclusion effect. The L-PAMPS produces an open flexible shell. The B-PAMPS produces a mesh which can exclude molecules larger than the mesh size. The release profile of the smaller protein EGF was also investigated to confirm the size exclusion hypothesis.

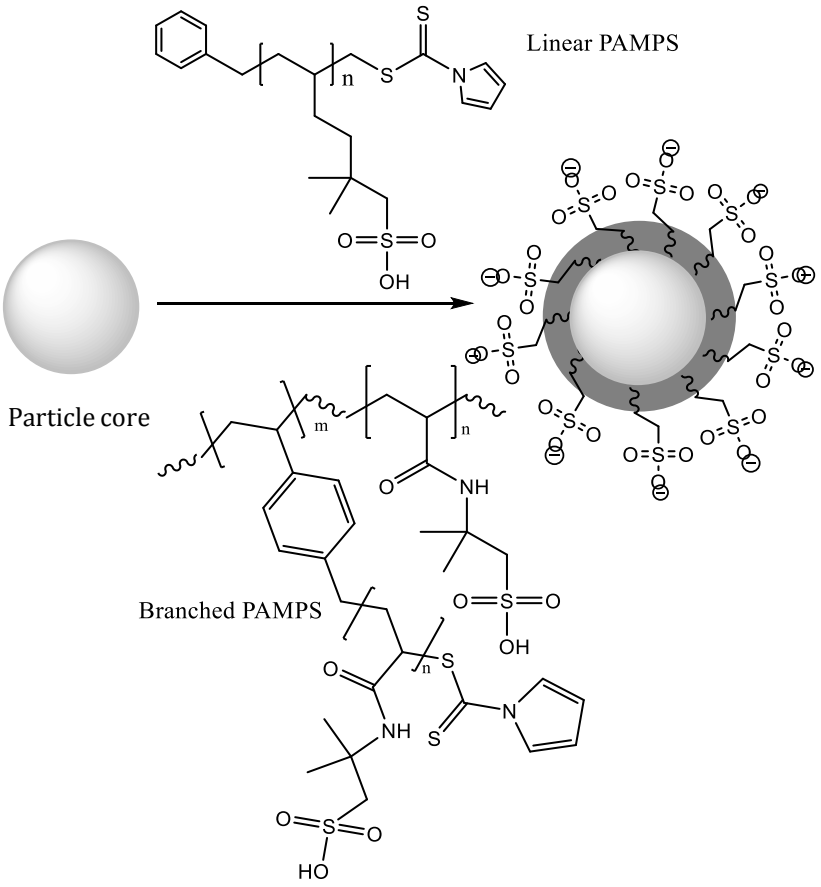

Figure 1.7 Hydrophobic PBMA core surrounded by a negatively charged hydrophilic PAMPS shell. Either L-PAMPS or B-PAMPS is added to stabilise the synthesis of PBMA.

1.12 *Fluorescent labelling of core-shell particles*

Fluorescently labelled materials can have a variety of applications, including: material tracking during *in vitro* and *in vivo* experiments; diagnostics; and imaging [230]. Small polymer particles are often labelled with a variety of fluorescent units for studying cell uptake and tracking with tissues [231]. There are a variety of factors that influence the cellular uptake of a polymer particle. The particle size and morphology dictate if the particle will be taken in by cells. Generally, the particle must be between 50-200 nm in diameter [232]. Finally, the use of a transfection agent in the form of an amphiphilic polymer also affect the uptake of polymer particles [232].

Rhodamine B is a fluorescent dye with an emission maximum at 570 nm which is often used in cell biology, histology or as a biochemical reagent [231]. Acrylated

forms of rhodamine B are commercially available and allow for incorporation of the fluorescent dye to polymers.

It is possible to use batch emulsion polymerisations to produce particles incorporating the fluorescent dye [233]. It is known that the addition of a fluorescent label can inhibit free radical emulsion polymerisation [234], therefore, inclusion of a dye is usually kept at 1 mol % [231]. The particles discussed in section 1.10 (page 25) and 1.11 (page 27) were synthesised with the fluorescent label acryloxyethyl thiocarbamoyl rhodamine B. 1:1 OPHP:EGDMA particles and 2:1:1 OPHP:GMAC:EGDMA particles were synthesised by a two-step emulsion process. This allowed the acryloxyethyl thiocarbamoyl rhodamine B to be contained within the particles core. L-PAMPS and B-PAMPS particles were synthesised in a one-step process, therefore the label was dispersed throughout the particle. Both methods produced pink latexes. Initial problems with particle aggregation got worse upon standing, finally resulting in an unstable and relatively unusable latex.

1.13 *Hydrogels with embedded core-shell particles*

Hydrogels are highly water swollen polymer networks. They are a popular choice of material for medical devices, cell scaffolds, wound dressing and drug delivery vehicles due to their similar mechanical properties to natural tissue. Hydrogels are easy to functionalise and can be synthesised to respond to a stimulus [8, 235-239]. Synthetic hydrogels are easier to maintain consistency over processing of natural tissue when produced in large quantities [240].

The term wound dressing covers everything from cotton bandages to new synthetic wound care systems that can promote healing by maintaining a constant environment and delivering drugs or anti-microbials [239]. Since wound care can be very varied there are many different types of wound dressing on the market, each tailored towards a particular type of wound. However, there are some common features that most wounds need for healing. These include: a warm moist environment, unimpeded epithelial cell movement, efficient oxygen circulation and protection from bacterial colonisation[8]. When choosing or designing a wound dressing the following must be taken into consideration. First, the wound must be

cleaned (debridement) to remove any necrotic tissue or bacteria. Hydrogels are unique compared with other wound dressings as they promote autolytic debridement [241]. The wound must be placed in a moist environment to prevent any further cell death, promote cell replication and enhance angiogenesis. Any excess exudate or blood must be removed as this can prevent new tissue formation. The gaseous exchange needs of the wound must be examined. Lower oxygen levels promote angiogenesis while higher oxygen levels stimulate growth of fibroblasts and epithelial cells. To promote dermal recovery the blood supply must be stimulated by maintaining the wound at body temperature. Finally, the dressing must have low adherence to the wound to prevent further trauma, must be cost effective and not need to be changed frequently [8].

Hydrogels can be tailored to suit all of these environments and therefore are a commonly used material for wound dressing. However, these types of dressing can occasionally need a second covering, such a gauze, or a semi-permeable polymer backing to allow gaseous exchange and prevent the gel from drying out [8]. Due to the high water content, hydrogels have been shown to have a cooling effect and have previously been used to reduce patient pain when treating chronic leg ulcers [242]. Hydrogels are suitable for wounds in each of the stages of wound healing, although they are not suitable for wounds that are extremely infected or are producing a lot of exudate [243].

Using hydrogels as a medium for inducing angiogenesis is the obvious choice. This is because hydrogels can incorporate biological molecules or drugs to promote angiogenesis whilst being a good candidate for a wound dressing. As previously discussed, there are many different growth factors that can be used to assist with angiogenesis and promote wound healing. Rather than discussing the particular proteins released, only the method of release will be discussed.

Ionic gelatin hydrogels have shown positive results of sustained protein release using cell culture and murine hind limb ischemia models [244]. Poly(ethylene glycol) diacrylate (PEGDA) hydrogels have generally low protein adsorption properties. However, various biological molecules and proteins can then be immobilised onto the surface of the hydrogel using covalent linking units [102, 245]. Injectable alginate gels blended with VEGF have been shown to be a potential easy

to administer pro-angiogenic material. Alginate gels containing VEGF were cooled forming a liquid. Upon warming up after injection they formed a solid gel that could administer VEGF and produce and angiogenic response in murine ischemic hindlimb models [246]. Natural molecules, such as heparin, incorporated into hydrogels have also shown some promising results. Poly(hyaluronan-co-PEGDA) gels can bind thiol modified heparin via the hyaluronan units in the hydrogel. This has been shown to induce angiogenesis in murine models [247]. Work by Gilmore *et. al.* used poly(n-vinyl-2-pyrrolidone-co-diethylene glycol bis-allyl carbonate-co-acrylic acid) hydrogels functionalised with peptides, RRR and KKK, followed by heparin to bind VEGF [248]. This showed low cytotoxicity and good ability to promote proliferation in human dermal microvascular endothelial cells (HUDMEC) on the surface of the hydrogel.

Poly(N-vinyl-2-pyrrolidone) (PVP) has commonly been used as a constituent in medical devices. This is because PVP is water soluble, biocompatible, has excellent haemocompatability and extremely low cytotoxicity [249]. PVP is crosslinked with flexible units to overcome the poor mechanical properties of PVP [250, 251]. Several different synthesis techniques have been used to produce PVP containing gels. These include: UV curing [252], electrospinning [253], and various radiation techniques [254-258]. Depending upon the use of the dressing it is possible to pre-cure the hydrogel or cure the gel *in situ*.

1.14 *Alternative protein analysis techniques*

Enzyme linked immunosorbant assays are often used to detect protein released from polymers. ELISA is an extremely sensitive technique that is commonly used in research and medical diagnostics. However, it is not without faults. Denatured or partially degraded protein is not always detected via ELISA and cross reactivity of various proteins can cause problems when analysing in-pure samples. This can give both false positive and false negative results. This is especially true when dealing with proteins where there is not a general agreement on the degradation products. Also, due to their sensitivity and use of anti-bodies, ELISA is can be an expensive analytical technique.

Other methods can be used to identify and quantify proteins present in a solution. Gel electrophoresis and mass spectrometry are two analytical techniques that are often used in protein synthesis. More recently they have been used in combination with antibodies to develop mass spectrometry based immunoassay diagnostic techniques [259]. The sensitivity is high and the techniques for protein detection are well established. Soft ionisation techniques such as MALDI and ESI are used to identify proteins. When dealing with unknown proteins, mass spectrometry is often coupled with gel electrophoresis then peptide sequence fingerprints can be compared to a database of other known proteins of similar origin [260].

2 Project Aims and Objectives

The aim of this project was to produce a system of delivering growth factors. The project was focused on the promotion of angiogenesis for increasing the healing time of chronic wound. Finding a delivery system that can promote angiogenesis successfully would have impacts in a variety of medical fields.

The project was designed to produce materials that are versatile, easy and cheap to produce delivery system. Scalable emulsion reactions were used to produce particles that can be tuned in size by varying the crosslinker. A negatively charged outer shell has been used rather than more traditional methods for binding growth factors. This was chosen because it can be synthesised on a larger scale compared to other methods and the charged groups can be easily incorporated into the polymer during a batch emulsion process.

The specific objectives where:

- Expand upon previous work based on OPHP functionalised core-shell particles. This will be done by increasing the number of monomers included in the particle shell and by expanding the range of proteins under investigation.
- Investigate the protein binding ability of PAMPS coated particles. Determine the effect of shell architecture using linear and branched PAMPS shell particles.
- Set particles into hydrogels to produce a wound dressing like system. This will also allow for direct comparison of the performance of materials studied with heparin functionalised hydrogels.
- Investigate the possibility of alternative protein detection techniques, such as mass spectroscopy and gel electrophoresis.

It was expected that the negative charge on the surface of the various core-shell particles would bind and release pro-angiogenic proteins over time. In this case the particles would be acting as a HS mimic. The quantity and availability of the particle charge and shell architecture was expected to have effects on the material performance.

3 Materials and Methods

3.1 *Synthesis of OPHP functionalised core-shell particles*

OPHP functionalised core-shell particles were made via a two-step batch emulsion process.

3.1.1 Synthesis of oleyl phenyl hydrogen phosphate (OPHP)

Synthesis of OPHP has previously been described by Gilmore [91, 116]. The synthesis below has been replicated from her PhD thesis.

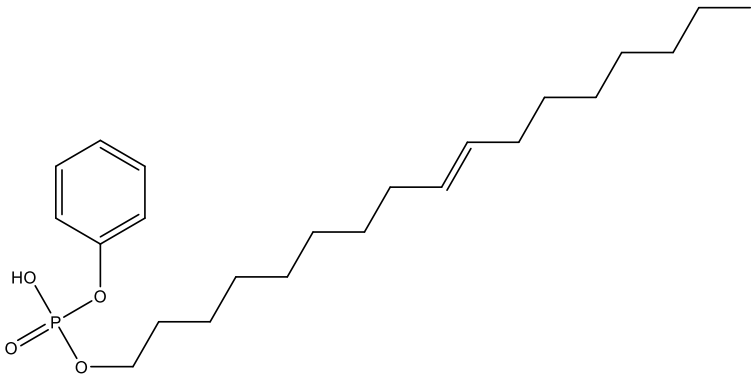

Figure 3.1 Structure of oleyl phenyl hydrogel phosphate

Oleyl alcohol (65.5g, Sigma Aldrich) was added drop wise over 30 minutes to stirring phenyl phosphodichloridate (50g, Sigma Aldrich). The mixture was stirred for 60 minutes at room temperature. The temperature was increased to 50°C and the reaction was stirred for 16 hours. The solution was added drop wise over 1 hour to rapidly stirring ice cold water (300ml). The reaction was left for 1 hour and then extracted into diethyl ether (3x100ml, Fisher). The organic extracts were dried with magnesium sulphate, followed by filtering and rotary evaporation. The resultant product was a brown oil. The product was purified on a silica column using a gradient from 90:10 DCM: methanol. Molecular formula: $C_{22}H_{37}O_4P$ (mass 396) % yield: 56.5 % Analysis was completed via elemental analysis (Expected: C 67.9%, H 9.73%. Analysis: C 67.27%, H 9.93%), ^{1}H NMR (($CDCl_3$, 250MHz) δH (ppm): 0.87 (t, 3H, CH_3), 1.26 (m, 22H, -CH_2-), 1.62 (dt, 2H, - CH_2CH_2-OP), 2.00 (dt, 4H, -CH_2CH=), 4.05 (d, 2H, -CH_2OP), 5.38 (dt, 2H, -CH=CH-), 7.10-7.32 (m, 5H, -C_6H_5-), 8.88 (s, 1H, OH)), ^{31}P NMR($CDCl_3$, 162MHz) δP (ppm): -4.0228) and mass spectrometry MH^+ : 425.

3.1.2 Synthesis of glycerol methacrylate acetonide (GMAC)

GMAC was routinely synthesised using the following protocol.

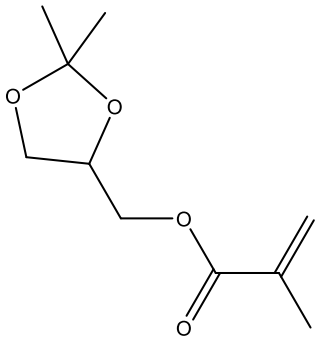

Figure 3.2 Structure of glycerol methacrylate acetonide.

Methacrylic anhydride (94.2g, Sigma Aldrich) was added drop wise to dry solketal (66.08g, Sigma Aldrich), pyridine (63.28g, Sigma Aldrich) and DCM (500ml, dry from Grubbs system) under nitrogen at 0°C. The solution was stirred at room temperature for 24 hours followed by the addition of water (250cm^3, 18.2 MΩ cm at 25°C, Millipore, UK). The organic phase was washed with water and solvent removed by rotary evaporation.

Amberlite IRA 402 was washed with 1M NaOH for 2 hours then washed with water followed by acetone. The crude GMAC was added and gently shaken overnight. The product was filtered and distilled under reduced pressure. Molecular formula: $C_{10}H_{16}O_4$ (mass: 200) % yield: 62.0 %. ^{1}H NMR (dDMSO): δ= 1.40 (s, O(O)C-C*H*$_3$), 1.85 (s, C*H*$_3$-C=CH$_2$), 3.75 (ddd, CH-C*H*$_2$-O), 3.83 (ddd, CH-C*H*$_2$-O), 4.05 (ddd, O-CH$_2$-C*H*), 4.20 (ddd, O-C*H*$_2$-CH), 4.95 (m, C*H*(H)=CH$_3$), 5.65 (d, CH(*H*)=CH$_2$).

3.1.3 Synthesis of poly (styrene-co-divinyl benzene) core

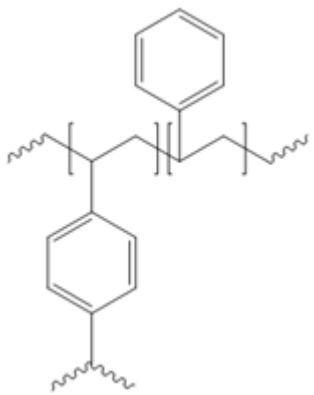

Figure 3.3 Structure of poly (styrene-co-divinyl benzene) produced by emulsion polymerisation.

Styrene (Sigma Aldrich) and divinyl benzene (Sigma Aldrich) were distilled before use.

A jacketed reaction vessel was heated to 70°C then purged with N_2. A solution of MES buffer (0.533g, Sigma Aldrich) in ultrapure water (45ml, 18.2 MΩ cm at 25°C, Millipore, UK) was purged with nitrogen for 5 minutes while stirring until solids were dissolved. Sodium dodecyl sulphate surfactant (1g, Alpha Aesar) and potassium carbonate (0.25g, Sigma Aldrich) were added and stirred until dissolved. The solution was sonicated for 10 minutes and adjusted to pH6 through the addition of NaOH. The buffer solution was added to the emulsion rig, purged with N_2 and stirred at 400rpm. Styrene (0.043 moles) and divinyl benzene (0.004 moles) purged with nitrogen was added over 30 minutes to stirring solution of buffer. Potassium persulphate (0.16g, Sigma Aldrich) dissolved in ultrapure water (7.5ml, 18.2 MΩ cm at 25°C, Millipore, UK) was purged with nitrogen for 15 minutes and added to the monomer dispersion in a one shot initiation. Polymerisation took place overnight. If needed, the reaction was ceased by turning the heat off and sample store at room temperature in water.

3.1.4 Synthesis of poly (oleyl phenyl hydrogen phosphate-co-ethylene glycol dimethacrylate) shell

The quantity of OPHP and EGDMA were varied in each latex to determine the importance of the availability of the phosphate for binding protein and the effect of crosslinker. The quantities of OPHP and EGDMA used can be found in Table 3-1.

Ethylene glycol dimethacrylate (Sigma Aldrich) and oleyl phenyl hydrogen phosphate were combined with ultrapure water (13.5ml, 18.2 MΩ cm at 25°C, Millipore, UK). The solution was purged with nitrogen for 5 minutes then added drop wise over 15 minutes to the PS-co-DVB core. The reaction was allowed to equilibrate for 1 hour. The initiator solution of potassium persulphate (Sigma Aldrich) in ultrapure water (8ml, 18.2 MΩ cm at 25°C, Millipore, UK) was purged with nitrogen for 15 minutes, then added to the reaction in a one shot initiation. The reaction was stirred at 400rpm and at 70°C overnight. The reaction was ceased by turning the heat off and sample store at room temperature in water.

Formulation	OPHP (moles)	EGDMA (moles)	Potassium Persulfate (moles)
1:3 OPHP:EGDMA	2.5×10^{-3}	9.6×10^{-3}	1.2×10^{-3}
1:1 OPHP:EGDMA	5.0×10^{-3}	4.8×10^{-3}	1.2×10^{-3}
3:1 OPHP:EGDMA	10.0×10^{-3}	2.4×10^{-3}	1.2×10^{-3}

Table 3-1 Formulation for poly (oleyl phenyl hydrogen phosphate-co-ethylene glycol dimethacrylate) shell.

3.1.5 Synthesis of poly (oleyl phenyl hydrogen phosphate-co-ethylene glycol dimethacrylate-co-glycerol methacrylate acetonide) shell

The quantity of EDGMA and glycerol methacrylate acetonide were varied in each latex to determine the effect of crosslinker. The quantities of OPHP, EGDMA and GMAC used can be found in Table 3-2.

Glycerol methacrylate acetonide, ethylene glycol dimethacrylate (Sigma Aldrich) and oleyl phenyl hydrogen phosphate were combined with ultrapure water (13.5ml, 18.2 MΩ cm at 25°C, Millipore, UK). The solution was purged with nitrogen for 5 minutes then added drop wise over 15 minutes to the PS-co-DVB core. The reaction was allowed to equilibrate for 1 hour. The initiator solution of potassium persulphate (Sigma Aldrich) in ultrapure water (8ml, 18.2 MΩ cm at 25°C, Millipore, UK) was purged with nitrogen for 15 minutes and then added to the reaction in a one shot initiation. The reaction was stirred at 400rpm and at 70°C for 2 hours. After 2 hours the temperature was increased to 80°C for 1 hour. The reaction was ceased by turning the heat off and sample store at room temperature in water.

Formulation	OPHP (moles)	EGDMA (moles)	GMAC (moles)	Potassium Persulfate (moles)
4:1:3 OPHP: GMAC:EGDMA	5.0×10^{-3}	7.1×10^{-4}	4.3×10^{-4}	6.3×10^{-4}
2:1:1 OPHP: GMAC:EGDMA	5.0×10^{-3}	5.7×10^{-4}	5.7×10^{-4}	4.2×10^{-4}
4:3:1 OPHP: GMAC:EGDMA	5.0×10^{-3}	4.3×10^{-4}	7.1×10^{-4}	6.3×10^{-4}

Table 3-2 Formulation for poly (oleyl phenyl hydrogen phosphate-co-ethylene glycol dimethacrylate-co-glycerol methacrylate acetonide) shell.

3.2 *Synthesis of PVP-co-DEGBAC hydrogels with embedded core-shell particles*

N-vinyl-2-pyrrolidone (Sigma Aldrich, UK) and acrylic acid (Sigma Aldrich, UK) were distilled under reduced pressure prior to use. Latex particles were washed and stored in propan-2-ol. Diethylene glycol bis-allyl carbonate (DEGBAC, Sigma Aldrich, UK), glycerol (Sigma Aldrich, UK), azobisisobutyronitrile (AIBN, Sigma Aldrich, UK) and hydroxyl-2-methylpropiophenone (2HMPP, Sigma Aldrich, UK) were used as supplied.

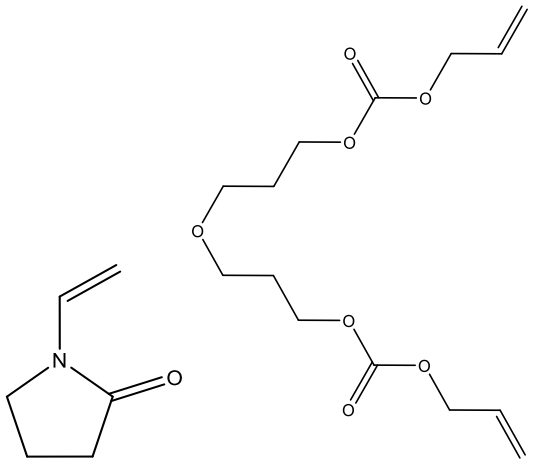

Figure 3.4 Monomers N-vinyl-2-pyrrolidone (NVP) and diethylene glycol bis-allyl carbonate (DEGBAC) that are the main constituents of the hydrogels produced. The synthesis was carried out with either thermal or UV curing.

3.2.1 Thermally cured hydrogels

Each monomer and initiator was weighed out according to Table 3-3. Propan-2-ol (Sigma Aldrich, UK) containing each latex was added. The solution was stirred under nitrogen for 30 minutes. The monomer mixture was injected in between glass plates containing a PTFE gasket. The hydrogel was thermally cured for 18 hours at 70^{o}C. After curing the glass plates and PTFE gasket was carefully removed and hydrogel stored under propan-2-ol.

Particle	NVP (moles)	DEGBAC (moles)	Latex (g)	IPA (moles)	AIBN (moles)	Glycerol (moles)
Control (PVP-co-DEGBAC)	3.6×10^{-2}	6.6×10^{-4}	-	-	3.7×10^{-4}	-
B PAMPS	3.6×10^{-2}	6.6×10^{-4}	1.2	-	3.7×10^{-4}	-
L PAMPS	3.6×10^{-2}	6.6×10^{-4}	1.4	-	3.7×10^{-4}	-
OPHP	3.6×10^{-2}	6.6×10^{-4}	1.4	-	3.7×10^{-4}	7.6×10^{-3}
GMAC	3.6×10^{-2}	6.6×10^{-4}	1.4	-	3.7×10^{-4}	7.6×10^{-3}

Table 3-3 Quantities used for thermally cured synthesis of PVP-co-DEGBAC hydrogels containing embedded latex particle.

3.2.2 UV cured hydrogels

Each monomer and initiator was weighed out according to Table 3-4. Propan-2-ol (Sigma Aldrich, UK) containing each latex was added. The solution was stirred under nitrogen for 30 minutes. The monomer mixture was injected in between quartz

plates containing a PTFE gasket. The hydrogel was UV cured for a total of 9 minutes, turning over after each minute. After curing the quartz plates and PTFE gasket was carefully removed and hydrogel stored under propan-2-ol.

Particle	NVP (moles)	DEGBAC (moles)	Latex (g)	IPA (moles)	2HMPP (g)	Glycerol (moles)
Control (PVP-co-DEGBAC)	8.6×10^{-2}	1.7×10^{-3}	-	4.0×10^{-2}	6.1×10^{-4}	-
B PAMPS	6.8×10^{-2}	1.7×10^{-3}	1.6	1.3×10^{-2}	6.1×10^{-4}	-
L PAMPS	6.8×10^{-2}	1.7×10^{-3}	1.6	1.3×10^{-2}	6.1×10^{-4}	-
OPHP	6.8×10^{-2}	1.7×10^{-3}	1.1	2.2×10^{-2}	6.1×10^{-4}	7.6×10^{-3}
GMAC	6.8×10^{-2}	1.7×10^{-3}	1.1	2.2×10^{-2}	6.1×10^{-4}	7.6×10^{-3}

Table 3-4 Quantities used for UV cured synthesis of PVP-co-DEGBAC hydrogels containing embedded latex particles.

3.3 *Synthesis of acryloxyethyl thiocarbamoyl rhodamine B labelled particles*

The emulsion reactor was protected from light throughout the synthesis.

Styrene (Sigma Aldrich, UK) and divinyl benzene (Sigma Aldrich, UK) and butyl methacrylate (Sigma Aldrich, UK) were distilled before use.

3.3.1 OPHP functionalised particles

3.3.1.1 Synthesis of poly (styrene-co-divinyl benzene) core containing acryloxyethyl thiocarbamoyl rhodamine B

The emulsion rig was heated to 70 ^{o}C then purged with N_2. A solution of MES buffer (0.533 g, Sigma Aldrich, UK) in deionised water (45 ml, 18.2 MΩ cm at 25^{o}C, Millipore, UK)) as purged with nitrogen for 5 minutes while stirring until solids were dissolved. Sodium dodecyl sulphate surfactant (1 g, Alpha Aesar, UK) and potassium carbonate (0.25 g, Sigma Aldrich, UK) were added and stirred until dissolved. The solution was sonicated for 10 minutes and adjusted to pH6 through the addition of NaOH. The buffer solution was added to the emulsion rig along with acryloxyethyl thiocarbomyl rhodamine B (4mg, Polysciences Inc. Germany) then purged with N_2 and stirred at 400rpm. Styrene (4.3×10^{-2} moles) and divinyl benzene (3.8×10^{-3} moles) purged with nitrogen was added over 30 minutes to the stirring buffer

solution. Potassium persulfate ($5.9x10^{-4}$ moles, Sigma Aldrich) dissolved in ultrapure water (7.5 ml, 18.2 MΩ cm at 25 °C, Millipore, UK) was purged with nitrogen for 15 minutes and added to the monomer solution in a one shot initiation. Polymerisation took place overnight.

3.3.1.2 Synthesis of 1:1 OPHP: EGDMA shell

Ethylene glycol dimethacrylate ($4.8x10^{-3}$ moles, Sigma Aldrich, UK) and oleyl phenyl hydrogen phosphate ($5.0x10^{-3}$ moles) were combined with ultrapure water (13.5 ml, 18.2 MΩ cm at 25°C, Millipore, UK). The solution was purged with nitrogen for 5 minutes then added drop wise over 15 minutes to the PS-co-DVB core. The reaction was allowed to equilibrate for 1 hour. The initiator solution of potassium persulfate ($1.2x10^{-3}$ moles, Sigma Aldrich, UK) in ultrapure water (8 ml, 18.2 MΩ cm at 25 °C, Millipore, UK) was purged with N_2 for 15 minutes, then added to the reaction in a one shot initiation. The reaction was stirred at 400 rpm and 70 °C overnight. After reaction was complete, the heat was turned off. Sample wound be stored in a sealed container, protected from light at 4°C.

3.3.1.3 Synthesis of 2:1:1 OPHP:EGDMA:GMAC shell

Glycerol methacrylate acetonide ($5.7x10^{-4}$ moles) ethylene glycol dimethacrylate ($5.7x10^{-4}$ moles, Sigma Aldrich, UK) and oleyl phenyl hydrogen phosphate ($5.0x10^{-3}$ moles) were combined with ultrapure water (13.5 ml, 18.2 MΩ cm at 25°C, Millipore, UK). The solution was purged with nitrogen for 5 minutes then added drop wise over 15 minutes to the PS-co-DVB core. The reaction was allowed to equilibrate for 1 hour. The initiator solution of potassium persulfate ($4.2x10^{-4}$ moles, Sigma Aldrich, UK) in ultrapure water (8 ml, 18.2 MΩ cm at 25°C, Millipore, UK) was purged with N_2 for 15 minutes, then added to the reaction in a one shot initiation. The reaction was stirred at 400 rpm and 70°C for 2 hours. The temperature was increased to 80°C for 1 hour. After reaction was complete, the heat was turned off. Sample wound be stored in a sealed container, protected from light at 4°C.

3.3.2 PAMPS functionalised particles

Linear or branched PAMPS (0.83 g) and acryloxyethyl thiocarbomyl rhodamine B (14.8 mg, Polysciences Inc., Germany) was dissolved in ultrapure water (72 ml, 18.2 MΩ cm at 25 °C, Millipore, UK). This was added to the emulsion reactor, purged with nitrogen and heated to 60 °C. Butyl methacrylate (0.1 moles, Sigma Aldrich, UK) was

added and stirred at 400rpm for 30 minutes. Potassium persulfate ($7.4x10^{-4}$ moles, Sigma Aldrich, UK) was dissolved in ultrapure water (10 ml, 18.2 MΩ cm at 25 °C, Millipore, UK) and added in a one shot initiation. The reaction ran for 8 hours. After reaction was complete, the heat was turned off. Sample wound be stored in a sealed container, protected from light at 4°C.

3.4 *Core-shell particle dialysis and analysis*

3.4.1 Dialysis and sterile dialysis of samples

12-14kDa MWCO dialysis tubing (Spectrum Laboratories Inc.) was soaked in ultrapure water (18.2 MΩ cm at 25°C, Millipore, UK). Excess water was tapped off and each tube was filled with latex. Dialysis solution of ultrapure water (500ml, 18.2 MΩ cm at 25°C , Millipore, UK), phosphoric acid (4.9g, Sigma Aldrich, UK) and sodium dodecyl sulphate (0.12 g ,2.5% by volume) was prepared. The dialysis solution was changed twice daily for 3 days. The dialysis solution was changed to ultrapure water (500ml, 18.2 MΩ cm at 25°C, Millipore, UK) and changed twice daily for 3 days. After removal from dialysis tubing, samples covered and stored at room temperature.

3.4.2 Deprotection of GMAC units

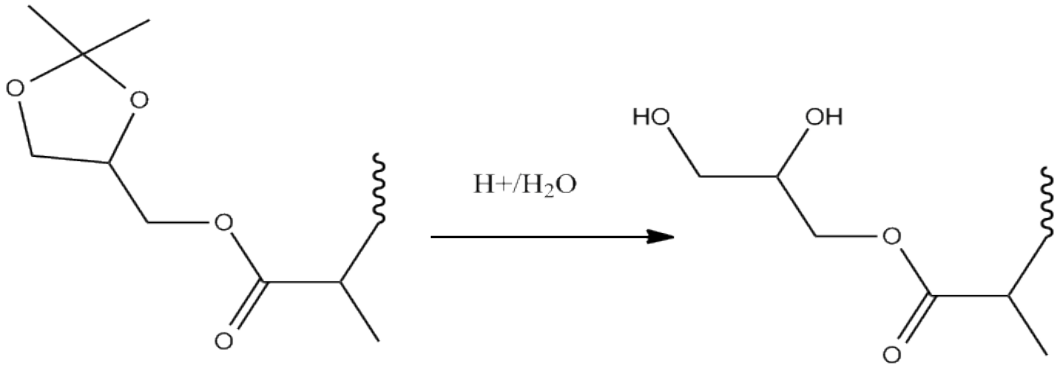

Figure 3.5 Deprotection of GMAC by removal of acetone group.

GMAC was deprotected by the addition of 1M HCl (1:4 by volume latex: HCl). This was heated in a water bath at 60°C for 5 hours.

3.4.3 Particle size analysis

10µl solution of each latex sample in 25 cm^3 10mM KCl was prepared. Particle size measurements were taken at 25°C using ZetaPALS zeta potential analyser (Brookhaven Instruments Corporation).

3.4.4 Zeta potential measurements

10µl solution of each latex sample in 25 cm^3 1mM KCl was prepared. References were taken for 1mM KCl solution, 10 mM KCl solution and B1-ZR3 reference solution. Zeta potential measurements were taken at 25°C using ZetaPALS zeta potential analyser (Brookhaven Instruments Corporation).

3.4.5 Solid content analysis

0.5ml latex was weighed then dried in a vacuum oven for 48 hours. The sample was then weighed again and mass lost and solid content determined. All samples were taken in triplicate.

$$\text{Solid Content (\%)} = (\text{mass dry latex (g)}/\text{mass wet latex (g)})\text{x}100$$

Material	Expected Mass Recovery (%)
1:3 OPHP:EGDMA	11.30
1:1 OPHP:EGDMA	9.92
3:1 OPHP:EGDMA	13.46
4:1:3 OPHP:GMAC:EGDMA	7.62
2:1:1 OPHP:GMAC:EGDMA	7.69
4:3:1 OPHP:GMAC:EGDMA	7.77

Table 3-5 Expected mass recovery of PS-co-DVB core OPHP:EGDMA shell and PS-co-DVB core OPHP:GMAC:EGDMA shell particles.

3.4.6 Transmission electron microscopy

TEM was carried out using an FEI Tecnai Spirit Microscope operating at 100kV. 50µl of 10:1 water to diluted latex were loaded onto gold mesh sample mounts. The sample was left for 60 seconds then the water was removed. Samples were stained with uranyl formate solution and fully air dried before imaging.

3.5 *Hydrogel analysis*

3.5.1 Water content analysis

Water content was determined by cutting and weighing small portions of each water swollen hydrogel in triplicate. These were then dried in a vacuum oven until constant weight. The water content was determined by the following:

$$\text{Water content (\%)} = ((W_{wet} - W_{Dry})/W_{wet}) \times 100$$

3.5.2 Residual monomer content

Residual monomer content was determined by gas chromatography. Controls of NVP and DEGBAC were ran prior to hydrogel samples so peak identity could be determined more easily. A Perkin Elmer Autosystem XL with a Phenomenex ZB-5 column was used throughout. Table 3-6 shows the parameters used for analysis.

Perkin Elmer Autosystem XL Operating Parameters	
Temperature range	40°C -250°C (temp ramp of 10°C/min)
Injection temperature	250°C
Carrier system	Helium
Flow rate	0.8ml/min
Injection system	Autosampler

Table 3-6 Gas chromatography operating conditions for determining residual monomer concentration.

3.5.3 Scanning electron microscopy

Polymer samples were dried using ethanol (50%-100% in steps) followed by hexamethyldsilazane (50%-10% in steps). Samples were transferred into 100% hexamethyldsilazane for 30 minutes followed by air drying the samples overnight. Samples were mounted onto aluminium pin-stubs with Leit-C carbon tabs and sputter coated (Edwards S150B) with gold. Samples were imaged using a Philips XL 20 microscope using associated software.

3.6 *Cell studies*

3.6.1 Normal human dermal fibroblast cell culture

NHDF were cultured in T75 cell culture flask (Corning Life Sciences, USA) with 20 ml Dulbeco's Modified Eagle Medium (DMEM, Life Technologies, UK) containing 10% FBS (Sigma Aldrich, UK) at 37°C with 5% CO_2. The media was changed every 3-4 days and passage occurred once per week when the cells were at 70-90% confluence. To passage the media was removed and 5 ml trypsin (Life Technologies, UK) was added to each flask. The trypsin was left on cells for approximately 5 minutes with gentle agitation. The process was monitored using a light microscope. 10 ml media was added to neutralise the trypsin. The cells were centrifuged to form a cell pellet and re-suspended in 10 ml media. Each flask was split into four.

3.6.2 Endocytosis study

Tissue culture plastic coated flat bottom 24 well plates (Corning Costar, USA) were used for cell culture. Initial studies used 100,000 cells per well. Half were cultured for 48 hours until 70-80% confluent and half were seeded and left for 3-4 hours to adhere to the surface of the well plate. Cells were cultured at 37°C with 5% CO_2. Each well contained 1.5 ml DMEM containing 10% FBS. The media was changed for media containing sterile rhodamine B labelled particles suspended in PBS. Table 3-7 contains the volume of particles and volume of media used in each well. The particle/media solution was left on the cells for 24 hours. The solution was removed and each well was wash 3 times with PBS. Cells were imaged using a fluorescent microscope in PBS and disposed of after imaging.

Particle Concentration	**Volume of Rhodamine B Labelled Particles in PBS (µl)**	**Volume of DMEM (10% FBS) (µl)**
High	500	1000
Medium	250	1250
Low	50	1450
Very Low	25	1475

Table 3-7 Volume of rhodamine B labelled particles used for cell culture experiments. All particles were sterilised and suspended in sterile PBS with a consistent solid content of 10%.

The cell seeding number was also altered. 20000, 40000, 70000 or 100000 cells were seeded into a 24 well plate. The cell culture condition were the same as stated above. Cells were left for 3-4 hours to adhere to the surface of the well plate and either medium or low volume of particles (Table 3-7) were added to each well. Cells were cultured for one data point then washed once with PBS and imaged using a fluorescent microscope.

Finally, 40000 cells were seeded onto each well of a 24 well plate, and cultured as stated above. A medium volume (Table 3-7) of particles were added and cells were cultured for 24 hours. Each well was washed once with PBS and imaged using a phase contrast microscope. A positive control of particles with no cells and a negative control of cells with no particles was used. Each experiment was carried out in triplicate.

3.7 *Protein studies*

3.7.1 Protein binding and release from particles

0.5ml phosphate buffered saline (PBS) was added to 0.5ml latex. The samples were agitated for 30 minutes then centrifuged until a solid polymer pellet had formed. The supernatant was removed leaving the solid polymer. 0.5ml PBS was added to the latex solid and agitated for 30 minutes. The sample was centrifuged at 13,000 rpm for 30 minutes and the supernatant removed. This process was continued until the supernatant was pH 7. A solution of 100ng/ml $VEGF_{165}$/PDGF-BB/EGF (Peprotech) solution was made up with the inclusion of 1% bovine serum albumin (Sigma Aldrich). 1 ml of this solution was added to each of the polymer samples and left at 4^{o}C for 18 hours with gentle agitation. The $VEGF_{165}$/PDGF-BB/EGF solution was removed and replaced with 1 ml PBS. Initial particle protein loading readings were taken by removing the supernatant after binding and analysing via ELISA. The samples were stored at 37^{o}C for the remainder of the experiment. Supernatant samples were initially taken at 1, 2, 6, 12, 24, 48 and 72 hours. This was later extended to 96, 120, 144, and 168 hours and finally extended up to 31 days. Samples were stored at -80^{o}C until analysis.

3.7.2 Protein binding and release from hydrogels

Each gel was cut into small circles using a cork borer. These were soaked in PBS with the solvent changed twice daily for 5 days. The PBS was removed and replaced with a solution of 100 ng/ml VEGF/PDGF/EGF in PBS containing 0.1 % BSA. This was left at 4^{o}C for 16 hours to bind to the hydrogel. The protein containing solution was removed and replaced with PBS containing 0.1 % BSA. The samples were stored at 37^{o}C for the release time period. Samples were taken at the following time points: 0, 1, 6, 12, 24, 48, 72 hours. Binding and release experiments were done in triplicate. Released samples were stored at -80^{o}C until analysis.

3.7.3 Protein interactions with heparin

A solution of 200ng/ml $VEGF_{165}$ (Peprotech) solution was made up in water with the inclusion of 0.1% bovine serum albumin (Sigma Aldrich) and 10% heparin (Sigma Aldrich). Samples were heated at 37^{o}C for 24 hours then stored at -80^{o}C until analysis.

3.7.4 Enzyme linked immunosorbant assay protocol

Either a sandwich ELISA kit from R&D Systems or a sandwich ELISA kit purchased from Peprotech were used for analysis. Each kit was utilised following the manufacturer's instructions. The standard protocol for ELISA is as follows (see kits instructions for quantities and timings):

If needed, prepare 96 well plate for by adding capture antibody to each well. Incubate then aspirate each well with wash buffer. Wash each well 4 times. Ensure sufficient washing by blotting the plate on a paper towel after each washing step. Add blocking buffer and incubate. Finish plate preparation by washing each well 4 times with wash buffer.

Standard protein calibration was produced by reconstituting protein standard and producing a serial dilution from 1000 pg/ml to 0 pg/ml. If needed, a higher concentration of standard protein could be used with Peprotech ELISA kits. Each standard was analysed in triplicate. If stated, assay diluent was added to each well, followed by sample or standard solution. The plate was then incubated at room temperature. After the incubation period the plate was washed and aspirated 4 times.

Detection antibody was added to each well. The plate was incubated at room temperature then washed 4 times with wash buffer. Peprotech plates then required addition of avidin-HRP conjugate and ABTS substrate as separate steps, whereas, R&D Systems plates added these together. After colour had developed, a stop solution was used to prevent further colour development.

The developed plate was read using MRX II plate reader (Dynex Technologies) with wavelengths and correction wavelengths as stated by the manufacturer. All samples and standards were analysed in triplicate.

3.7.5 Mass spectrometry

Samples were prepared as described in section 3.7.1-3.7.3. After collection, samples were flash frozen and stored at -80^{o}C until analysis. When needed, samples were quickly defrosted. Analysis was ran on using ESI on a waters LTC mass spectrometer with TOF analysis.

3.7.6 Gel electrophoresis

Mini-Protean TGX pre-cast electrophoresis gels (Bio-Rad, UK) were loaded into a Mini-Protean tetra cell tank (Bio-Rad, UK). TGS buffer (Bio-Rad, UK) was diluted to 1x concentration and added to the tank. For each well 20µl of protein was diluted with 20µl Laemmli sample buffer (Sigma Aldrich) and loaded into an electrophoresis gel well. All protein samples were ran in triplicate. 10µl protein standard (precision plus protein dual colour standard, Bio-Rad) was added to at least three wells on each gel. 300V was applied for 5 minutes then 180V for approximately 25 minutes. The movement of the coloured standard wells was monitored for progression down the gel. The gels were removed from their cases and a scalpel was used to remove the top wells.

3.7.6.1 Staining

Staining was done using Bio-Rad silver stain plus kit. All glassware was acid washed prior to being used with staining solutions. All volumes given are for staining two mini gels. All solvent and reagents not supplied in the staining kit were from Sigma Aldrich.

Reagent	Volume (ml)
Methanol	200
Acetic Acid	40
Fixative Enhancer Concentrate	40
Distilled Water	120

Table 3-8 Fixative step for 2 mini electrophoresis gels. Fixative enhancer concentrate was supplied in Bio-Rad silver stain plus kit.

Table 3-8 shows the solution used for fixing electrophoresis gels before staining. The gels were placed in the solution and left with gentle agitation for 20 minutes. The gels were rinsed and washed with 400ml distilled water for 10 minutes. The wash solution was decanted off and replaced with a further 400ml distilled water for 10 minutes.

Reagent	Volume (ml)
Distilled water	35
Silver Complex Solution	5
Reduction Moderator Solution	5
Image Development Reagent	5
Development Accelerator Solution	50

Table 3-9 Staining and development step for 2 mini electrophoresis gels. All solutions were supplied in Bio-Rad silver stain plus kit.

The staining and development solution was stirred prior to use. The development accelerator solution was added just prior to adding solution to the gel. The electrophoresis gels were stained for approximately 20 minutes with gentle agitation. When staining was complete, it was stopped using 5% acetic acid solution.

4 Results

4.1 *Analysis of OPHP functionalised core-shell particles*

Particles were designed with a functional phosphate unit polymerised into the outer shell of a PS-co-DVB core particle. The shell was altered by varying the ratio of cross linker (EGDMA) and by the inclusion of GMAC, which is assumed to produces a large open shell on the particles.

After dialysis, to remove surfactant, the particle size, zeta potential and solid content of the latexes were determined as shown in Figure 4.1. All latexes were stable, with a negative surface charge and within the expected size range [196]. The solid content measurements for OPHP:EGDMA particles are consistent with normal emulsion polymerisation.

Figure 4.1 shows that as the ratio of OPHP:EGDMA changes there is an effect on the particle size. As the ratio of OPHP:EGDMA increases, particle size also increases. The less OPHP and more EGDMA the smaller the particle. In this case, EGDMA is a crosslinker and an increase in crosslinker quantity leads to a more tightly porous structure. This reduced the size of the outer shell of the particle leading to a net decrease in particle size. Comparison of batch variation shows that the synthesis produced particles that showed no significant difference (T-Test) when the dynamic light scattering and zeta potential measurements where compared.

A

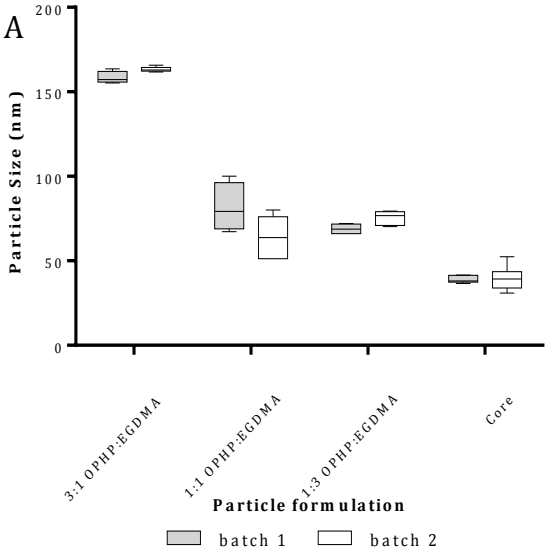

B

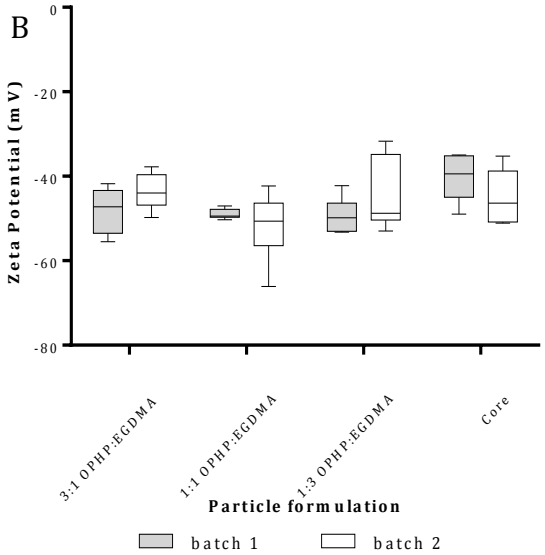

C

Formulation	Particle Size (nm)	Zeta Potential (mV)	Solid Content (%)
Core	40.4±1.0	-40.2±1.8	10.3±0.6
1:3 OPHP:EGDMA	72.5±1.8	-49.8±1.5	14.2±0.3
1:1 OPHP:EGDMA	100.0±6.7	-47.7±1.8	10.0±0.7
3:1 OPHP:EGDMA	161.1±1.6	-49.3±0.5	13.2±0.1

Figure 4.1 (A) Particle size analysis of OPHP:EGDMA latex. Batch variation analysed via Mann-Whitney T-Test. (B) Zeta potential analysis of OPHP:EGDMA latex. Batch variation analysed via Mann-Whitney T-Test. (C) Particle size, zeta potential and solid content measurements.

The solid content analysis of OPHP:GMAC:EGDMA particles (Table 4-1) was less than those for OPHP:EGDMA particles but still within the normal range for this types of emulsion polymerisation. After deprotection of the GMAC shell, the deprotected and protected particle size were compared, as shown in Figure 4.2. The deprotection

step increases the swelling of the GMAC shell. The size range of the latex particles showed a wide variation depending upon the quantity of GMAC in the sample. As the quantity of GMAC was increased, the particle size also increased. There was only a small increase in particle size between 2:1:1 OPHP:GMAC:EGDMA and 4:3:1 OPHP:GMAC:EGDMA before deprotection. However, after deprotection this size difference increased. It is thought that before deprotection, GMAC was only a small crosslinking unit so additional protected GMAC in the particle shell does not have a vast effect upon particle size. After deprotection of the GMAC, the shell expanded in size and produced a porous layer. This effect was large enough to produce a noticeable effect on the net particle size.

Comparison of batch variation shows that the synthesis produces particles in which the batch variation changes with a change in composition. There was a significant difference between the batch variation for particle size measurements for protected variants of 2:1:1 OPHP:GMAC:EGDMA particles (P=0.03) and 4:1:3 OPHP:GMAC:EGDMA particles (P=0.04). Protected 4:3:1 OPHP:GMAC:EGDMA particles showed no significant difference in batch variation for zeta potential or particle size analysis. Protected 4:1:3 OPHP:GMAC:EGDMA particles also showed a significant batch variation for zeta potential measurements (P=0.009). Deprotected OPHP:GMAC:EGDMA showed no significant difference in batch variation when particle size or zeta potential where analysed.

Formulation	Solid Content (%)
4:1:3 OPHP: GMAC:EGDMA	7.5±0.04
2:1:1 OPHP: GMAC:EGDMA	7.9±0.05
4:3:1 OPHP: GMAC:EGDMA	7.6±0.6

Table 4-1 Solid content analysis of 4:1:3 OPHP:GMAC:EGDMA, 2:1:1 OPHP:GMAC:EGDMA and 4:3:1 OPHP:GMAC:EGDMA shell particles.

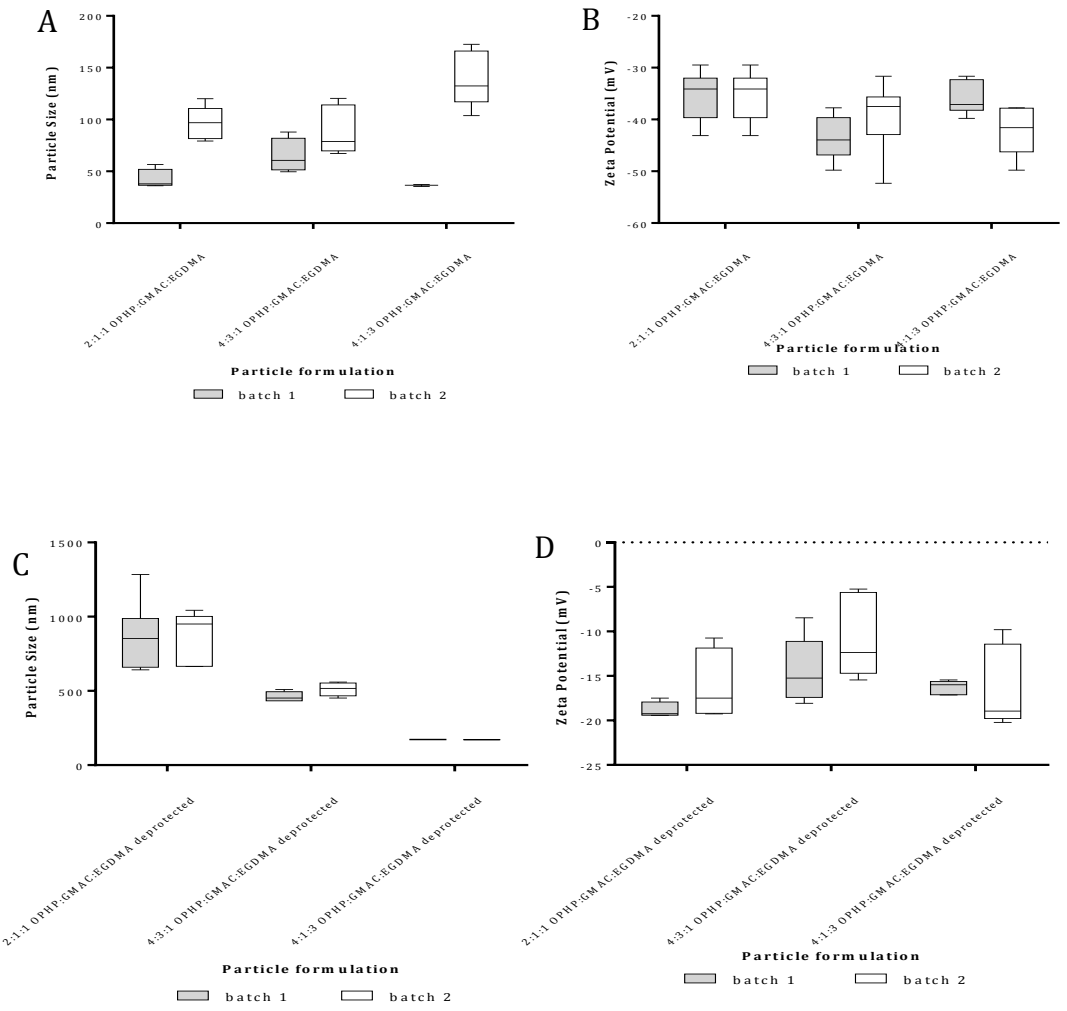

E

Formulation	Zeta Potential Before De-protection (mV)	Zeta Potential After De-protection (mV)	Particle Size Before De-protection (nm)	Particle Size After De-protection (nm)
4:1:3 OPHP: GMAC:EGDMA	-39.13±2.29	-16.28±1.76	78.37±4.83	172.09±1.17
2:1:1 OPHP: GMAC:EGDMA	-35.36±2.18	-17.23±1.78	72.18±5.59	486.59±6.74
4:3:1 OPHP: GMAC:EGDMA	-41.45±2.46	-12.53±2.12	101.03±7.5	861.22±14.09

Figure 4.2 (A) Particle size measurements from protected GMAC containing latexes. (B) Zeta potential measurements from protected GMAC containing latexes. (C) Particle size measurements from deprotected GMAC containing latexes. (D) Zeta potential measurements from deprotected GMAC containing latexes. (E) Particle size, zeta potential and solid content analysis of GMAC containing latexes. Bach variation analysed via Mann-Whitney T-Test.

TEM imaging was undertaken on 1:1 OPHP:EGDMA and 2:1:1 OPHP:GMAC:EGDMA particles. These were chosen as they showed the best performance in initial protein release studies (discussed in section 4.3). TEM imaging was used to confirm dynamic light scattering measurements and to examine particle morphology. Unfortunately TEM could only be performed upon protected OPHP:GMAC:EGDMA particles as the deprotected OPHP:GMAC:EGDMA particles showed significant aggregation and instability when imaged. This can be seen in Figure 4.3.

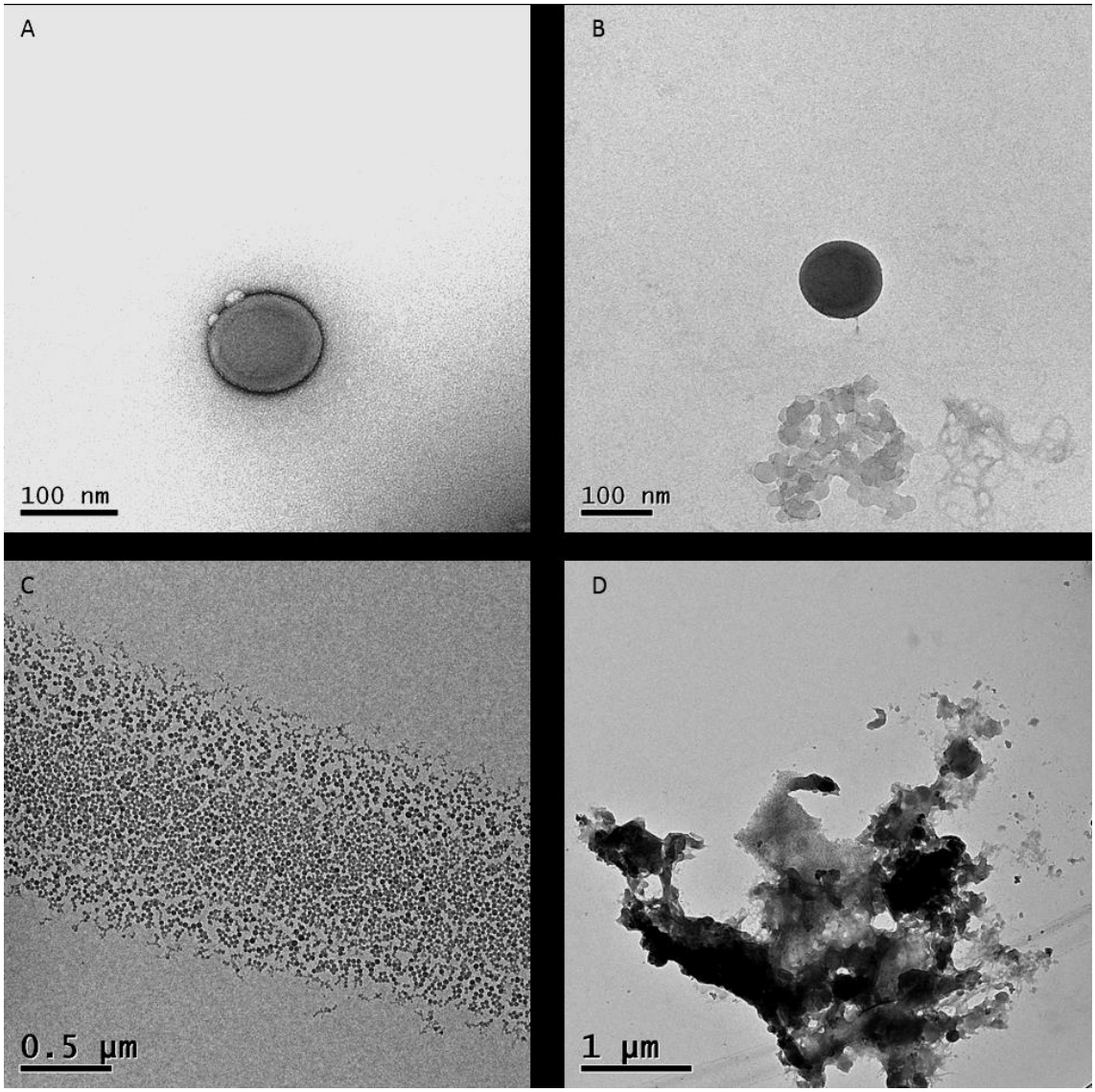

Figure 4.3 (A) TEM image of 50:50 OPHP:EGDMA. (B) TEM image of protected 50:50 OPHP:GMAC:EGDMA particle. The core shell structure can be seen on both images. Particles stained with uranyl formate. (C) TEM image of PS-co-DVB particle core. Particles stained with uranyl formate. (D) TEM image of deprotected 50:50 OPHP:GMAC:EGDMA particles. Aggregation and instability during the imaging process is seen.

4.2 *Analysis of PAMPS functionalised core-shell particles*

Particles containing L-PAMPS and B-PAMPS should bind heparin binding growth factors through the sulfonic acid groups present within the particle shell. It was hypothesised that a variation in shell architecture would affect the protein release. The L-PAMPS forms a grafted comb around the PBMA core. This makes the particle shell flexible and non-porous. Alternatively, the B-PAMPS forms a network around the PBMA [221].

Before protein studies could be carried out, the branched and L-PAMPS were washed with PBS. The particle size measurements before washing showed that there are two distinct particle sizes present in the latex sample [221]. Figure 4.4 shows the change in particle size distribution after washing. Each sample had narrow size distributions and only one particle size region is seen. This is due to the smaller particles being removed during the washing process. When the samples were centrifuged the smaller particles did not fully settle into a pellet. After several series of washings this resulted in the smaller particles being removed from the sample.

Comparison of batch variation shows that the synthesis produced materials that exhibited some batch variation when analysing the particle size and zeta potential of the latexes. There was no batch variation in L-PAMPS when measuring particle size but did show batch variation when analysed for zeta potential ($P=0.001$). B-PAMPS exhibited batch variation when analysed for particle size ($P=0.01$) but not when the zeta potential was measured.

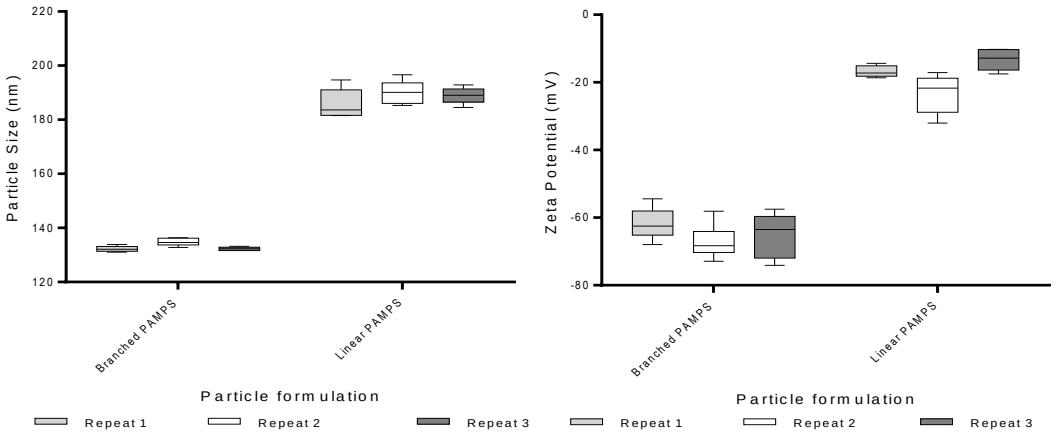

	Particle size (nm)	Zeta potential (mV)
Linear PAMPS	188.2±1.2	-17.9±1.6
Branched PAMPS	113.1±0.4	-65.5±1.3

Figure 4.4 (A) Particle size distribution of repeated particle size measurements of L-PAMPS and B-PAMPS. (B) Zeta potential distribution of repeated measurments of L-PAMPS and B-PAMPS. (C) Average particle size and zeta potential measurements of L-PAMPS and B-PAMPS. Batch variation analysed by one-way ANOVA.

4.3 *Protein release from OPHP functionalised core-shell particles*

The various ratios of phosphate to crosslinker were initially investigated for the release of VEGF. The aim was to produce a system that did not exhibit the normal burst release that is seen with similar protein delivery polymers [116].

4.3.1 Release of VEGF$_{165}$

4.3.1.1 Preliminary studies

Figure 4.5 shows the release of VEGF from 1:1 OPHP:EGDMA, 1:4 OPHP:EGDMA and 3:1 OPHP: EGDMA shells over 72 hours. All particles show the same behaviour up to 48 hours. At 72 hours the 1:3 OPHP: EGDMA and 3:1 OPHP:EGDMA release considerably more VEGF than the 1:1 particle. The 1:1 OPHP:EGDMA particles showed a more stable release profile. These particles were used for extended studies and also for comparison studies using different proteins.

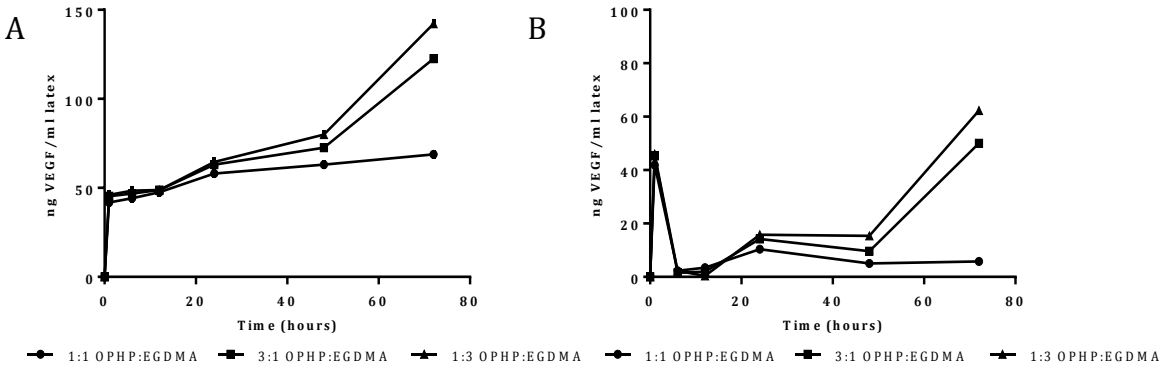

Figure 4.5 Release of VEGF from various OPHP:EGDMA shell particles . 200ng protein initially loaded onto each sample. Analysis was performed with ELISA and all samples were ran in triplicate. (A) Cumulative release of VEGF over 72 hours. (B) Instantaneous release of VEGF at each time point over 72 hours.

The release of VEGF from particles containing the various ratios of OPHP:GMAC:EGDMA was also investigated for 72 hours (Figure 4.6). From 0-12 hours the release of VEGF from each particle is very similar. After 12 hours the varying ratios of GMAC have an effect on the release profile of VEGF. The release from 4:3:1 OPHP:GMAC:EGDMA plateaued after 12 hours. Finally, the release from the 2:1:1 OPHP:GMAC:EGDMA particles is sustained over the 72 hours of the investigation. It is hypothesised that the VEGF is able to bind within the shell and is stabilised sufficiently to give a sustained release. The 2:1:1 OPHP:GMAC:EGDMA particles were chosen for further study and comparison studies with different growth factors. However, all particles show a burst release profile in the initial time points.

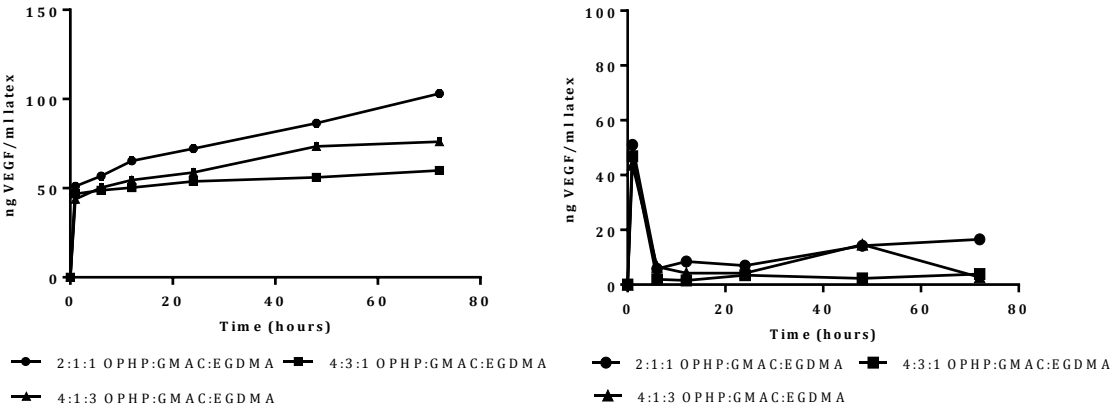

Figure 4.6 Release of VEGF from various OPHP:GMAC:EGDMA shell particles . 200ng protein initially loaded onto each sample. Analysis was performed with ELISA and all samples were ran in triplicate. (A) Cumulative release of VEGF over 72 hours. (B) Instantaneous release of VEGF at each time point over 72 hours.

4.3.1.2 31 day release studies

For the full release profile of VEGF from phosphate functionalised core-shell particles to be determined, the study was extended to 31 days. Table 4-2 shows high initial VEGF uptake for both OPHP:EGDMA and OPHP:GMAC:EGDMA particles. This would be expected as both particles contain the same quantity of functional phosphate units. However, the initial VEGF loading data must not be viewed alone. The final quantity of VEGF retrieved from the particles must also be taken into consideration when determining which particles have better stabilisation properties. Figure 4.7 shows the release of VEGF for 31 days. After 31 days approximately 69% of VEGF had been retrieved from OPHP:EGDMA particles whereas 100% VEGF had been retrieved from OPHP:GMAC:EGDMA particles. This indicates that the GMAC containing particles were better at stabilising VEGF compared to OPHP:EGDMA particles.

Particle shell	**1:1 OPHP:EGDMA**	**2:1:1 OPHP:GMAC:EGDMA**
Initial VEGF loading (%)	97.9±0.62	97.8±0.65

Table 4-2 Initial VEGF uptake from 1:1 OPHP:EGDMA and 2:1:1 OPHP:GMAC:EGDMA. VEGF loading was determined by analysis (ELISA) of the supernatant after loading protein onto the particles.

After 24 hours the release profile of OPHP:EGDMA and OPHP:GMAC:EGDMA particles began to vary significantly (RM two-way ANOVA with Tukey post hoc analysis, P=0.0018). Figure 4.7 shows that OPHP:EGDMA released VEGF in a slower sustained manner whereas VEGF release from OPHP:GMAC:EGDMA particles plateaued after 24 days. Since both particles contained the same quantity of phosphates (the unit that can bind to VEGF) the variety in release profile must be due to the shell architecture. However, when all the data are taken into consideration, OPHP:GMAC:EGDMA particles are better at stabilising VEGF than OPHP:EGDMA.

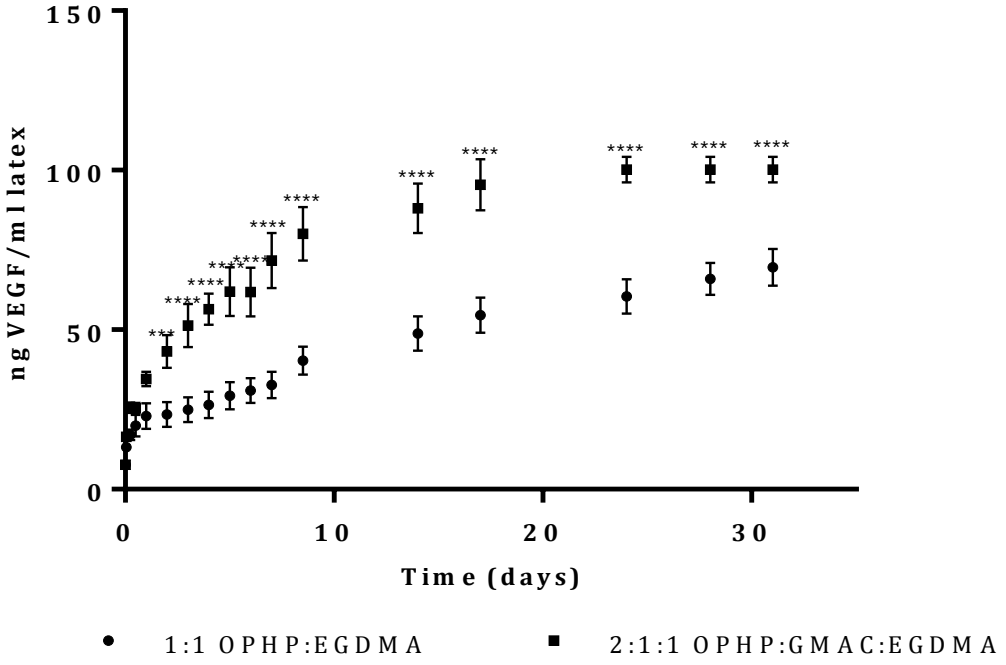

Figure 4.7 Release of VEGF over 31 days from OPHP:EGDMA and OPHP:GMAC:EGDMA particles. Particles were initially loaded with 100ng/ml VEGF solution. All samples were ran in triplicate and analysis was performed via ELISA. Data analysis was performed using RM-two-way ANOVA with Tukey post hoc analysis.

4.3.2 Release of PDGF-BB

The release profile of PDGF from 1:1 OPHP:EGDMA and 2:1:1 OPHP:GMAC:EGDMA was determined. Table 4-3 shows the initial loading onto the particles. Both OPHP:EGDMA and OPHP:GMAC:EGDMA particles show good uptake. However, as previously discussed, these data must be considered alongside the data shown in Figure 4.8. When this is taken into consideration it shows that neither particles exhibited exceptional stabilisation of PDGF. OPHP:GMAC:EGDMA particles (53.1% recovery) were significantly better at stabilising PDGF compared to OPHP:EGDMA particles (29.7% recovery).

Particle Shell	**1:1 OPHP:EGDMA**	**2:1:1 OPHP:GMAC:EGDMA**
Initial PDGF loading (%)	96.5±0.2	96.2±0.08

Table 4-3 Initial PDGF uptake of 1:1 OPHP:EGDMA and 2:1:1 OPHP:GMAC:EGDMA particles. Uptake was determined by analysis (ELISA) of the supernatant after PDGF loading.

The release of PDGF from OPHP:EGDMA and OPHP:GMAC:EGDMA particles produced similar release profiles, but significantly different quantities of protein were detected after release. Both particle compositions gave an initial burst release then began to plateau after 7 days. OPHP:GMAC:EGDMA particles stopped releasing

any significant amount of PDGF after 10 days whereas small quantities of PDGF were detected from OPHP:EGDMA particles for the full 31 days.

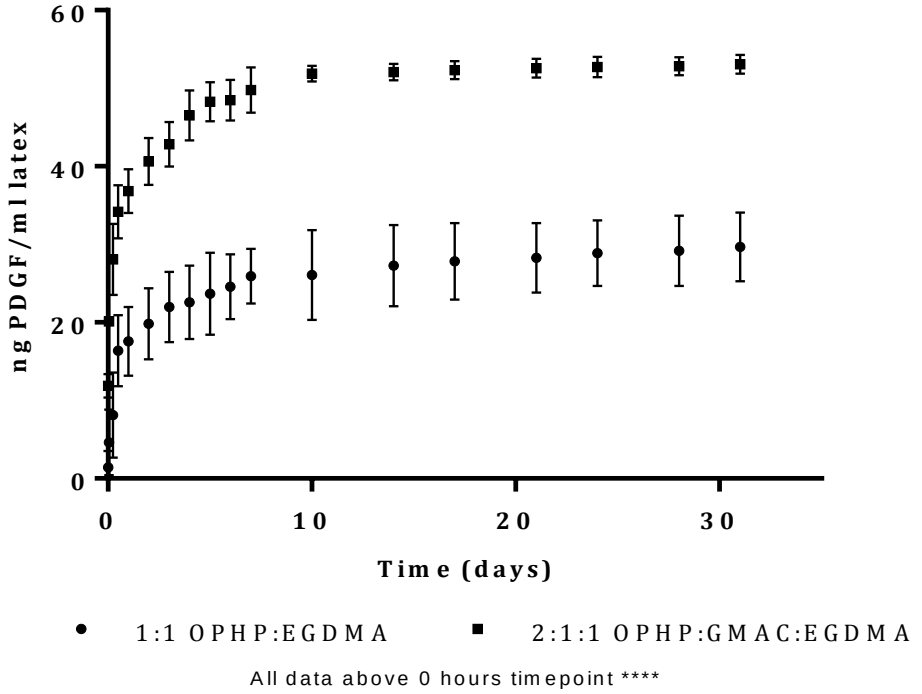

Figure 4.8 Release of PDGF over 31 days from OPHP:EGDMA and OPHP:GMAC:EGDMA particles. Particles were initially loaded with 100ng/ml PDGF solution. All samples were ran in triplicate and analysis was performed via ELISA. Data analysis was performed using RM-two-way ANOVA followed by Tukey post hoc analysis.

PDGF is smaller than VEGF (PDGF 24.4KDa compared to VEGF 38.2KDa) and this results in PDGF being released faster from OPHP:GMAC:EGDMA than OPHP:EGDMA particles. The pores of the OPHP:GMAC:EGDMA shell would not necessarily slow the release of PDGF as it would be too small for a size exclusion effect to be exerted by the GMAC shell. The pores in the OPHP:EGDMA shell are smaller than those in the OPHP:GMAC:EGDMA shell. The PDGF was able to bind deep within the OPHP:EGDMA shell, slowing the release profile.

4.3.3 Release of EGF

The release of EGF from 1:1 OPHP:EGDMA and 2:1:1 OPHP:GMAC:EGDMA particles was investigated. EGF is a small protein that does not specifically bind to heparin. It was chosen as a candidate for investigation due to its size and presence of arginine and lysine units. Table 4-4 showed good protein uptake from each of the particles. However, the data shown in Table 4-4 is not necessarily correct. The particles did

not bind a high proportion of the protein. Instead, the protein was not stabilised and was unable to be detected by ELISA, as shown in Figure 4.9. This gives the initial impression that there is no EGF left in the supernatant after protein binding.

Particle Shell	1:1 OPHP:EGDMA	2:1:1 OPHP:GMAC:EGDMA
Initial EGF loading (%)	99.6±1.92	99.6±0.97

Table 4-4 Initial EGF uptake of 1:1 OPHP:EGDMA and 2:1:1 OPHP:GMAC:EGDMA particles. Uptake was determined by analysis of the supernatant after EGF loading.

The release profile of EGF from 1:1 OPHP:EGDMA and 2:1:1 OPHP:GMAC:EGDMA is almost identical. The release profile is steady over 24 hours but very small quantities of protein are released. This could be because the protein was not stabilised sufficiently by the particles. Once the protein was degraded it could no longer be detected by ELISA. This would explain why there was such small protein recovery from OPHP and GMAC particles.

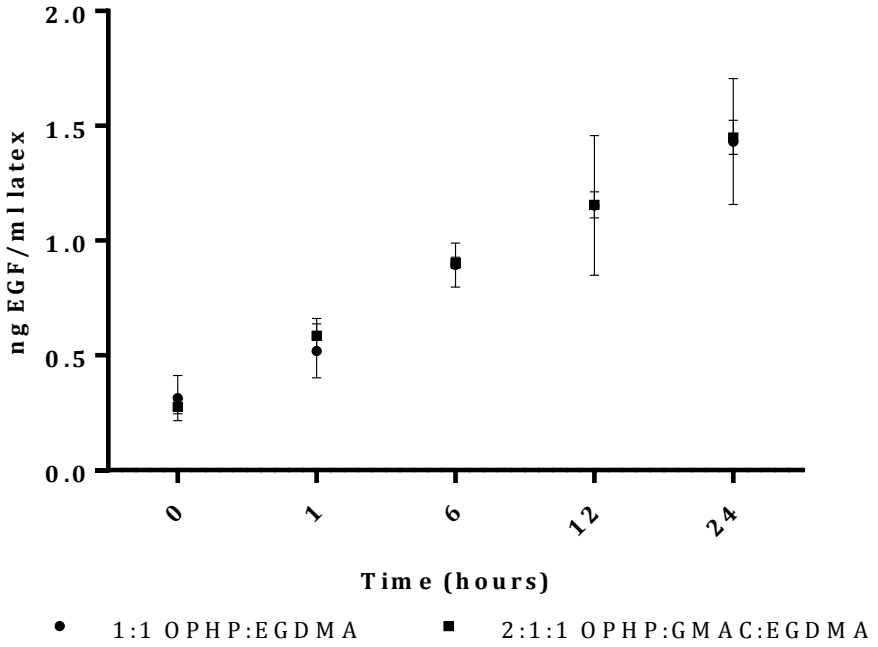

Figure 4.9 Release of EGF over 24 hours from OPHP:EGDMA and OPHP:GMAC:EGDMA particles. Particles were initially loaded with 100ng/ml EGF solution. All samples were ran in triplicate and analysis was performed via ELISA. Data analysis was performed using RM-two-way ANOVA followed by Tukey post hoc analysis.

Figure 4.9 shows that the particle shell architecture had no effect on the release of EGF. This was because EGF is extremely small compared to the other proteins (EGF 6.3kDa, PDGF 24.3kDa and VEGF 38.2kDa). The large pores in OPHP:GMAC:EGDMA shell and small pores in OPHP:EGDMA shell had no effect on the release of EGF as it

was too small to have significant size exclusion effect on release. This resulted in a fast release with little to no stabilisation.

4.4 *Protein release from PAMPS functionalised core-shell particles*

4.4.1 Release of $VEGF_{165}$

The binding and subsequent release of VEGF was studied over 31 days. The quantity of PAMPS and the architecture of the particle shell were varied. The release profile indicates that the quantity of PAMPS plays a less significant role in the release of VEGF than the shell architecture (see Figure 4.10). This is due to the large excess of potential binding points on the particles. This means that even the lower quantity of PAMPS included in the particles still has many free sulfonic acid groups that VEGF could bind to. Increasing the available sulfonic acid groups, therefore, does not affect the ability to bind VEGF and the subsequent release profile.

The initial protein uptake was high for L-PAMPS and B-PAMPS (Table 4-5). Branched particle data initially indicated that they were able to bind slightly higher amounts of VEGF than linear particles. However, when viewed in combination with the final detectable protein shown in Figure 4.10 this may not be the case. Any denatured protein cannot be detected by the ELISA protocol so if the branched particles could not stabilise the VEGF sufficiently, this may give a misleading result for initial protein uptake.

Particle shell	**1g Linear PAMPS**	**4g Linear PAMPS**	**1g Branched PAMPS**	**4g Branched PAMPS**
Initial VEGF loading (%)	97.7±0.27	98.7±0.3	99.7±0.3	99.7±0.24

Table 4-5 Initial uptake of VEGF from a solution containing VEGF in PBS with 0.1 % BSA bound to PAMPS coated latex particles. Protein analysis carried out via ELISA.

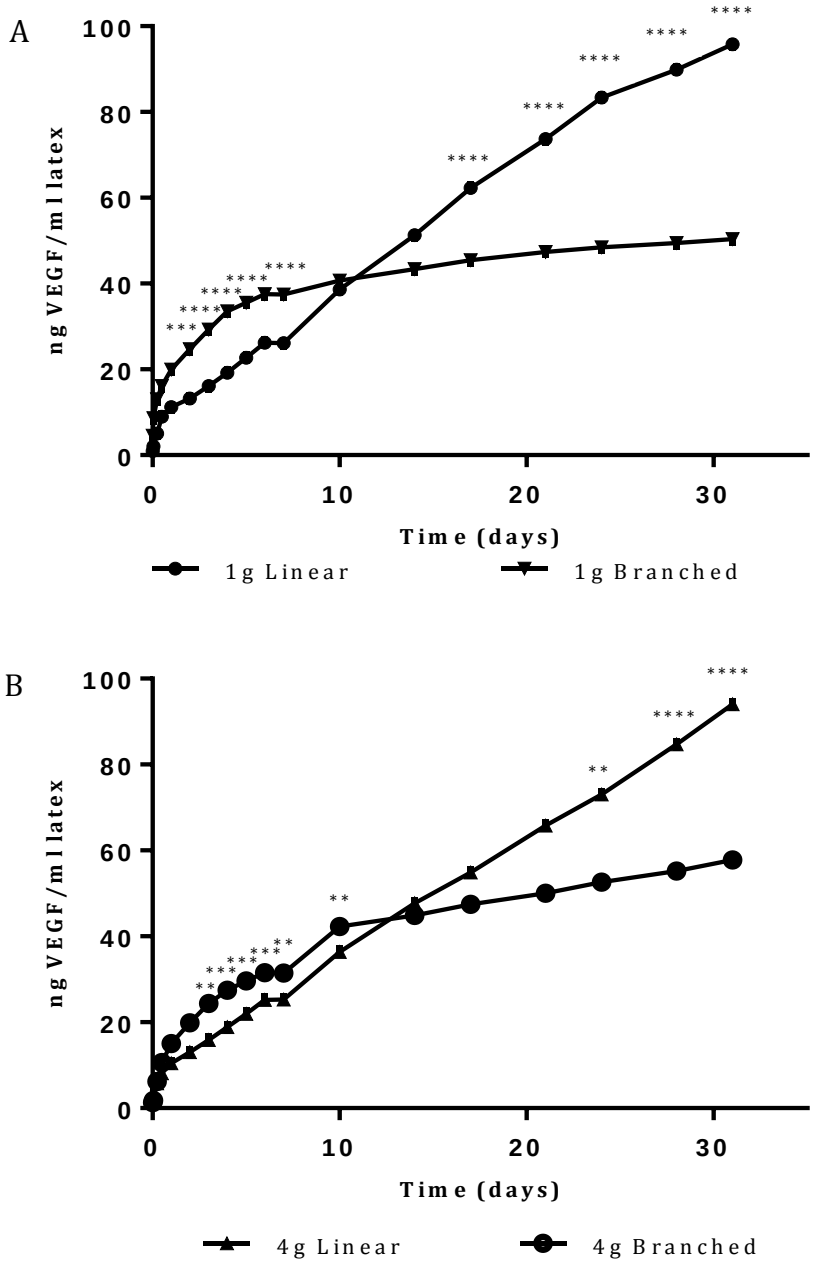

Figure 4.10 Release of 100ng/ml VEGF from particles containing either L- or B-PAMPS. (A) 1g PAMPS surrounding a PBMA core. (B) 4g PAMPS surrounding a PBMA core. All samples were studied in triplicate and analysed by ELISA. RM-two-way ANOVA with Tukey post hoc analysis was used.

The general release profiles are similar for both quantities of PAMPS. The L-PAMPS shows a release profile with sustained release up to 31 days and no burst release phase was seen in the initial time points. The B-PAMPS shows initial release that begins to slow or plateau after 9-10 days. This could be due to the protein size, PAMPS shell architecture and shell flexibility. The recombinant VEGF used has a molecular weight of 38.2 KDa. It can be reasoned that the L-PAMPS shell is flexible and can accommodate a protein of this size. This could stabilises the protein (in a similar manner as HS) whilst it is bound to the PAMPS and slows the release by

binding to many sulfonic acid groups as it moved through the particle shell. This leads to a high binding and stabilisation, followed by a slow sustained release that yields approximately 95% for 1g L-PAMPS particles and 94% for 4g L-PAMPS after 31 days. In comparison, the branched particle shell can be thought of as a rigid porous structure. If the VEGF is not of the correct size to fit within these pores, the protein can only bind to the sulfonic acid groups available on the particle surface. This would reduce the stabilisation of protein, reducing the ability of detection once released and would produce a particle that exhibits a burst release profile. This is what can be seen with both 1g and 4g B-PAMPS. Due to reduced protein stabilisation, after 31 days only approximately 50% for 1g B-PAMPS and 58% for 4g B-PAMPS of the initial VEGF was detected.

4.4.2 Release of PDGF-BB

The release of PDGF was also studied over 31 days. As discussed in section 4.4.1, the particle architecture played a greater role in tailoring the release profile than the quantity of PAMPS included in the particle shell. The initial uptake (seen in Table 4-6) indicates that L-PAMPS has a marginally better initial protein uptake when compared to B- PAMPS. However, when the final protein recovery data (Figure 4.11) are taken into consideration, the initial uptake data may not be an accurate representation of protein binding and stabilisation.

Particle shell	1g Linear PAMPS	4g Linear PAMPS	1g Branched PAMPS	4g Branched PAMPS
Initial PDGF loading (%)	99.5±0.24	99.0±0.25	98.7±0.47	96.9±0.28

Table 4-6 Initial uptake of PDGF from a solution containing PDGF with 0.1 % BSA bound to PAMPS coated latex particles. Protein analysis carried out via ELISA.

PDGF is a relatively small protein of 24.4 KDa. The size of PDGF compared to VEGF affects how the PAMPS shell can stabilise and release the protein. Both the 1g and 4g PAMPS particles showed that B-PAMPS releases more detectable PDGF over 31 days then L-PAMPS.

Two effects could be occurring with the PDGF release data. The first is that the branched porous shell allows the PDGF to bind within the particle. This would produce better stabilisation of the PDGF over the study time, allowing for more PDGF to be detected at each time point. The linear shell cannot stabilise the protein over long periods of time, so less protein is detected at each time point.

Alternatively, PDGF is well stabilised and was released extremely slowly by both the L-PAMPS and B-PAMPS shells. However, the data indicated that the first case is the most likely in this example. This is because as the quantity of B-PAMPS in the shell was increased from 1g to 4g, slightly more protein was detectable after 31 days (30.5ng to 36.3ng PDGF). This provides evidence that more available PAMPS increases the ability to stabilise more PDGF, hence more is detected at final time points. Overall, the protein retrieval is low after 31 days (between 10.8-14.3% for L-PAMPS and 30.5-36.3% for B-PAMPS).

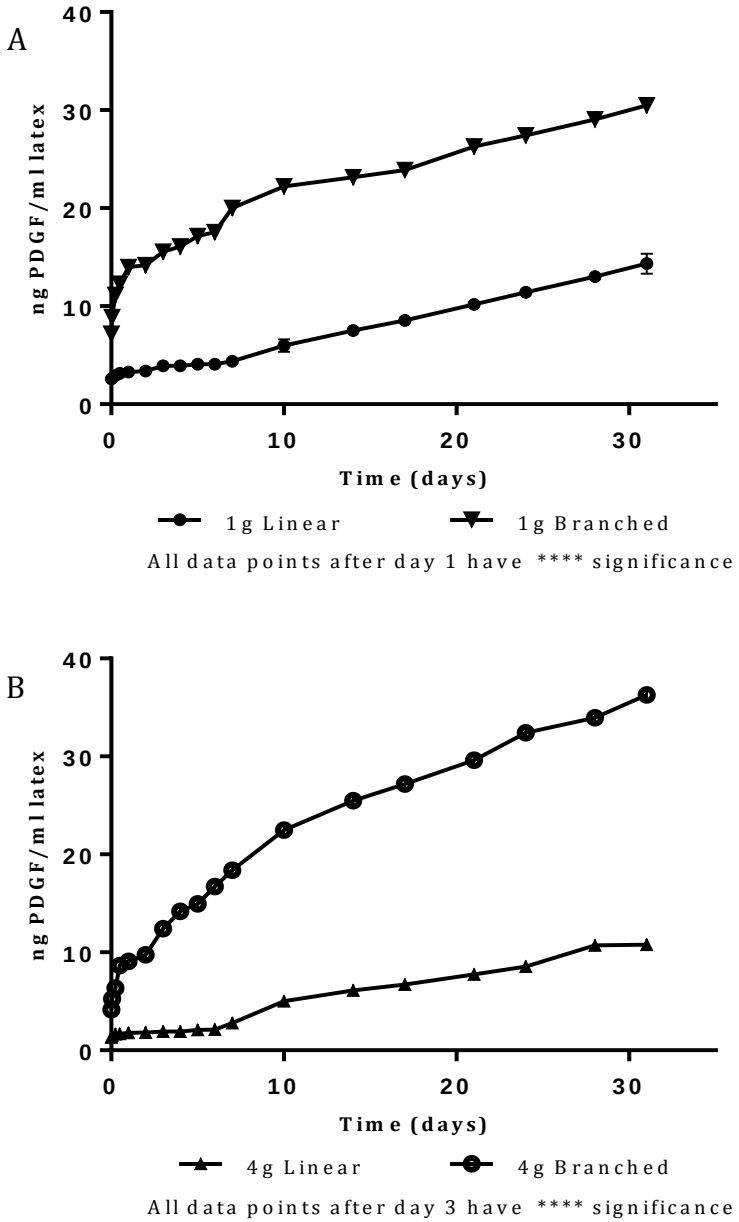

Figure 4.11 Release of 100ng/ml PDGF from particles containing either L- or B-PAMPS. (A)1g PAMPS surrounding a PBMA core. (B) 4g PAMPS surrounding a PBMA core. All samples were studied in triplicate and analysed by ELISA. RM-two-way ANOVA with Tukey post hoc analysis was performed.

4.4.3 Release of EGF

EGF was released from linear and branched PAMPS over 24 hours. The initial EGF loading shows high percentage of protein uptake. However, as previously discussed, this is not an accurate representation of what was occurring. When viewed with Figure 4.12 it shows that the EGF was not sufficiently stabilised by the 1g PAMPS particles, leading to little or no detection in the supernatant.

Particle shell	Linear PAMPS	Branched PAMPS
Initial EGF loading (%)	81.9±2.98	99.6±0.64

Table 4-7 Initial uptake of EGF from a solution containing EGF with 0.1 % BSA bound to PAMPS coated latex particles. Protein analysis carried out via ELISA.

The release profile of EGF from L-PAMPS and B-PAMPS is shown in Figure 4.12. There is no significant difference between the release from L-PAMPS or B-PAMPS. Both B-PAMPS and L-PAMPS showed a plateau region beginning to form after 12 hours. The linear particles showed a slight increase in the quantity of released EGF compared to branched particles. However, the quantity of protein released from each was extremely small and would not be practically useful.

As previously discussed, EGF is not a heparin binding growth factor but does have characteristics similar to VEGF and PDGF. When compared to VEGF and PDGF, EGF is a significantly smaller protein. The pores produced in the B-PAMPS shell have no influence on the release of EGF, as the protein is too small to have any significant electrostatic interactions as it is released. This resulted in poor initial binding, reduced stabilisation of the protein and finally very little intact protein release from the particles.

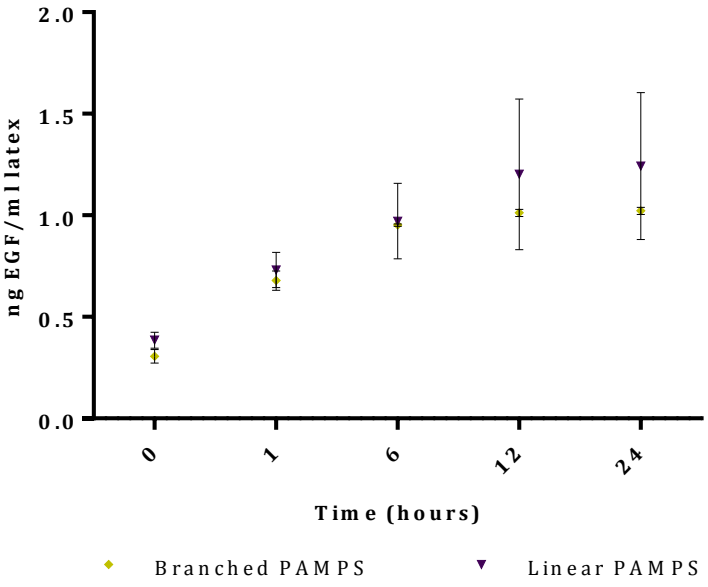

Figure 4.12 Release of EGF from 1g L- and B-PAMPS over 24 hours. Samples were loaded with 100ng/ml EGF and analysed in triplicate via ELISA. Statistical analysis was doen using RM-two-way ANOVA with Tukey post hoc analysis.

4.5 *Analysis of NVP-co-DEGBAC hydrogels*

PVP-co-DEGBAC hydrogels with embedded core-shell polymer particles can be synthesised by thermal and UV curing. The four types of core-shell particles embedded in the gel shows some variation in the water content analysis.

Initial formulation experiments were completed with thermally cured hydrogels. The percentage of latex embedded was varied from 5% to 40% latex. The smaller weight % of particles had no detrimental effect on the composition of the latex and the larger weight % prevented the hydrogel from successfully curing. The quantities stated in Table 3-4 produced the easiest to handle hydrogels. Thermally curing the hydrogels highlighted two problems. The first was the slow production rate due to the need for an overnight cure. The second was small nitrogen bubbles forming in the gel upon curing. This was due to the nitrogen release from the azo-initiator. Even with thorough degassing this problem was maintained. UV curing was chosen to be the main method of curing the hydrogels. All protein experiments were completed using UV cured hydrogels. This is because there is a faster synthesis rate with UV cured hydrogels and they produced a more consistent gel (no bubbles formed). With a medium to low percentage of latex included in the hydrogel, the polymer could still cure using UV, indicating that the solid particles were not significantly negatively affecting radical production and curing efficiency. All hydrogels were extremely brittle without the inclusion of propan-2-ol as a solvent. Upon adding solvent the hydrogels were softer and could be cut using a cork borer.

Table 4-8 shows the water content of each hydrogel. They are all within the region of 81-88% water content. These hydrogels are designed as wound dressing and a high water content is a desirable feature [241]. The PVP-co-DEGBAC control hydrogel and those containing L-PAMPS, OPHP and GMAC all have very similar water contents. This would be expected as the percentage of components in each gel is very similar. The PVP-co-DEGBAC hydrogel containing B-PAMPS has a higher water content. This hydrogel has the same ratios of monomers as the PVP-co-DEGBAC L PAMPS gel. This indicated that the increase in water content is due to the B-PAMPS present on the surface of the core shell particles embedded within the hydrogel. Previous studies have shown that as the molar ratio of PAMPS is increased

this can increase the polymer swelling in water [261]. The shell on the B-PAMPS particles is more porous and has the ability to hold slightly more water than the L-PAMPS shell.

Material	Water content (%)
PVP-co-DEGBAC control	85.37 ± 1.2
PVP-co-DEGBAC B PAMPS	88.68 ± 0.9
PVP-co-DEGBAC L PAMPS	86.35 ± 0.66
PVP-co-DEGBAC OPHP	86.56 ± 0.87
PVP-co-DEGBAC GMAC	86.21 ±2.26

Table 4-8 Water content (%) of UV cured hydrogel controls and hydrogels containing core shell polymer particles.

Figure 4.13 shows the SEM images taken of the surface of the gel and the edge of the gel. The control material and those containing particles both had a ridged surface; this is from the drying process. When water was lost from the hydrogel the polymer collapsed in on itself forming a material with a ridged appearance. The edges of the hydrogels show a fractured polymer. This is because the material becomes brittle when dried. Debris is also present around the edges of the hydrogels. The details of the internal structure may be lost when the gel is dried.

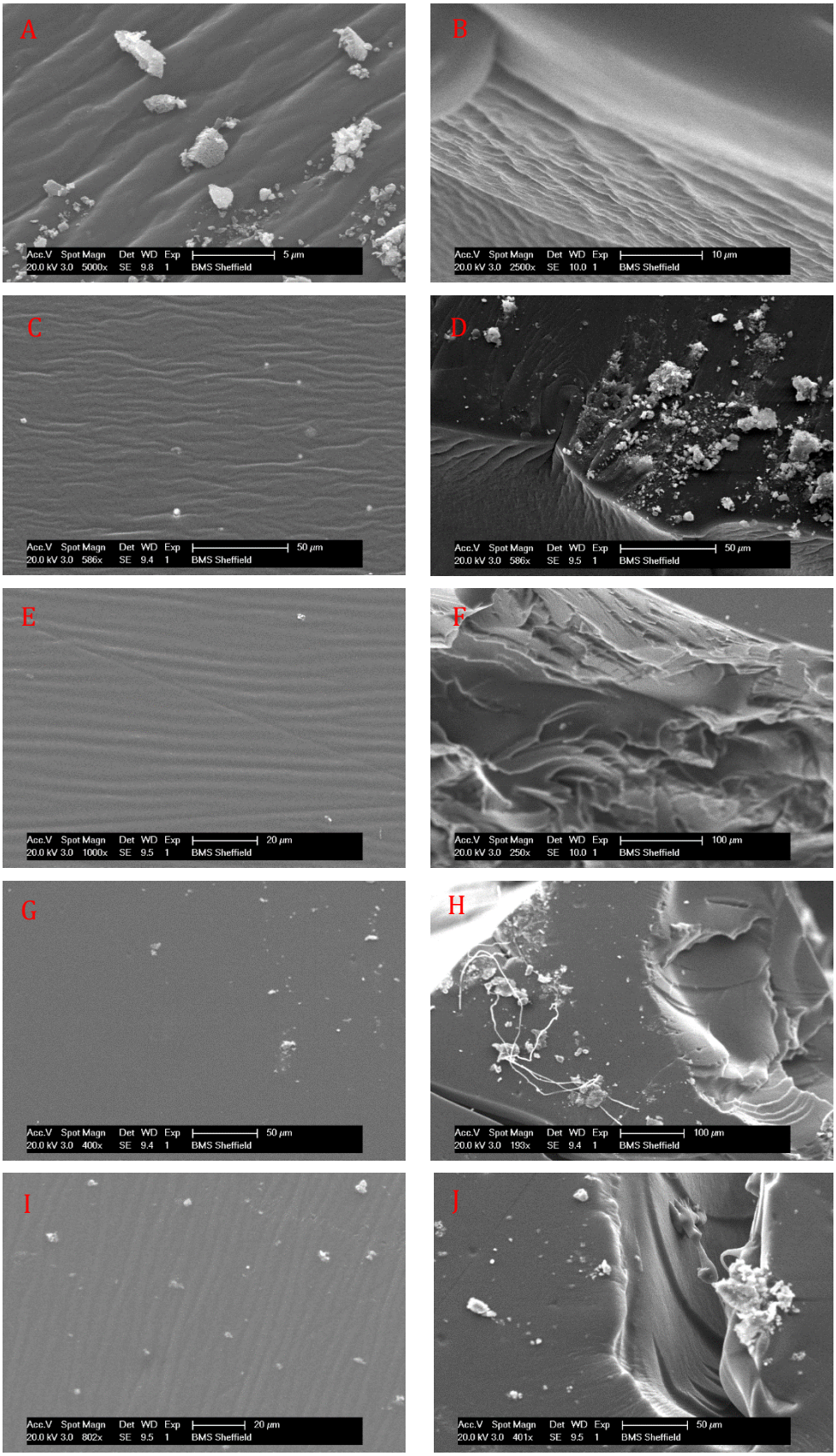

Figure 4.13 SEM images of PVP-co-DEGBAC hydrogels containing the core shell particles. (A) surface of control (B) edge of control (C) surface of OPHP:EGDMA particle containing polymer (D) edge of OPHP:EGDMA particle containing polymer (E) surface of OPHP:GMAC:EGDMA particle containing polymer (F) edge of OPHP:GMAC:EGDMA particle containing polymer (G) surface of L-PAMPS particle containing polymer (H) edge of L-PAMPS particle containing polymer (I) surface of B-PAMPS particle containing polymer (J) edge of B-PAMPS containing polymer.

4.6 *Protein release from particles embedded in NVP-co-DEGBAC hydrogels*

The release of VEGF, PDGF and EGF over 3 days was investigated. The release profile would be expected to be similar to that determined in chapters 3 and 4. The PVP-co-DEGBAC control gel should not bind any significant quantities of protein because there is not a binding target on the surface of the hydrogel.

4.6.1 Release of VEGF

Figure 4.14 shows VEGF release from PVP-co-DEGBAC control gels and hydrogels with either 1:1 OPHP:EGDMA, 2:1:1 OPHP:GMAC:EGDMA, L-PAMPS or B-PAMPS. The release from the control, 1:1 OPHP:EGDMA and 2:1:1 OPHP:GMAC:EGDMA showed no significant difference in release. VEGF was initially released in a burst between 0 and 1 hour. After this point the release plateaus and no more VEGF is released.

The release profile from L-PAMPS embedded in PVP-co-DEGBAC gels closely matched those of the particle alone. The release profile is linear and significantly differs from the control after 1 hour. The release profiles of B-PAMPS particles are similar to that of the L-PAMPS particles. The release profile from B-PAMPS embedded in PVP-co-DEGBAC gels closely matched those of the particle alone up to the same time point.

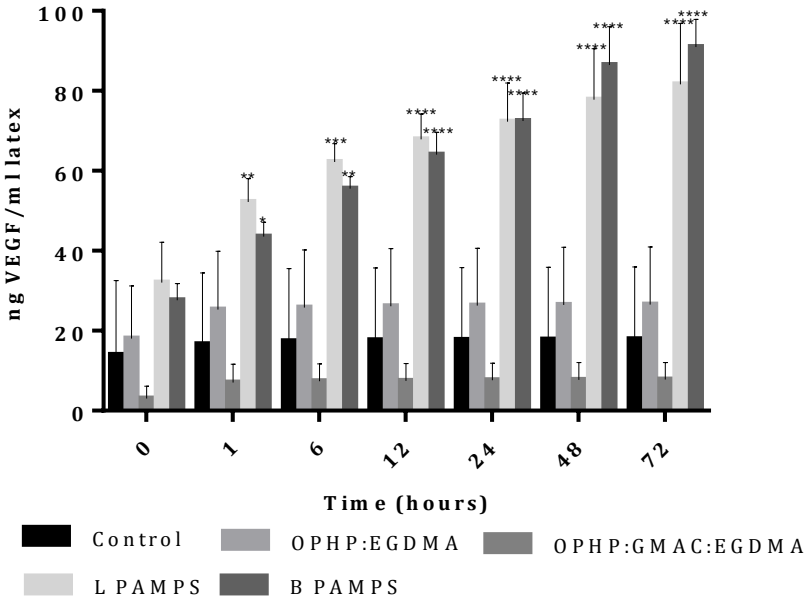

Figure 4.14 Release of VEGF from 1:1 OPHP:EGDMA, 2:1:1 OPHP:GMAC:EGDMA, B-PAMPS and L-PAMPS particles embedded in PVP-co-DEGBAC hydrogel. The control is PVP-co-DEGBAC hydrogel with no embedded particles. Two-way ANOVA with TUKEY post-hoc analysis was performed

4.6.2 Release of PDGF

Figure 4.15 shows the release of PDGF from PVP-co-DEGBAC control hydrogels and hydrogels with 1:1 OPHP:EGDMA, 2:1:1 OPHP:GMAC:EGDMA, L-PAMPS and B-PAMPS particles embedded in the gel. The control hydrogel, 1:1 OPHP:EGDMA and 2:1:1 OPHP:GMAC:EGDMA show no significant difference in the release profile of PDGF. There was a large percentage of the PDGF washed off the hydrogels at time point 0 (between 40-60% of the protein loaded). After this there was a small burst release between time point 0 and 1 hour. The release profile of PDGF from 1:1 OPHP:EGDMA and 2:1:1 OPHP:GMAC:EGDMA particles without the hydrogel showed protein released at each time point up to 72 hours.

L-PAMPS and B-PAMPS show some difference in release profile compared to the control. They are both lower than the control and show little to no release over the 72 hours. L-PAMPS hydrogels show only very small amounts of protein detected at each time point. There is approximated 30% of the loaded protein detected at time point 0 from the B-PAMPS hydrogel and this does not vary over the course of 72 hours. This suggest that neither the L-PAMPS or B-PAMPS are stabilising the PDGF enough for degradation to be prevented and the protein to be detectable. The release profiles differ considerably to the data from the particles with no hydrogel.

Over the same time period studied by the hydrogel experiment, both L-PAMPS and B-PAMPS showed cumulative release of PDGF. L-PAMPS only released small portions of PDGF, however, more PDGF was released with the particles alone than those embedded in hydrogels. B-PAMPS released larger portions of PDGF in a relatively linear fashion.

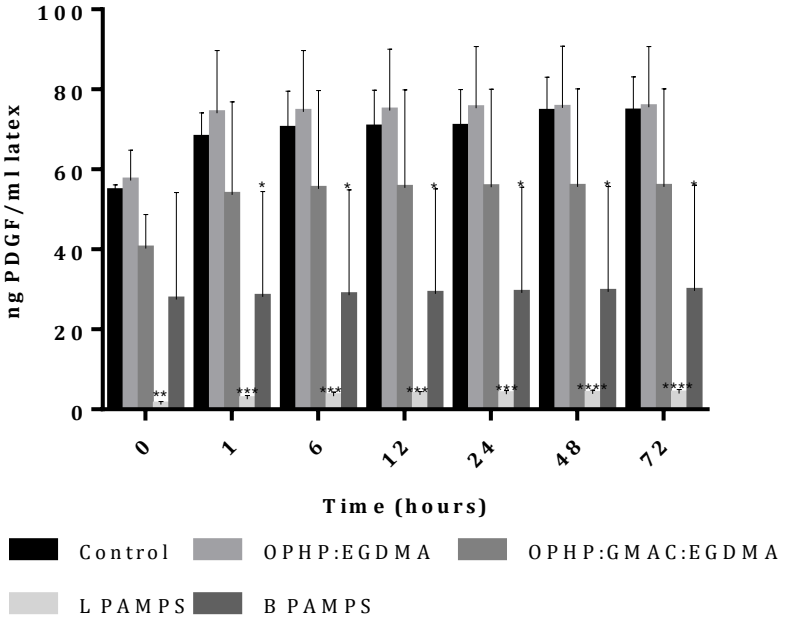

Figure 4.15 Release of PDGF from 1:1 OPHP:EGDMA, 2:1:1 OPHP:GMAC:EGDMA, B-PAMPS and L-PAMPS particles embedded in PVP-co-DEGBAC hydrogel. The control is PVP-co-DEGBAC hydrogel with no embedded particles. Two-way ANOVA with TUKEY post-hoc analysis was performed

4.6.3 Release of EGF

Figure 4.16 shows the release profile of EGF from PVP-co-DEGBAC control hydrogels and hydrogels with 1:1 OPHP:EGDMA, 2:1:1 OPHP:GMAC:EGDMA, L-PAMPS and B-PAMPS particles embedded in the gel. There is no significant difference between the control and any gels containing particles. The protein recovery is low and the release profile is similar to that of the particles with no hydrogel. Due to the release profile of the particle containing hydrogels being so similar to that of the control, this suggests that the EGF is not sufficiently electrostatically bound to the negative charges present on the particles to stabilise the protein. This results in small quantities being detected (between 2.1-3.9% proteins recovered after 72 hours) and there being no difference between charged particles and a neutral hydrogel.

The overall efficiency of binding and release of all proteins from each material is reduced or equal to that of the particles alone. This is due to the hydrogel reducing the functionality of the particles and the availability of phosphate and sulphonic acid groups leading to a reduction in protein binding, stability and release. The behaviour of the particles within the gel is not yet fully understood.

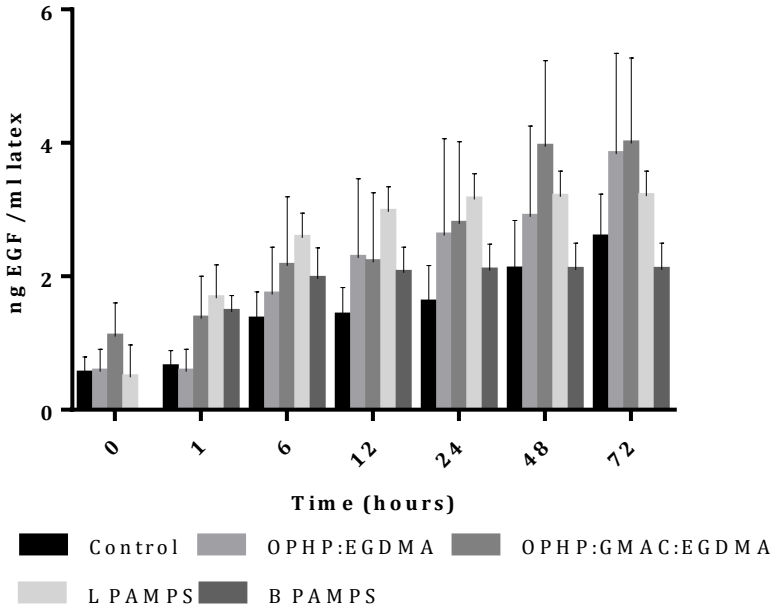

Figure 4.16 Release of EGF from 1:1 OPHP:EGDMA, 2:1:1 OPHP:GMAC:EGDMA, B-PAMPS and L-PAMPS particles embedded in PVP-co-DEGBAC hydrogel. The control is PVP-co-DEGBAC hydrogel with no embedded particles. Two-way ANOVA with TUKEY post-hoc analysis was performed

4.7 *Synthesis and analysis of acryloxyethyl thiocarbamoyl rhodamine B labelled particles*

The aim was to produce fluorescent particles that could be used to track particle movement *in vivo*. Acryloxyethyl thiocarbamoyl rhodamine B was successfully incorporated into four different formulations. However, the long term stability was poor resulting in aggregation and coagulation. This reduced the practicality of the material.

4.7.1 Synthesis of acryloxyethyl thiocarbamoyl rhodamine B labelled particles

The synthesis of acryloxyethyl thiocarbamoyl rhodamine B labelled particles was attempted using a variety of methods. To begin with the fluorescent dye was added

to the shell of PS-co-DVB core poly (OPHP-co-EGDMA) shell latexes. This lead to significant coagulation after 16-18 hours at 4^{o}C. This was deemed to be because the positive charge on the acryloxyethyl thiocarbamoyl rhodamine B was destabilising the latex, acting as a salt. Hence for the syntheses described the acryloxyethyl thiocarbamoyl rhodamine B was added to the PS-co-DVB core and poly (OPHP-co-EGDMA) shell and PS-co-DVB core poly(OPHP-co-EGDMA-co-GMAC) shell added after incorporation of acryloxyethyl thiocarbamoyl rhodamine B. The second reaction was completed in a continuous process and the remaining acryloxyethyl thiocarbamoyl rhodamine B core was not isolated from the reaction mixture. Therefore, it was assumed that although the majority of the label was in the particle core, there was a possibility that the label was also present in the particle shell.

The synthesis of both L PAMPS and B PAMPS stabilised PBMA particles was attempted using the equivalent of 1g PAMPS. Initially these latexes appeared stable, however, after 3 days the latexes coagulated. The quantity of PAMPS was too low to act as a sufficient surfactant for the BMA core when acryloxyethyl thiocarbamoyl rhodamine B was added to the system. A larger quantity (equivalent to 4g) of both L-PAMPS and B-PAMPS was used for the synthesis. This remained visually stable for several weeks at 4^{o}C. Due to the one-step method used to synthesise PAMPS shell particles, the exact location of acryloxyethyl thiocarbamoyl rhodamine B cannot be determined. It will be incorporated in both the shell and core of the particle.

All particles were unstable if left in the original reaction mixture without dialysis. Dialysis was carried out at 4^{o}C straight after completion of the reaction. As the latex was dialysed some of the acryloxyethyl thiocarbamoyl rhodamine B label was being washed out of the solution. This occurred until 3-4 cycles of dialysis had been completed. After this the label could no longer be seen in the wash solutions. The instability of the particles when un-dialysed and the obvious washing out of some label indicated that even at 0.1% label, not all was incorporated into the polymer. If free label was present in the reaction mixture it would destabilise the particles because rhodamine B contains a positive charge and the particles contain a negative change.

4.7.2 Analysis by dynamic light scattering, zeta potential measurements and solid content analysis

Dynamic light scattering showed that the particles containing the label have a relatively uniform size and similar size distribution to those with no label [221]. The PS-co-DVB core was considerably larger than the core with no acryloxyethyl thiocarbamoyl rhodamine B (see Figure 4.1). The size of 1:1 OPHP:EGDMA core-shell system was also increased compared to those that did not contain a label in the core (Figure 4.1). This size increase indicates that the label has been polymerised into the particle [262]. Zeta potential measurements (Table 4-9) show all particles to be stable and contain a negative charge. The solid content is also in the expected region.

Formulation	Particle Size (nm)	Zeta Potential (mV)	Solid Content (%)
PS-co-DVB core	121.9 ± 1.0	-37.4 ± 1.5	12.9 ± 0.2
1:1 OPHP:EGDMA	265.3 ± 3.2	-44.9 ± 1.3	10.2 ± 0.7
2:1:1 OPHP:GMAC:EGDMA	See Table 4-10	See Table 4-10	See Table 4-10
Linear PAMPS	149.0 ± 1.0	-45.3 ± 1.6	16.6 ± 0.1
Branched PAMPS	112.2 ± 1.8	-47.3 ± 2.1	14.8 ± 0.4

Table 4-9 Particle size, zeta potential and solid content analysis of core shell particles synthesised with acryloxyethyl thiocarbamoyl rhodamine B. All samples ran in triplicate. Data shows mean ± SE.

2:1:1 OPHP:GMAC:EGDMA particles behaved differently to the others when acryloxyethyl thiocarbamoyl rhodamine B label was incorporated in the polymerisation. Table 4-10 shows the values for particle size, zeta potential and solid contents of protected and de-protected particles. The particle size of 2:1:1 OPHP:GMAC:EGDMA particles containing a label is smaller than that of the particles with no label even though the core is larger with a label (see Figure 4.2) for comparison with no label). One reason for this may be that the presence of acryloxyethyl thiocarbamoyl rhodamine B is retarding the polymerisation in both the core and the shell. It is well documented that fluorescent labels can retard polymerisation [234]. If the polymerisation of the core is not complete before the shell monomers are added the overall particle size will be smaller than anticipated. This is potentially what is occurring with the rhodamine B labelled GMAC polymers.

The particle size increases as expected upon de-protection therefore the shell is present on the particle. The lower than anticipated solid content also indicates that complete monomer conversion is not occurring. The OPHP:GMAC:EGDMA shell is less stable than OPHP:EGDMA shell (as indicated by zeta potential measurements). The incomplete particle core will have less of an obvious effect on the particle size since the more stable OPHP:EGDMA shell is able to accommodate the incorporation of a small quantity of acryloxyethyl thiocarbamoyl rhodamine B. This will destabilise the shell to some degree and this can be seen by comparing zeta potential measurements shown in Figure 4.1 (no label) and Table 4-9 (containing acryloxyethyl thiocarbamoyl rhodamine B). The OPHP:GMAC:EGDMA shell is less stable and cannot incorporate acryloxyethyl thiocarbamoyl rhodamine B without significant colloid disruption, hence a smaller particle is formed with a lower solid content.

	Protected			**De-protected**		
Formulation	**Particle Size (nm)**	**Zeta Potential (mV)**	**Solid Content (%)**	**Particle Size (nm)**	**Zeta Potential (mV)**	**Solid Content (%)**
2:1:1 OPHP:GMAC:EGDMA	56.3 ± 0.9	-41.5 ± 2.1	8.1 ± 0.1	314.8 ± 6.9	-35.2 ± 1.7	3.6 ± 1.3

Table 4-10 Particle size, zeta potential and solid content analysis of GMAC containing core shell particles synthesised with acryloxyethyl thiocarbamoyl rhodamine B before and after the deprotection of GMAC. All samples ran in triplicate. Data shows mean ± SE.

4.7.3 Cell culture and endocytosis of particles

Labelling of particles would enable them to be tracked when used in bio-assays *in vitro* and *in vivo.* First, it must be determined if cells envelop the labelled particles. Initial experiments resulted in problems when washing the cells and removing residual particles. This resulted in mechanical removal of cells in the centre of each well plate. Gentle washing was not always sufficient to remove any particles that had settled on the surface of the well plate and some settled particles could be seen. Figure 4.17 shows the result of too much or too little washing. By removing any

particles that are within the media the only particles visible should be those taken up by cells.

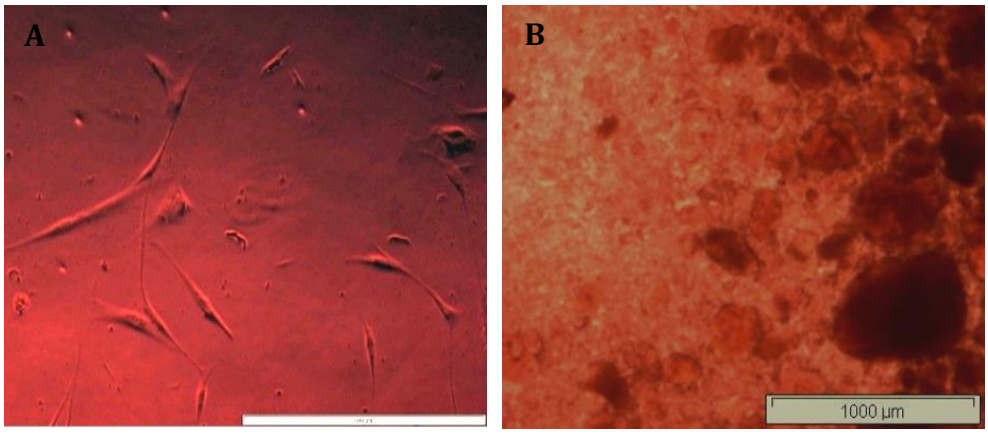

Figure 4.17 40000 NHDF seeded onto 24 well plates with 250 µl OPHP:EGDMA shell fluorescent particles. (A) Imaged after heavy washing of surface to remove particles. Particle remnants and low cell count can be seen. (B) After removing particles by not washing surface. Scale bar 1000µm.

Figure 4.17 also shows the effect of salt on the particles. For the cells to be able to survive the particles must be re-suspended in PBS followed by DMEM. This was shown to significantly de-stabilise OPHP:EGDMA and OPHP:GMAC:EGDMA particles. This resulted in the particles aggregating together, preventing cell uptake and limiting further use of the materials. L-PAMPS and B-PAMPS particles containing a label showed a small amount of aggregation in DMEM. However, the aggregation was considerable enough to hind any further use of the fluorescent particles.

4.8 *Protein degradation and analysis by alternative techniques*

Gel electrophoresis and mass spectrometry was used to determine if they are suitable analytical techniques for the release of proteins from negatively charged core-shell particles. The degradation of proteins was also investigated. Heparin was used as a comparison for the release of VEGF as VEGF binds to heparin when naturally released in the body.

Gel electrophoresis with silver staining showed little difference between pure VEGF or PDGF and degraded VEGF or PDGF. The VEGF gel shows a marker for VEGF just higher that the marker for 37 KDa. This would be expected as the molecular weight of VEGF studies is 38.2 KDa. From visual inspection of the gel, the VEGF band is the

same in both the degraded and non-degraded proteins. There is also a band present around the 25 KDa mark. This is stronger stained and thicker in the degraded protein than the non-degraded protein. This band can be attributed to the VEGF dimer breaking in half. The fact that this is still present in the non-degraded gel indicates how sensitive to the aqueous environment and easily denatured VEGF can be. The strong peak present at approximately 60-70 KDa is the BSA that is present in both the lyophilised protein and when made into solution. Mass spectrometry data confirmed the BSA peak at 66.4 KDa in both degraded and non-degraded samples. A peak present at 73.9 KDa was attributed to complexed VEGF and was present in both spectra. This peak may have ran into the BSA on the gel which would explain the thicker than expected band present. Small peaks were seen on both spectra between 45 KDa and 30 KDa. These peaks have been dwarfed by the larger BSA peak so the quantifying these peaks proved difficult.

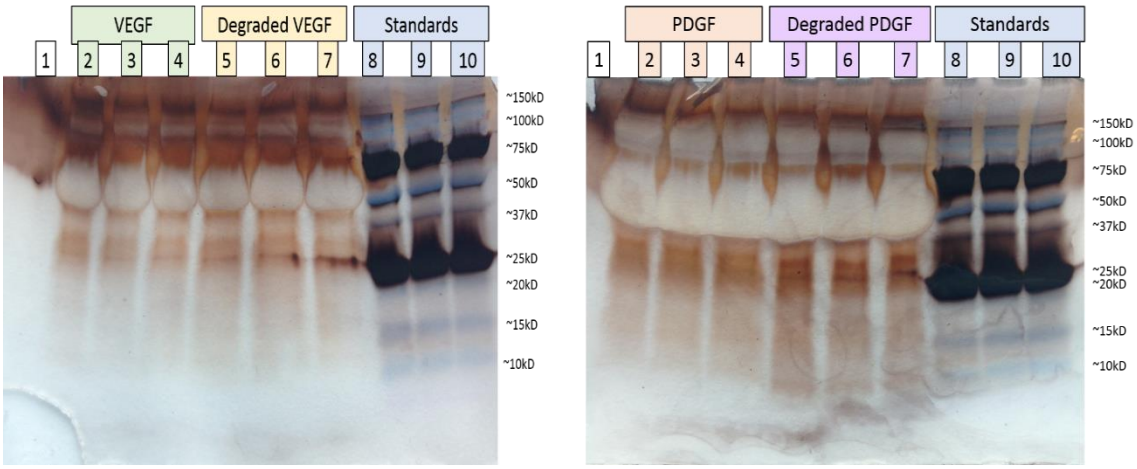

Figure 4.18 Electrophoresis gels showing degraded protein and non-degraded protein. All samples, including standards, were run in triplicate.

The PDGF gel shows a marker for PDGF around the marker for 25 KDa. This would be expected as the molecular weight of PDGF studied is 24.4 KDa. The PDGF band looks stronger in the degraded protein than the non-degraded protein. However, the bands are the same width, so the depth of staining may not be representative of the quantity of protein present. There are three bands present between the 25-20 KDa bands. These are thicker and more obvious in the degraded protein. This would indicate that these are products of protein degradation, although the exact products cannot be determined from this data alone. The BSA band at approximately 66.5 KDa

can also be seen on the PDGF gel. Mass spectrometry data confirmed the BSA peak at 66.4 KDa in both degraded and non-degraded samples. A peak at 73.8 KDa in the degraded protein spectra and 73.9 KDa in the non-degraded spectra was attributed to a complex of three PDGF proteins. A further peak at 44.3 KDa was present in both spectra and was a complex of two proteins.

VEGF was released from core-shell particles in the same manner as described in chapters 3 and 4. Both gels show a band for BSA and a band at ~38 KDa for VEGF. Both gels show light thin bands below 37 KDa that relate to degradation products. These would be expected as the protein has been released for 48 hours. The protein released in the early stages of the experiment would have begun to degrade in solution. In each gel well 7 shows darker bands at the same band position as the standard wells. This can be attributed to the standard wells running slightly. In all wells relating to the protein released from particles there is a dark band above 250 KDa. This is any residual polymer that may have been in suspension after centrifuging the polymer/protein samples. The polymers are designed to be highly charged and because of this would not run down the gel. This is stronger in L-PAMPS and B-PAMPS compared to OPHP or GMAC wells. When centrifuging L-PAMPS and B-PAMPS particles it can take some time before a fine suspension is no longer present, therefore it is difficult to ensure no polymer contaminates supernatant samples. This behaviour has been explained by Platt *et. al.* as PAMPS particles were found to produce two defined particle sizes during colloid synthesis [221]. The mass spectrometry from released proteins was the same as those for VEGF as described above.

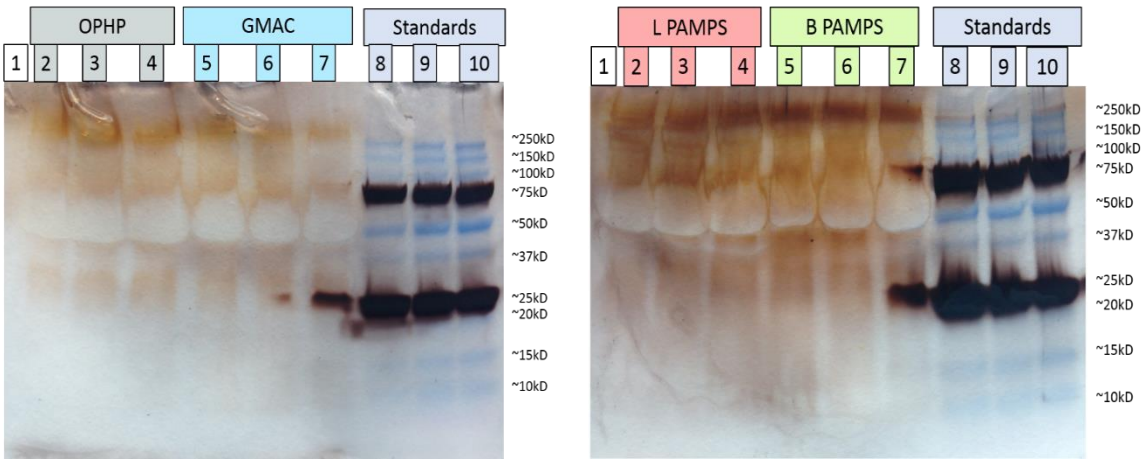

Figure 4.19 Electrophoresis gels showing VEGF that had been released from various core shell particles. All samples, including standards, were run in triplicate.

When released in the body VEGF is bound and stabilised by heparin that is present as part of the ECM. To investigate the effectiveness of core-shell particles for releasing VEGF, heparin was used as a comparison. The electrophoresis gel shows bands for BSA and a band at approximately 150 KDa that can be attributed to heparin. Because heparin is naturally derived, a definitive molecular weight is not given as the heparin may be a range of molecular weights. Wells 5-7 contain heparin with VEGF bound. The VEGF cannot be seen on the gel. This may be due to the heparin not running down the gel sufficiently. As discussed in chapter 1, heparin is a highly charged molecule. This can prevent movement down the electrophoresis gel when a voltage is applied. The lack of protein showing on the gel indicates that this is what has occurred. It also suggests that VEGF is bound tightly to heparin and is not continuously released as seen with core-shell particles. The highly charged nature of heparin also prevented any more information being gained from mass spectrometry.

5 Discussion

5.1 *Analysis of OPHP functionalised core-shell particles*

When producing a polymer for eventual large scale production, it is important to investigate the batch variation of particles synthesised by emulsion polymerisation. Figure 4.1 and Figure 4.2 show the batch variation in dynamic light scattering (DLS) and zeta potential analysis for OPHP:EGDMA and OPHP:GMAC:EGDMA latexes. Box and whisker plots not only show any batch variation, but also show the range of variation. The information gained from visual representation of the interquartile range is useful if the batch variation needed to be reduced.

OPHP:EGDMA particles showed no significant difference between batch variation. OPHP:GMAC:EGDMA particles showed some significant difference when protected (2:1:1 OPHP:GMAC:EGDMA particle size, P=0.03; 4:1:3 OPHP:GMAC:EGDMA particle size, P=0.04, zeta potential, P=0.009) but no significant difference after deprotection of the GMAC unit. All materials containing GMAC exhibited an increase in size after deprotection. It is thought that this is due to the removal of acetone from GMAC units, producing glycerol mono-methacrylate polymerised into the particle shell. This unit is much more hydrophilic than GMAC, therefore, it can bind more water into the particle shell. This would cause the particle shell to swell, thereby, increasing the overall particle size that is measured via DLS. The data shown in Figure 4.2 validates the hypothesis that the particle size increase is due to deprotection of the GMAC unit. The material with the largest quantity of GMAC (4:3:1 OPHP:GMAC:EGDMA) has the largest particle size (861.22±14.09 nm) and the material with the smallest quantity of GMAC (4:1:3 OPHP:GMAC:EGDMA) has the smallest particle size (172.09±1.17 nm).

Particle size was confirmed using TEM (Figure 4.3). However, deprotected OPHP:GMAC:EGDMA particles could not be successfully imaged using standard TEM techniques. When preparing samples for TEM imaging, the deprotected OPHP:GMAC:EGDMA particles became instable, aggregated into polymer clumps, and finally burnt or melted in the electron beam. This did not occur with protected OPHP:GMAC:EGDMA particles. This could be due to the reduction in the particle zeta potential upon deprotection. Figure 4.2 shows that for all GMAC containing

materials, the zeta potential is decreased upon deprotection. This would be expected. The negative charge on the polymer shell arises due to the negative phosphate groups present on the OPHP monomer. The quantity and availability of these groups does not change when the GMAC groups are deprotected, however, the size changes drastically. This results in the negative charge being spread over a larger surface area. If the particle charge is reduced upon deprotection, the particles would be less colloidally stable and more prone to aggregation. The future work section discusses alternative to standard TEM imaging for colloidally instable particles.

Percentage solid content was determined for OPHP:EGDMA and OPHP:GMAC:EGDMA particles (shown in Figure 4.1 and Table 4-1). In emulsion polymerisations that produce insoluble cross-linked materials, solid content analysis can give insight into the degree of polymerisation. Comparison between the expected mass recovery (Table 3-5) and the actual mass recovery (Table 4-1 and Figure 4.1) shows that all syntheses were completed to a high degree of polymerisation. Any insignificant mass loss or gain when determining the percentage solid content could be due to material loss when weighing or residual water in the samples after drying.

5.2 *Analysis of PAMPS functionalised core-shell particles*

Before use in protein release studies, L- and B-PAMPS particles had to be washed with distilled water. The particle size and zeta potential measurements were determined to ensure the washing steps did not affect the particles. Zeta potential and DLS analysis prior to washing can be found in the paper by Platt. e*t. Al.* [221]. L-PAMPS was shown to be larger (188.2±1.2 nm) and have a lower zeta potential (-17.9±1.6 mv) than B-PAMPS. Both the L- and B-PAMPS containing the same quantity of PAMPS monomer (in this case 1g). The structure of each monomer (Figure 1.7) shows that B-PAMPS has more negative charges per repeating unit than L-PAMPS. B-PAMPS is also smaller (113.1±0.4 nm) than L-PAMPS, therefore, has a smaller size: charge ratio. Consequently, it could be predicted that L-PAMPS containing particles would have a lower zeta potential than B-PAMPS containing particles.

The L- and B-PAMPS macro-monomers were produced by RAFT polymerisation (protocol detailed in [221]). RAFT allows for the production of polymers with controlled chain lengths and controlled degrees of branching. It was for these reasons that RAFT was chosen as the synthesis method for PAMPS macro-monomers. In future, it could be possible to finely control the particle shell size by altering the chain length or degree of branching of the PAMPS macro-monomer.

5.3 *Protein release from OPHP functionalised core-shell particles*

Colloidally stable core-shell particles have been synthesised in a two-step batch emulsion process. These particles can be altered by differing cross-linking density and by varying cross-linking units. The inclusion of OPHP was to provide a negatively charged unit in the outer shell of the particle. OPHP has previously been identified as being able to bind and release VEGF for short periods of time [116]. This was expanded upon to act as a HS mimic for a variety of growth factors. $VEGF_{165}$, PDGF-BB and EGF all showed different release profiles when released from 1:1 OPHP:EGDMA and 2:1:1 OPHP:GMAC:EGDMA particles.

It is thought that the particles not only electrostatically bind proteins, but also, exert a size exclusion effect on the protein bound within the outer shell. The particle shell can be thought of as a mesh-like structure. The size and density of the mesh can be altered by altering the degree of cross-linking or by altering the cross-linking units. (Varying the ratio of OPHP:EGDMA was the former variation and the inclusion of GMAC was the latter alteration). If a protein is large compared to the particle shell mesh size, it cannot bind within the particle shell. However, if the protein is small compared to the particle shell mesh size, it can bind within the particle shell, as the protein is able to pass though the polymer mesh. A protein bound and enclosed by the particle shell will have access to more electrostatic binding sites than a protein bound to the outer surface of the particle shell. Upon release, the protein would be move through the particle shell by diffusion and would be forced into contact with other electrostatic binding sites. Access to more electrostatic binding sites will hold the protein in the correct conformation for longer periods of time. If there is a large disparity in size between the protein and polymer mesh size (for example, a very

small protein in a large mesh), the effect of the sequential electrostatic binding may not be felt and would have little effect on the protein release profile.

Figure 4.5 shows the release of VEGF from 1:3, 1:1 and 3:1 OPHP:EGDMA shell particles. The variation of the quantity of EGDMA could produce a particle shells with a differing mesh-like structure. Increasing the amount of EGDMA present in the particle shell could produce a looser mesh structure and decreasing the amount of EGDMA could produce a tighter, smaller mesh structure. DLS measurements (Figure 4.1) shows increasing particle size with increasing quantity of EGDMA, which would be consistent with this theory. Figure 4.5 shows that increasing the quantity of OPHP (or negatively charges phosphate groups) in the shell did not result in more VEGF released from the particle shell.

Figure 4.6 shows the release of VEGF from 4:1:3, 2:1:1 and 4:3:1 OPHP:GMAC:EGDMA shell particles. The quantity of OPHP remained the same throughout the three materials, therefore, any variation on binding would be due to the particle shell structure. The ratio of OPHP: cross-linker was the same as that for 1:1 OPHP:EGDMA. When deprotected, GMAC is more hydrophilic than EGDMA. It is thought that this could bind more water within the particle shell producing a swollen mesh-like structure. As previously discussed, Figure 4.2 shows an increase in particle size as more GMAC is incorporated into the polymer.

1:1 OPHP:EGDMA and 2:1:1 OPHP:GMAC:EGDMA particles were chosen for further study because they showed a favourable release profile for the release of VEGF over 72 hours. They also have comparable quantities of phosphate within the polymer shell, therefore, any variation in protein release is due to the particle structure. Figure 4.7, Figure 4.8 and Figure 4.9 show the release of VEGF, PDGF and EGF respectfully. For the release of VEGF and PDGF, 1:1 OPHP:EGDMA consistently showed less protein detected at each time point and a smaller burst release than 2:1:1 OPHP:GMAC:EGDMA. 2:1:1 OPHP:GMAC:EGDMA particles show more VEGF and PDGF detection at each time point but also exhibits a larger burst release phase and earlier plateau region than 1:1 OPHP:EGDMA particles do. There was no significant difference between the release of EGF from either material.

The three proteins studies varied in size: VEGF 38.2 KDa, PDGF. 24.4 KDa and EGF 6.3 KDa. It is hypothesised that the variation in protein size and the variation in particle shell structure would have an effect of the release profiles on said proteins. It can be assumed that all the proteins have a similar proficiency for electrostatically binding to negatively charged phosphate groups. This assumption is based on the number of arginine and lysing units in the protein backbone but, the conformational arrangement of these groups is not taken into consideration at this time. For VEGF to bind within the particle shell, the shell mesh size would have to be larger than for either PDGF or EGF to bind within the particle shell. Alternatively, for the particle shell mesh-size to have both an electrostatic binding effect and a size exclusion effect on EGF, the shell mesh-size would need to be smaller than for VEGF or PDGF binding.

Figure 4.7, Figure 4.8 and Figure 4.9 show that the larger protein (VEGF) has a slower release from the particles with the largest particle shell mesh size (2:1:1 OPHP:GMAC:EGDMA). The medium sized protein (PDGF) has an initial burst release where we can assume the protein has been stabilised and released from the surface of the particles. Finally, the smallest protein (EGF) shows very little extra stability produced by the two different shells. This could be because the particle shell mesh sizes are both large in comparison to the protein and not slowing the release of EGF by sequential binding to phosphate groups within the particle shell.

Analysis of protein by ELISA is a sensitive analysis technique that is commonly used in research and diagnostics. However, it is not without problems. Some of these are address in the introduction chapter (alternative protein analysis techniques, page 35). When protein is released from core-shell particles it is only detected with ELISA if the protein is still intact. Table 4-2, Table 4-3 and Table 4-4 show the initial protein uptake of VEGF, PDGF and EGF by 1:1 OPHP:EGDMA and 2:1:1 OPHP:GMAC:EGDMA particles. This data alone cannot be used to definitively determine the successful or unsuccessful protein uptake by a material. If the protein has been denatured or undergone any primary structure damage the ELISA may not detect the protein. This must always be kept in mind when analysing data from ELISA. However, there are complimentary techniques that can be adopted alongside ELISA. One possible option would be to use FTIR to detect any free peptide bonds. The presence of these would indicate that there have been breakage of the primary amino acid sequence.

If the amino acid primary structure is broken, it would therefore, be unlikely that all of the protein present in the sample is being detected. This technique would be quick to run and immediately give information on the state of the proteins present. However, practically this may prove difficult as the protein sample contains BSA and other biological molecules that may result in FTIR data not definitively coming from the protein of interest.

The ability to release VEGF and PDGF over long periods of time would be greatly advantageous for wound healing. Table 1-1 and Table 1-2 give examples of other materials for release of VEGF and PDGF respectively. VEGF was released over 31 days which is considerably longer than those studies of VEGF release from microparticles by Karal-Yilmaz *et. al.* and Patel *et. al.* [121, 124]. Biodegradable PLGA Gd-doped microspheres released VEGF for up to six week but a large burst release phase was not overcome [127]. Injectable PLG gels were able to release PDGF for 2-4 weeks and is a promising avenue for the stimulation of angiogenesis [130]. However, this system may not be as promising as first assumed when treating conditions, such as burns, where the material would not able to be injected. By looking at other GF release systems it is clear there is still a clinical need that has not been fully met.

5.4 *Protein release from PAMPS functionalised core-shell particles*

Particles with a BMA core and either L-PAMPS or B-PAMPS shell can bind, stabilise and release a variety of growth factors over a period of 1-31 days. Negatively charged sulfonic acid groups present on PAMPS produce a HS mimic that can bind to arginine and lysine amino acids present in various proteins. The structure of the particle shell and size of protein have a profound effect on the release profile.

As previously described, the particles are thought to not just electrostatically bind to the protein released, the shell architecture is thought to play an equally important role in the binding and release of proteins. L-PAMPS could form a micelle like structure around the BMA core. The hydrophilic sulfonic acid groups would be mainly on the outside and the hydrophobic chain would surround the BMA centre.

These linear chains would be flexible and could accommodate proteins of varying sizes.

B-PAMPS would produce a more rigid mesh structure around the BMA core. Although not cross-linked, the branching of the PAMPS would intertwine. To ease explanation, it is assumed the B-PAMPS shell is a rigid or semi rigid structure with holes or pores in the shell. In the case of B-PAMPS, hydrophilic sulfonic acid groups would be available on the surface of the particle and within the pores in the particle shell. If a protein is large compared to the B-PAMPS pore size, it cannot bind within the particle shell and would only bind on the particle surface. However, if the protein is small compared to the B-PAMPS pore size, it can bind within the particle shell, as the protein is able to pass into the polymer pores. Since it is assumed that in the B-PAMPS shell, sulfonic acid groups are present throughout, a protein bound and enclosed by the particle shell will have access to more electrostatic binding sites than a protein bound to the outer surface of the particle shell. When the protein is release by diffusion, it would move through the pore in the B-PAMPS shell and be forced into contact with other electrostatic binding sites. This will slow release and prevent the protein from denaturing in the aqueous environment. As with previously described particles, if there is a large disparity in size between the protein and B-PAMPS pore size (for example, a very small protein in a large pore), the effect of the sequential electrostatic binding may not be felt and would have little effect on the protein release profile.

Figure 4.10 and Figure 4.11 show there was a significant difference in the release of VEGF and PDGF when comparing linear and branched shells. As with OPHP functionalised materials, it was found that the quantity of negative electrostatic binding groups in the shell produced little difference in the protein release profile. L-PAMPS released VEGF in a linear fashion over 31 days. The release of VEGF from B-PAMPS began to slow after approximately 14 days. L-PAMPS released PDGF slowly over 31 days. There was no obvious burst release seen and no plateau region but only small amounts of protein was detected. B-PAMPS released PDGF in a close to linear fashion for 31 days. There was no significant difference between L- and B-PAMPS with the release of EGF.

These release profiles could be explained by the architecture of the particle shell. L-PAMPS shell is flexible and can move to accommodate different sized proteins. B-PAMPS shell can be thought of as a rigid structure containing pores. VEGF was the largest protein investigated and the release from B-PAMPS was slow and eventually plateaued. This could be because VEGF was too large to bind deep within the B-PAMPS shell, whereas, the flexible chains on L-PAMPS could wrap around VEGF giving access to a greater number of electrostatic binding sites and resulting in a slow, linear release of protein. PDGF is smaller than VEGF, meaning it could fit within the pores created in the B-PAMPS shell. This would mean that the protein could interact with the shell in various places as PDGF is released, thereby, slowing the release of PDGF from a B-PAMPS shell. The smaller size of PDGF means that the flexible linear chains can move to accommodate the protein. However, there is only one negative sulfonic acid group per AMPS unit, therefore, a smaller protein will come into contact with less electrostatic binding sites than a larger protein. This would reduce the stabilisation of the protein and result in lower protein recovery when compared to B-PAMPS. Neither L-PAMPS nor B-PAMPS shells produced a sustained release of EGF. This could be due to EGFs small size. The protein may be too small to be affected by sequential electrostatic binding within the pores of the B-PAMPS shell. This would result in proteins being less stabile (and unable to be detected by ELISA) and release not being sustained over longer periods of time. The small size of EGF could also prevented it from binding sufficiently to L-PAMPS. As the L-PAMPS chains try to arrange themselves around the small protein, repulsion from the neighbouring negatively charged regions may be felt. This would result in little electrostatic binding occurring and L-PAMPS having little effect on the binding and release of EGF.

The release of VEGF, PDGF and EGF from L- and B-PAMPS was similar to that of 1:1 OPHP:EGDMA and 2:1:1 OPHP:GMAC:EGDMA particles. All release data displayed the importance of particle shell architecture. It can be assumed that the phosphate groups on OPHP and the sulfonic acid groups on PAMPS are acting as a HS mimic and are binding to the proteins via arginine and lysine amino acids. VEGF had the best protein recovery with all materials studied (1:1 OPHP:EGDMA, 69%; 2:1:1 OPHP:GMAC:EGDMA, 99%; L-PAMPS, 95%; B-PAMPS, 54%). PDGF had varied protein recovery (1:1 OPHP:EGDMA 30%; 2:1:1 OPHP:GMAC:EGDMA 53%; L-

PAMPS, 12%; B-PAMPS, 33%) and EGF had very poor protein recovery (1:1 OPHP:EGDMA and 2:1:1 OPHP:GMAC:EGDMA, 1.5%; L-PAMPS, 1%; B-PAMPS, 0.8%). As previously discussed, techniques complimentary to ELISA would be needed to determine why any remaining protein was not detected. From comparing all the core-shell particles studied, it is clear that different materials are better suited to releasing certain proteins.

PAMPS stabilised emulsion polymers have not been previously used for release of VEGF, PDGF or EGF. However, work by Liekens *et. al.* and Garcia-Fernandez *et. al.* showed that sulfonic acid groups can bind growth factors from cell culture media [218, 219]. L- and B-PAMPS shell particles exhibited excellent protein uptake (Table 4-5, Table 4-6 and Table 4-7) and it is reasonable to assume that there may be unprotected protein remaining bound to the sulfonic acid groups on the particle shell.

5.5 *Analysis of NVP-co-DEGBAC hydrogels*

Different wounds needs different environments to promote healing. A wound must often be kept in a moist environment. This is to prevent any further cell death; promote cell replication and angiogenesis; and to help relieve pain to the patient [241]. However, skin can be damaged by continued exposure to incorrect water levels. This is known as maceration and refers to any damage caused to the skin by excessing water or bodily fluids. This can result in death of healthy tissue and an increased risk of infection [242]. It is for these reasons that it is important to monitor the water content of hydrogels produced for wound dressing systems.

Table 4-8 shows the water content of PVP-co-DEGBAC control hydrogel and PVP-co-DEGBAC gels containing L-PAMPS, B-PAMPS, 1:1 OPHP:EGDMA, 2:1:1 OPHP:GMAC:EGDMA particles. The water content of the hydrogels containing embedded particles (86.12±2.26 – 88.68±0.9 %) is higher than the control gel (85.37±1.2 %). This would be expected as the all the particles contain hydrophilic groups, either in the form of negatively charged group, or hydrophilic cross-linking units. It could be possibly to control the water content of PVP-co-DEGBAC hydrogels

by altering the ratio of hydrophilic and hydrophobic units. Additional hydrophilic groups could increase the water content of a hydrogel and a reduction in hydrophilic units could decrease the water content. This would allow for the material to be tailored to the needs of a particular wound. However, the overall mechanical effects of altered water content must be taken into account. The resultant hydrogel must still be flexible, offer a barrier to bacterial colonisation and release growth factors over a useful time frame.

To gain an understanding of how the particles were embedded in the hydrogel SEM images were taken. Figure 4.13 shows surface and edge images of the PVP-co-DEGBAC control and particle embedded gels. Very little information could be gained from these images as the hydrogels must be dry prior to imaging. This resulted in the internal hydrogel structure collapsing. This can be seen by the characteristic wrinkled effect on the surface of the gel. Alternative imaging techniques will be discussed later.

For a hydrogel to be used as a wound dressing it must be able to be sterilised. The PVP-co-DEGBAC hydrogels used were sterilised with a series of ethanol washing steps. This sterilised the materials but is time consuming and could be ineffectual for thicker materials, as it relies on the ethanol soaking throughout the hydrogel. Alternative sterilisation techniques could be heat treatment or irradiation. The effect of heat sterilisation would have to be investigated as it is possible that high temperatures needed for heat sterilisation may affect the structure of the hydrogel [263]. Studies on UV irradiation for sterilisation of hydrogels had limited success. I was found that UV irradiation did not mean cGMP standards for sterilisation of a biomaterial [264]. Gamma irradiation of NVP based materials have shown that it can be an effective method for sterilisation of hydrogels [265, 266]. However, gamma irradiation was shown to increase crosslinking in the polymer, which may results in differing performance, particularly water content [266]. Furthermore, in these particle embedded PVP-co-DEGBAC hydrogels the effect of any sterilisation treatment of the core-shell particles must also be addressed.

5.6 *Protein release from particles embedded in NVP-co-DEGBAC hydrogels*

A set of NVP-co-DEGBAC hydrogels containing embedded core-shell particles were synthesised. The hydrogels contained either 1:1 OPHP:EGDMA, 2:1:1 OPHP:GMAC:EGDMA, L-PAMPS or B-PAMPS particles. Figure 4.14-4.16 show the release of VEGF, PDGF and EGF. They show that the hydrogels containing core-shell particles performed worse than the core-shell particles tested alone. However, the exception to this was hydrogels containing L-PAMPS and B-PAMPS particles releasing VEGF. These hydrogels performed equal to or better than the particles alone. The behaviour of these materials is still not understood. The structure of the L- and B-PAMPS shells may prevent the hydrogel material from penetrating the particle shell. This could allow the sulfonic acid groups on the PAMPS macro-monomer to remain available for binding to proteins.

Previous work by Gilmore *et. al.* used PVP-co-DEGBAC-co-AA hydrogels functionalised with tri-arginine (RRR) and heparin [248]. The release profile of VEGF was studied over 72 hours. Over the course of 72 hours, the best performing material released approximately 26% of the protein loaded. The cumulative release showed an initial burst phase and then released small portions of VEGF over the course of the study. When heparin functionalised material is compared to the particle embedded hydrogels, the particle embedded materials initially seem to perform better. L-PAMPS and B-PAMPS embedded particles both release a higher payload during the experimental time period. This would be desirable for a VEGF release system, as VEGF is needed in the initial stages of angiogenesis. More importantly, they are easier and cheaper to synthesise than producing a peptide functionalised material. The batch variance that is often found with natural materials (in this case heparin) can also be eliminated.

One method for increasing the performance of the particle embedded hydrogels could be to pre-load the core-shell particles with protein prior to embedding into the hydrogel. This is a method that is often used when releasing proteins or drugs from encapsulated particles (see Table 1-1and Table 1-2). This may prevent the bulk hydrogel material (NVP and DEGBAC) from blocking binding sites on the particles, resulting in the core-shell particles maintaining their protein release behaviour.

However, there is one main problem that a technique such as this faces. The hydrogels are cured by either UV photo-curing or heat curing. Obviously, heat curing is not an option with pre-loaded particles embedded into the gel structure. UV curing has potential but the gels are synthesised un-swollen with propan-2-ol as a solvent. This environment would not be accommodating to environmentally sensitive proteins, such as VEGF and PDGF. For this to be successful, a different synthesis protocol for UV curing would have to be developed to allow the gels to be cured with water as a solvent.

Although the quantity of protein released from the hydrogel can be estimated via ELISA, the binding site within the hydrogel is not known. It is assumed that the proteins bind to either the phosphoric acid or sulfonic acid sites on the embedded core-shell particles but this has not been confirmed. It is possible that there is protein non-specifically bound within the bulk hydrogel material. It is possible to radio label proteins prior to binding to the hydrogel material. An autoradiograph can then be produced of the hydrogel. This would show the spatial arrangement of the protein within the gel. If the protein was only bound to particles, you would expect to see high concentration clumps of radiolabelled protein within the gel. If there was non-specifically bound protein present, you would expect to see a consistent distribution throughout the hydrogel. This technique would also give information about the concentrations of protein bound and if there is any protein bound that cannot be detected by ELISA. A variety of peptide radio labels are available for binding to proteins, with new ones developed specifically for VEGF to assist with cancer diagnosis [267].

5.7 *Analysis of acryloxyethyl thiocarbamoyl rhodamine B labelled particles*

Water stable fluorescent particles have been produced by incorporating acryloxyethyl thiocarbamoyl rhodamine B into the core and throughout the particle. A two-step batch emulsion system was used to produce particles with a polystyrene divinyl benzene acryloxyethyl thiocarbamoyl rhodamine B core and 1:1 OPHP:EGDMA or 2:1:1 OPHP:GMAC:EGDMA shell. By using this two-step system it was hypothesised that the fluorescent label was mainly confined to the core of the

particle. Acryloxyethyl thiocarbamoyl rhodamine B has large hydrophobic areas that could preferentially arrange themselves into the hydrophobic PS-co-DVB core. However, acryloxyethyl thiocarbamoyl rhodamine B is still partially water soluble so some could remain in the aqueous phase during the polymerisation of the particle core. If there was fluorescent label in the aqueous phase upon addition of the shell monomers, it could be assumed that some label will also be incorporated into the particle shell. Table 4-9 and Table 4-10 show particle size, zeta potential and sold content analysis for fluorescently labelled 1:1 OPHP:EGDMA and 2:1:1 OPHP:GMAC:EGDMA shell particles. Zeta potential measurements indicate the particles are colloidally stable and have a negative surface charge. This supports the theory that the fluorescent label (which contains a positive charge) is not within the shell in large quantities. The PS-co-DVB core is larger than that shown in Figure 4.1, which again indicates that the fluorescent label is polymerised within the core.

A single step batch emulsion system was used to synthesis particles containing acryloxyethyl thiocarbamoyl rhodamine B in to BMA core with L-PAMPS or B-PAMPS shell. Due to the method of production, it was impossible to definitively determine if the label would be contained solely in either the core or shell. Table 4-9 shows that L- and B-PAMPS shell materials are colloidally stable and the incorporation of the fluorescent label is not exerting a detrimental effect on the stability of the particles.

It was found that the equivalent to 1g PAMPS was not enough to act as a surfactant for the polymerisation of BMA and acryloxyethyl thiocarbamoyl rhodamine B. When the quantity of PAMPS was increased to the equivalent of 4g PAMPS, the macro-monomer was a sufficient surfactant for the polymerisation. To fully understand why this occurs a full investigation into the kinetics of the reaction would need to be completed, as described by Platt *et. al.* [221].

All particles labelled with acryloxyethyl thiocarbamoyl rhodamine B were instable in salt solutions. This is a known feature of latexes produced by emulsion polymerisation. However, the labelled particles were considerably less stable than their none labelled equivalents. This may be due to the positive charge present on the acryloxyethyl thiocarbamoyl rhodamine B label. One way of overcoming problems associated with salt instability would be to embed the labelled particles

into PVP-co-DEGBAC hydrogels, as previously described for none labelled particles. This would hold the particles in place and prevent them from aggregating when places in PBS or cell culture media. These materials would have the same problems associated with sterilisation as previously discussed in section 5.6. Although embedding the fluorescently labelled particles in the hydrogel would prevent aggregation in PBS and cell culture media, it would not allow for tracking of the cells *in vivo*. This would be useful if the materials were tested in animal models.

5.8 *Protein degradation and analysis by alternative techniques*

Analysis of denatured and non-denatured proteins by electrophoresis showed a small difference between the two samples. Some peaks were confirmed by mass spectrometry however this was not as successful at determining protein stability as electrophoresis. Release of VEGF from OPHP:EGDMA, OPHP:GMAC:EGDMA, L-PAMPS and B-PAMPS coated core-shell particles show some noticeable difference between the stability of the protein. A comparative release from heparin proved unsuccessful. There is a clean need for complimentary protein analysis techniques to be used alongside ELISA. Alternative protein detection techniques have been heavily debated throughout and will be further addressed in the future work section.

6 Conclusions

This project has produced a set of materials that are candidates for future inclusion in wound dressings. All materials produced where easy to synthesis, have the potential for scale up, and do not require expensive peptides or ECM components to release pro-angiogenic growth factors. The binding of protein to particles (or hydrogel) was via negatively charged groups within the particle shell. It was hypothesised that these groups were acting as a HS mimic, thereby, stabilising the protein in the aqueous environment.

The conclusions are as follows:

- Particles containing OPHP were reproducible and gave acceptable batch variation when comparing particle size and zeta potential measurements.
- The inclusion of GMAC made the particle size significantly larger after deprotection.
- The variation of shell composition had an effect on the release of VEGF and PDGF but no significant effect on EGF release.
- Varying the quantity of PAMPS in the particle shell showed no significant difference in the release of protein but varying shell structure showed a significant difference in release of protein.
- PAMPS particles could release VEGF and PDGF over 31 days but there was little release of EGF.
- OPHP and PAMPS functionalised particles can be embedded into NVP-co-DEGBAC hydrogels.
- When embedded, most particles showed little functionality. The exception to this was L- and B-PAMPS, which release VEGF over 72 hours.
- The L- and B-PAMPS particles embedded in NVP-co-DEGBAC performed comparably to previously studies heparin functionalised materials.
- OPHP and PAMPS functionalised materials labelled with acryloxyethyl thiocarbamoyl rhodamine B produced latex particles with the fluorescent label incorporated, however, the particles aggregated over time.
- Alternative protein analysis techniques did not prove as successful as ELISA.

7 Future Work

The materials produced are a promising choice for potential future uses for wound dressings. However, the full capabilities of the materials have not been explored and there are still many questions to be answered. The main area of future work would need to focus on is confirming the size exclusion effect occurring within the particle shells. This could be done by expanding the number of proteins under investigation. The three proteins chosen (VEGF, PDGF and EGF) where done because of their size and also the biochemical and physiological relevance to angiogenesis during wound healing. Other potential protein release candidates would either have to bind to the ECM via heparin or contain areas with a high concentration of arginine and lysine units. Useful proteins to investigate could include: various forms of FGF (FGF-acidic, 16.8kDa, FHF-basic, 16.4-17.2kDa), PlGF (29.7-45.7kDa) and HB-EGF (9.7kDa). There are several reasons this work has not been carried out to date. The first is that the range of proteins studied was deemed sufficient for giving an overview of the size limitations of the material. Rather than studying a wider variety of protein sizes, time was spent on finding out other limitations of the core-shell particles, such as embedding in hydrogels and the potential for inclusion of fluorescent labels for tracking movement of particles.

One way of determining the sensitivity of the size exclusion effect is to alter the monomer units. Only one phosphate based monomer has been included in this work. The size of the particle shell was altered by changing the phosphate unit to crosslinker ratio. By including a large crosslinking unit the shell size was able to be substantially altered. However, it could be possible to finely tune the shell by changing the chain length of the phosphate monomer. This along with altering crosslinking units would give a system that has the potential to be finely tuned to release a particular protein at a desired time frame. By doing this the release plateau could be eliminated.

Particles containing either L-PAMPS or B-PAMPS showed that shell architecture also has an effect on the release of proteins. This could be investigated further by altering the degree of branching of the PAMPS to produce a series of materials with various degrees of branching. The degree of branching of the PAMPS can be altered by changing the ratio of monomer to chain transfer agent. If more chain transfer agent

is used, the degree of branching increases. The production of PAMPS with varying degrees of branching has been investigated within the research group during an undergraduate masters project by John De Crescenzo. The PAMPS was used during emulsion polymerisation but PAMPS with high degrees of branching had insufficient surfactant-like properties which lead to unstable latex formation. If this work was re-visited it could be possible to produce a set of particles with different sized pores in the particle shell. This would align with the theory that shell architecture also plays an important role in protein binding to be tested.

Embedding the particles in a gel would be essential for this system to be used as a wound dressing. The gel not only allows for easier handling but also can keep the wound moist and reduce bacterial colonisation [241]. To produce an ideal wound dressing the specific conditions created by the hydrogel would need to be investigated. These include: water content, oxygen and air flow and whether a second layer would need to be added to the hydrogel. To produce a usable wound dressing a collaboration with clinicians and potentially industry would be needed. This would give access to applicable expertise and industrially relevant research and development practices. Tissue and bacteria culture would also have to be undertaken to ensure the dressing does not allow bacteria to cross though the dressing and skin is still able to grow in close proximity to the material. PVP is frequently used as a material for wound dressing however crosslinking unit ratios and solvent ratios may need to be altered to produce a system that is more suited to particular types of wounds [243].

The manner in which the particles are set in the hydrogels also needs to be determined. It was found that upon drying in preparation for SEM the hydrogels collapse slightly resulting in a creased surface to the gel. Due to this is was difficult to gain an insight into how the particles sat within the gel. However, imaging using an alternative SEM technique may prevent this. Environmental SEM would allow for the hydrogels to remain semi-swollen. Cryo-TEM would be able to give a cross section of the hydrogel with the embedded particles. Since the sample is frozen, there should not be problems associated with the collapse of the material upon drying as with standard SEM techniques.

The release data from the hydrogels shows potential specificity for particular proteins. This would need to be further investigated to determine if the hydrogel system can be used to specifically select proteins from a mixed solution. This could be done simply by soaking the hydrogel in a protein solution, as described in section 3.7.2 (page 52). The released proteins could be analysed by ELISA as previously described. If the hydrogel system was specifically selecting one protein over others there should be a significantly higher quantity of one protein detected. Obviously, any potential ELISA cross-reactivity would have to be investigated prior and any proteins that show cross-reactivity could not be used. If the hydrogel system is capable of specifically selecting a particular protein from a mixed solution and release the protein in a biologically viable state, it could have a potential application in protein separation and purification.

The inclusion of rhodamine B into particles resulted in a pink latex that fluoresces within the red region of the spectrum. Although rhodamine B could be successfully incorporated into the polymer, the level of label incorporation was low. The quantity of rhodamine B incorporated into the polymer was not determined in the above work. One way this could be done is by monitoring the quantity of label washed out during dialysis. It can be assumed that if the label diffuses out during dialysis, it is not bound to the polymer chains. At each stage during dialysis (at each solvent change), a sample of the dialysis solution could be taken and analysed by UV-visible spectroscopy. This allows for the quantity of rhodamine B to be monitored over time. However, one problem associated with this method is photo-degradation of rhodamine B over time [268]. This could lead to lower rhodamine B levels being recorded.

The main problem associated with the particles containing rhodamine B is aggregation over time. This was concluded to be due to salt instability mainly from the positively charged unit on free rhodamine B. This was partially reduced by immediate dialysis after polymerisation has finished. However, if these were to be synthesised on a larger scale, the aggregation would need to be reduced as much as possible. One way this may be achieved, is to use a different label with no charged regions. There are a plethora of fluorescent labels that could be chosen, however there are a few criteria they must adhere to. First, is they must contain a region that

could be polymerised into the particles. This is usually a double bond in the form of an acrylate or methacrylate group. The second criteria is that the label should not contain charged regions because this has been shown to cause aggregation if any free label is left in solution. Finally, the label cannot be too large, as this could potentially disrupt the core-shell structure of the particles. Any change in core-shell structure could be monitored by TEM.

A clear, definitive ideal time frame for protein release must be determined. This would need to be done for each protein released from the material. During healing, each protein will have a different role that would be needed at different timepoints. However, the exact role of each protein involved in healing has not been fully determined and the extent of their importance has not been realised. Until this information is available, it would be difficult to have a perfect system that could release all the proteins needed at the ideal timepoints.

The practicalities of protein loading must also be addressed. In an ideal situation, the wound dressing would not need to be pre-loaded with protein. It would be put on a recent wound and could capture, stabilise and slowly release the vast mixture of proteins that are produced by the body after injury. In reality, these proteins are released and quickly degrade in the body, resulting in the majority of the proteins not interacting with cells. This type of dressing would need to be able to selectively capture proteins of interest and not be damaged or fouled by other biomolecules and cells that are present in a wound. Obviously, a system such as this would need many years of development and *in vitro* and *in vivo* testing. When determining the suitability of the materials for a wound dressing, the long term degradation must be looked at. This would determine if the material undergoes detrimental biofouling and how often the dressing would need to be changed. An incubator at 37^{o}C could be used for determining any chemical degradation that occurs. TEM would be a good tool to use to visualise any change in structure with time. Protein release studies should be done at various time points to see how older materials interact with proteins. To investigate how the material acts in the body, animal models would have to be used. *In vivo* studies would need to be completed for the materials to be deemed suitable as a wound dressing.

The bioactivity of any protein released must be determined. All of the techniques previously discussed, including gold standard protocols, have limitations associated with them. Matrigel assays are commonly used for assessing endothelial cell growth in response to a pro-angiogenic stimuli [139, 149-151]. It could be used to assess endothelial cell response (via cell replication) to supernatant from particles containing released protein. A matrigel assay could also be used to assess cell movement towards the source of growth factors by using particle embedded hydrogels. However, as previously discussed, matrigel has problems with giving false positive results [148]. A matrigel assay would be a good starting point for assessing bioactivity.

After an *in vitro* model had been used to assess bioactivity an *in vivo* model must be performed. *In vivo* work is expensive, time consuming and often requires ethical approval. The gold standard for assessing angiogenesis *in vivo* is the ischemic hind limb model. Initially, it is possible to reduce costs and ethics approval by using zebrafish as a candidate for *in vivo* study. However, this does not allow for long term (greater than 4 days) release or implantation studies.

An *in vitro* or/and an *in vivo* wound healing model would also be appropriate to use. *In vitro* models mimic the healing process using cells from the dermis and epidermis by culturing on a hydrogel like material [269]. Other cells, such as macrophages, can be added to mimic the extracellular environment. *In vivo* models allow for more complex wounds to be modelled, such as, diabetic wounds, chronic and acute wounds, and wounds in aging populations. Porcine models are the ideal candidate for human wound healing. However, this model is not as popular as small animal models, such as rodents, due to the animal size and husbandry requirements. Rather than a porcine model, the mouse dorsal trunk skin model is the most popular for *in vivo* wound healing [270].

8 Supplier Information

Chemical Suppliers	Cell Culture Suppliers	Gel Electrophoresis Suppliers	ELISA kit Suppliers	Equipment Suppliers
Sigma-Aldrich Company Ltd The Old Brickyard New Road Gillingham Dorset SP8 4XT **Merck Millipore** Suite 3 & 5, Building 6, Croxley Green Business Park Watford Hertfordshire WD18 8YH **Fisher Scientific UK Ltd** Bishop Meadow Road Loughborough LE11 5RG **Alfa Aesar** Shore Road Port Heysham Industrial Park Heysham Lancashire LA3 2XY **Polysciences Europe** Handelsstasse 3 D-69214 Eppleheim Germany **Thermo Fisher Scientific** Stafford House 1 Boundary Park Boundary Way Hemel Hempstead Hertfordshire HP2 7GE **Bio-Rad Laboratories Ltd** Bio-Rad House Maxted Road Hemel Hempstead Hertfordshire HP2 7DX	**PromoCell** Sickingenstr 63/65 69126 Heidelberg Germany **VWR** Hunter Boulevard Magna Park Lutterworth Leicestershire LE17 4XN	**Bio-Rad Laboratories Ltd** Bio-Rad House Maxted Road Hemel Hempstead Hertfordshire HP2 7DX	R**&D Systems** 19 Barton Lane Abingdon Science Park Abingdon, OX14 3NB **Peprotech** PeproTech House 29 Margravine Road London W6 8LL	**Spectrum Laboratories Inc.** P.O. Box 3262 4800 DG Breda The Netherlands **Brookhaven Instruments Corporation** 750 Blue Point Road Holtsville NY 11742 **FEI** 5350 NE Dawson Creek Drive Hillsboro Oregon 97124 USA **Dynex Technologies GmbH** Heerweg 15D 73770 Denkendorf Germany **Perkin Elmer** Chalfont Road Seer Green Buckinghamshire HP9 2FX

9 Appendix

Calibration graphs for $VEGF_{165}$, PDGF-BB and EGF. The concentration of released protein can be determined using these graphs.

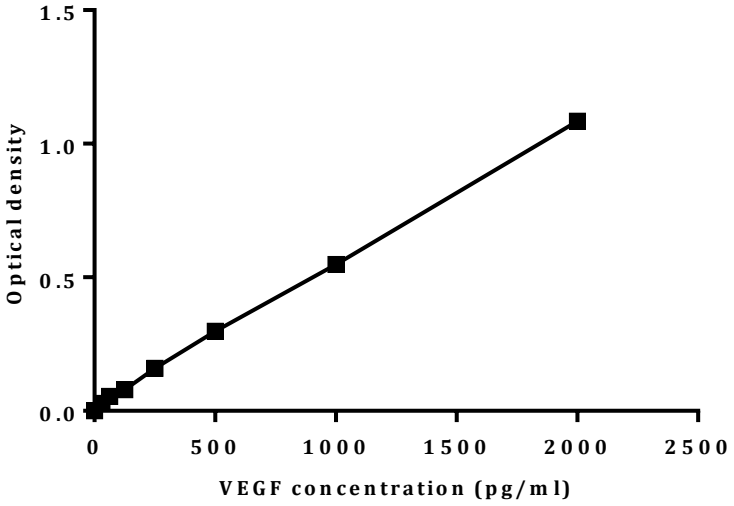

Figure 9.1 Example calibration graph for VEGF ELISA. For each 96 well ELISA plate ran an optical density to concentration calibration must be performed.

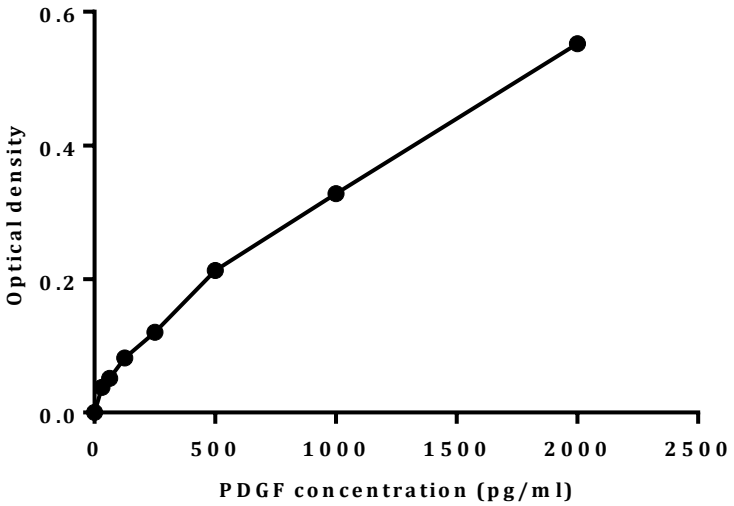

Figure 9.2 Example calibration graph for PDGF ELISA. For each 96 well ELISA plate ran an optical density to concentration calibration must be performed.

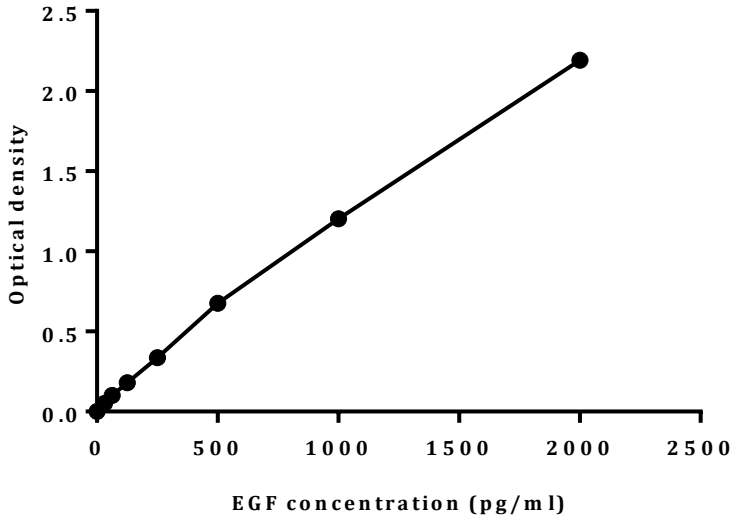

Figure 9.3 Example calibration graph for EGF ELISA. For each 96 well ELISA plate ran an optical density to concentration calibration must be performed.

10 References

1. Risau, W., *Mechanisms of angiogenesis.* Nature, 1997. **386**(6626): p. 671-674.
2. Beck, L. and P. D'Amore, *Vascular development: cellular and molecular regulation.* The FASEB Journal, 1997. **11**(5): p. 365-373.
3. Carmeliet, P., *Mechanisms of angiogenesis and arteriogenesis.* Nature Medicine, 2000. **6**(4): p. 389-395.
4. Otrock, Z.K., et al., *Understanding the biology of angiogenesis: Review of the most important molecular mechanisms.* Blood Cells Molecules and Diseases, 2007. **39**(2): p. 212-220.
5. Lamalice, L., F. Le Boeuf, and J. Huot, *Endothelial cell migration during angiogenesis.* Circulation Research, 2007. **100**(6): p. 782-794.
6. Nguyen, M., J. Folkman, and J. Bischoff, *1-Deoxymannojirimycin inhibits capillary tube formation in vitro. Analysis of N-linked oligosaccharides in bovine capillary endothelial cells.* Journal of Biological Chemistry, 1992. **267**(36): p. 26157-65.
7. Klagsbrun, M. and M.A. Moses, *Molecular angiogenesis.* Chemistry & Biology, 1999. **6**(8): p. R217-R224.
8. Boateng, J.S., et al., *Wound healing dressings and drug delivery systems: A review.* Journal of Pharmaceutical Sciences, 2008. **97**(8): p. 2892-2923.
9. Percival, N.J., *Classification of Wounds and their Management.* Surgery (Oxford), 2002. **20**(5): p. 114-117.
10. Miller, L. *Understanding Chronic Wounds*. 2013 [cited 2014 23/1/14].
11. Strodtbeck, F., *Physiology of wound healing.* Newborn and Infant Nursing Reviews, 2001. **1**(1): p. 43-52.
12. Clark, R., *Wound repair: Overview and general considerations.* Hort Notes, 1995. **6**: p. 3.
13. Martin, P., *Wound healing - Aiming for perfect skin regeneration.* Science, 1997. **276**(5309): p. 75-81.
14. Hübner, G., et al., *Differential regulation of pro-inflammatory cytokines during wound healing in normal and glucocorticoid-treated mice.* Cytokine, 1996. **8**(7): p. 548-556.
15. Kerstein, M.D., *The scientific basis of healing.* Advances in wound care : the journal for prevention and healing, 1997. **10**(3): p. 30-36.
16. Cooper, D.M., *Wound healing: New understandings.* Nurse Practitioner Forum: Current Topics and Communications, 1999. **10**(2): p. 74-86.
17. Levenson, S.M., et al., *The healing of rat skin wounds.* Annals of surgery, 1965. **161**: p. 293-308.
18. Gordillo, G.M. and C.K. Sen, *Revisiting the essential role of oxygen in wound healing.* The American Journal of Surgery, 2003. **186**(3): p. 259-263.
19. Schreml, S., et al., *Oxygen in acute and chronic wound healing.* British Journal of Dermatology, 2010. **163**(2): p. 257-268.
20. Harris, A.L., *Hypoxia - A key regulatory factor in tumour growth.* Nature Reviews Cancer, 2002. **2**(1): p. 38-47.
21. Prabhakar, N.R., *Invited Review: Oxygen sensing during intermittent hypoxia: cellular and molecular mechanisms.* Journal of Applied Physiology, 2001. **90**(5): p. 1986-1994.

22. Chen, L., A. Endler, and F. Shibasaki, *Hypoxia and angiogenesis: regulation of hypoxia-inducible factors via novel binding factors.* Experimental and Molecular Medicine, 2009. **41**(12): p. 849-857.
23. Norrby, K., *Mast cells and angiogenesis.* Apmis, 2002. **110**(5): p. 355-371.
24. Vacca, A., et al., *Human lymphoblastoid cells produce extracellular matrix degrading enzymes and induce endothelial cell proliferation, migration, morphogenesis, and angiogenesis.* International Journal of Clinical & Laboratory Research, 1998. **28**(1): p. 55-68.
25. Brovkovych, V., et al., *Nitric oxide release from normal and dysfunctional endothelium.* Journal of Physiology and Pharmacology, 1999. **50**(4): p. 575-586.
26. Soneja, A., M. Drews, and T. Malinski, *Role of nitric oxide, nitroxidative and oxidative stress in wound healing.* Pharmacological Reports, 2005. **57**: p. 108-119.
27. Sen, C.K., *The general case for redox control of wound repair.* Wound Repair and Regeneration, 2003. **11**(6): p. 431-438.
28. Schaffer, M.R., et al., *Nitric oxide regulates wound healing.* Journal of Surgical Research, 1996. **63**(1): p. 237-240.
29. Droge, W., *Free radicals in the physiological control of cell function.* Physiological Reviews, 2002. **82**(1): p. 47-95.
30. Battegay, E.J., R. Thommen, and R. Humar, *Platelet-derived growth factor and angiogenesis.* Trends in Glycoscience and Glycotechnology, 1996. **8**(42): p. 231-251.
31. Folkman, J. and Y. Shing, *Angiogenesis.* Journal of Biological Chemistry, 1992. **267**(16): p. 10931-10934.
32. Sage, R.B.V.a.E.H., *Between molecules and morphology. Extracellular matrix and creation of vascular form.* American Journal of Pathology, 1995. **147**(4): p. 873 - 883.
33. Takeshita, S., et al., *Therapeutic angiogenesis - A single intra-arterial bolus of vascular endothelial growth factor augments revascularization in a rabbit ischemic hind limb model.* Journal of Clinical Investigation, 1994. **93**(2): p. 662-670.
34. Barrientos, S., et al., *Growth factors and cytokines in wound healing.* Wound Repair and Regeneration, 2008. **16**(5): p. 585-601.
35. Yancopoulos, G.D., et al., *Vascular-specific growth factors and blood vessel formation.* Nature, 2000. **407**(6801): p. 242-248.
36. Odorisio, T., et al., *The placenta growth factor in skin angiogenesis.* Journal of Dermatological Science, 2006. **41**(1): p. 11-19.
37. Richardson, T.P., et al., *Polymeric system for dual growth factor delivery.* Nat Biotech, 2001. **19**(11): p. 1029-1034.
38. Ferrara, N. and W.J. Henzel, *Pituitary follicular cells secrete a novel heparin-binding growth factor specific for vascular endothellial cells.* Biochemical and Biophysical Research Communications, 1989. **161**(2): p. 851-858.
39. Senger, D.R., et al., *Tumor-cells secrete a vascular- permeablility factor that promotes accumulation of ascites-fluid.* Science, 1983. **219**(4587): p. 983-985.
40. Muller, Y.A., et al., *The crystal structure of vascular endothelial growth factor (VEGF) refined to 1.93 angstrom resolution: multiple copy flexibility and receptor binding.* Structure, 1997. **5**(10): p. 1325-1338.

41. Klagsbrun, M. and P. A. D'Amore, *Vascular endothelial growth factor and its receptors.* Cytokine & Growth Factor Reviews, 1996. **7**(3): p. 259-270.
42. Robinson, C.J. and S.E. Stringer, *The splice variants of vascular endothelial growth factor (VEGF) and their receptors.* Journal of Cell Science, 2001. **114**(5): p. 853-865.
43. Kim, K.J., et al., *Inhibition of vascular endothelial growth factor-induced angiogenesis suppresses tumor-growth in vivo.* Nature, 1993. **362**(6423): p. 841-844.
44. Fong, G.-H., et al., *Regulation of flt-1 expression during mouse embryogenesis suggests a role in the establishment of vascular endothelium.* Developmental Dynamics, 1996. **207**(1): p. 1-10.
45. Terman, B.I., et al., *Identification of the KDR tyrosine kinase as a receptor for vascular endothelial-cell growth factor.* Biochemical and Biophysical Research Communications, 1992. **187**(3): p. 1579-1586.
46. Heldin, C.H. and B. Westermark, *Mechanism of action and in vivo role of platelet-derived growth factor.* Physiological Reviews, 1999. **79**(4): p. 1283-1316.
47. Claessonwelsh, L., *Platelet derived growth factor receptor signals.* Journal of Biological Chemistry, 1994. **269**(51): p. 32023-32026.
48. Heldin, C.H., *Structural and function studies on platelet derived growth factor.* Embo Journal, 1992. **11**(12): p. 4251-4259.
49. Battegay, E.J., et al., *PDGF-BB modulates endothelial proliferation and angiogenesis in vitro via PDGF beta-receptors.* The Journal of Cell Biology, 1994. **125**(4): p. 917-928.
50. Bar, R.S., et al., *The effects of platelet-derived growth factor in cultured microvessel endothelial cells.* Endocrinology, 1989. **124**(4): p. 1841-1848.
51. Edelberg, J.M., et al., *PDGF mediates cardiac microvascular communication.* Journal of Clinical Investigation, 1998. **102**(4): p. 837-843.
52. Nicosia, R.F., S.V. Nicosia, and M. Smith, *Vascular endothelial growth factor, platelet-derived growth factor, and insulin-like growth factor-1 promote rat aortic angiogenesis in vitro.* American Journal of Pathology, 1994. **145**(5): p. 1023-1029.
53. Reuterdahl, C., et al., *Tissue localization of beta-receptors for platelet derived growth factor and platelet derived growth factor-B chain during wound repair in humans.* Journal of Clinical Investigation, 1993. **91**(5): p. 2065-2075.
54. Jaye, M., et al., *Modulation of the sis gene transcript during endothelial cell differentiation in vitro.* Science, 1985. **228**(4701): p. 882-885.
55. Rabenstein, D.L., *Heparin and heparan sulfate: structure and function.* Natural Product Reports, 2002. **19**(3): p. 312-331.
56. Korir, A.K. and C.K. Larive, *Advances in the separation, sensitive detection, and characterization of heparin and heparan sulfate.* Analytical and Bioanalytical Chemistry, 2009. **393**(1): p. 155-169.
57. Whitelock, J.M. and R.V. Iozzo, *Heparan Sulfate: A Complex Polymer Charged with Biological Activity.* Chemical Reviews, 2005. **105**(7): p. 2745-2764.
58. Noti, C. and P.H. Seeberger, *Chemical Approaches to Define the Structure-Activity Relationship of Heparin-like Glycosaminoglycans.* Chemistry & Biology, 2005. **12**(7): p. 731-756.

59. Munoz, E.M. and R.J. Linhardt, *Heparin-binding domains in vascular biology.* Arteriosclerosis Thrombosis and Vascular Biology, 2004. **24**(9): p. 1549-1557.
60. Capila, I. and R.J. Linhardt, *Heparin - Protein interactions.* Angewandte Chemie-International Edition, 2002. **41**(3): p. 391-412.
61. Fromm, J.R., et al., *Differences in the Interaction of Heparin with Arginine and Lysine and the Importance of these Basic Amino Acids in the Binding of Heparin to Acidic Fibroblast Growth Factor.* Archives of Biochemistry and Biophysics, 1995. **323**(2): p. 279-287.
62. Cardin, A.D. and H.J. Weintraub, *Molecular modeling of protein-glycosaminoglycan interactions.* Arteriosclerosis, Thrombosis, and Vascular Biology, 1989. **9**(1): p. 21-32.
63. Margalit, H., N. Fischer, and S.A. Ben-Sasson, *Comparative analysis of structurally defined heparin binding sequences reveals a distinct spatial distribution of basic residues.* Journal of Biological Chemistry, 1993. **268**(26): p. 19228-19231.
64. Gitaygoren, H., et al., *The binding of vascular endothelial growth-factor to its receptors is dependent on cell surface-associated heparin-like molecules.* Journal of Biological Chemistry, 1992. **267**(9): p. 6093-6098.
65. Fager, G., et al., *Heparin-like glycosaminoglycans influence growth and phenotype of human arterial smooth-muscle cells in vitro.* In Vitro Cellular & Developmental Biology-Animal, 1992. **28A**(3): p. 176-180.
66. Zhao, W.J., et al., *Binding affinities of vascular endothelial growth factor (VEGF) for heparin-derived oligosaccharides.* Bioscience Reports, 2012. **32**(1): p. 71-81.
67. Feyzi, E., et al., *Characterization of heparin and heparan sulfate domains binding to the long splice variant of platelet-derived growth factor A chain.* Journal of Biological Chemistry, 1997. **272**(9): p. 5518-5524.
68. Wirostko, B., T.Y. Wong, and R. Simo, *Vascular endothelial growth factor and diabetic complications.* Progress in Retinal and Eye Research, 2008. **27**(6): p. 608-621.
69. Lerman, O.Z., et al., *Cellular dysfunction in the diabetic fibroblast: Impairment in migration, vascular endothelial growth factor production, and response to hypoxia.* American Journal of Pathology, 2003. **162**(1): p. 303-312.
70. Maruyama, K., et al., *Decreased macrophage number and activation lead to reduced lymphatic vessel formation and contribute to impaired diabetic wound healing.* American Journal of Pathology, 2007. **170**(4): p. 1178-1191.
71. Verheul, H.M.W. and H.M. Pinedo, *Possible molecular mechanisms involved in the toxicity of angiogenesis inhibition.* Nature Reviews Cancer, 2007. **7**(6): p. 475-485.
72. Kusumanto, Y.H., et al., *Treatment with intramuscular vascular endothelial growth factor gene compared with placebo for patients with diabetes mellitus and critical limb ischemia: A double-blind randomized trial.* Human Gene Therapy, 2006. **17**(6): p. 683-691.
73. Saaristo, A., et al., *Vascular endothelial growth factor-C accelerates diabetic wound healing.* American Journal of Pathology, 2006. **169**(3): p. 1080-1087.
74. Cox, O.T., et al., *Sources of PDGF expression in murine retina and the effect of short-term diabetes.* Molecular Vision, 2003. **9**: p. 665-672.

75. Li, H.H., et al., *Research of PDGF-BB gel on the wound healing of diabetic rats and its pharmacodynamics.* Journal of Surgical Research, 2008. **145**(1): p. 41-48.
76. Cheng, B., et al., *Recombinant human platelet-derived growth factor enhanced dermal wound heating by a pathway involving ERK and c-fos in diabetic rats.* Journal of Dermatological Science, 2007. **45**(3): p. 193-201.
77. Cohen, M.A. and W.H. Eaglstein, *Recombinant human platelet-derived growth factor gel speeds healing of acute full-thickness punch biopsy wounds.* Journal of the American Academy of Dermatology, 2001. **45**(6): p. 857-862.
78. Monstrey, S., et al., *Assessment of burn depth and burn wound healing potential.* Burns, 2008. **34**(6): p. 761-769.
79. Catty, R.H.C., *Healing and contraction of experimental full-thickness wounds in the human.* British Journal of Surgery, 1965. **52**(7): p. 542-548.
80. Harrison, C.A., A.J. Dalley, and S. Mac Neil, *A simple in vitro model for investigating epithelial/mesenchymal interactions: keratinocyte inhibition of fibroblast proliferation and fibronectin synthesis.* Wound Repair and Regeneration, 2005. **13**(6): p. 543-550.
81. Guo, R., et al., *The healing of full-thickness burns treated by using plasmid DNA encoding VEGF-165 activated collagen-chitosan dermal equivalents.* Biomaterials, 2011. **32**(4): p. 1019-1031.
82. Zhang, F., et al., *Improvement of full-thickness skin graft survival by application of vascular endothelial growth factor in rats.* Annals of Plastic Surgery, 2008. **60**(5): p. 589-593.
83. Richter, G.T., et al., *Effect of vascular endothelial growth factor on skin graft survival in Sprague-Dawley rats.* Archives of Otolaryngology-Head & Neck Surgery, 2006. **132**(6): p. 637-641.
84. Wang, H.J., et al., *Acceleration of skin graft healing by growth factors.* Burns, 1996. **22**(1): p. 10-14.
85. Hill, E., et al., *The effect of PDGF on the healing of full thickness wounds in hairless guinea pigs.* Comparative Biochemistry and Physiology a-Physiology, 1991. **100**(2): p. 365-370.
86. Ennett, A.B., D. Kaigler, and D.J. Mooney, *Temporally regulated delivery of VEGF in vitro and in vivo.* Journal of Biomedical Materials Research Part A, 2006. **79A**(1): p. 176-184.
87. Mollica, F., et al., *Mathematical modelling of the evolution of protein distribution within single PLGA microspheres: prediction of local concentration profiles and release kinetics.* Journal of Materials Science-Materials in Medicine, 2008. **19**(4): p. 1587-1593.
88. Batycky, R.P., et al., *A theoretical model of erosion and macromolecular drug release from biodegrading microspheres.* Journal of Pharmaceutical Sciences, 1997. **86**(12): p. 1464-1477.
89. Zhang, M., et al., *Simulation of drug release from biodegradable polymeric microspheres with bulk and surface erosions.* Journal of Pharmaceutical Sciences, 2003. **92**(10): p. 2040-2056.
90. Epstein, S.E., et al., *Therapeutic interventions for enhancing collateral development by administration of growth factors: basic principles, early results and potential hazards.* Cardiovascular Research, 2001. **49**(3): p. 532-542.

91. Gilmore, L.J., *Synthetic Polymers for Interaction with Vascular Endothelial Growth Factor*, in *Department of Chemistry*. 2009, University of Sheffield: Sheffield.
92. Eppler, S.M., et al., *A target-mediated model to describe the pharmacokinetics and hemodynamic effects of recombinant human vascular endothelial growth factor in humans.* Clinical Pharmacology & Therapeutics, 2002. **72**(1): p. 20-32.
93. Jay, S.M. and W.M. Saltzman, *Controlled delivery of VEGF via modulation of alginate microparticle ionic crosslinking.* Journal of Controlled Release, 2009. **134**(1): p. 26-34.
94. Fischbach, C. and D.J. Mooney, *Polymers for pro- and anti-angiogenic therapy.* Biomaterials, 2007. **28**(12): p. 2069-2076.
95. Lee, H., H.J. Chung, and T.G. Park, *Perspectives on: Local and sustained delivery of angiogenic growth factors.* Journal of Bioactive and Compatible Polymers, 2007. **22**(1): p. 89-114.
96. Zisch, A.H., M.P. Lutolf, and J.A. Hubbell, *Biopolymeric delivery matrices for angiogenic growth factors.* Cardiovascular Pathology, 2003. **12**(6): p. 295-310.
97. Tessmar, J.K. and A.M. Göpferich, *Matrices and scaffolds for protein delivery in tissue engineering.* Advanced Drug Delivery Reviews, 2007. **59**(4–5): p. 274-291.
98. ZISCH, A.H., et al., *Cell-demanded release of VEGF from synthetic, biointeractive cell ingrowth matrices for vascularized tissue growth.* The FASEB Journal, 2003. **17**(15): p. 2260-2262.
99. Backer, M.V., et al., *Surface immobilization of active vascular endothelial growth factor via a cysteine-containing tag.* Biomaterials, 2006. **27**(31): p. 5452-5458.
100. Bentz, H., J.A. Schroeder, and T.D. Estridge, *Improved local delivery of TGF-β2 by binding to injectable fibrillar collagen via difunctional polyethylene glycol.* Journal of Biomedical Materials Research, 1998. **39**(4): p. 539-548.
101. Mann, B.K., R.H. Schmedlen, and J.L. West, *Tethered-TGF-β increases extracellular matrix production of vascular smooth muscle cells.* Biomaterials, 2001. **22**(5): p. 439-444.
102. DeLong, S.A., J.J. Moon, and J.L. West, *Covalently immobilized gradients of bFGF on hydrogel scaffolds for directed cell migration.* Biomaterials, 2005. **26**(16): p. 3227-3234.
103. Shen, Y.H., M.S. Shoichet, and M. Radisic, *Vascular endothelial growth factor immobilized in collagen scaffold promotes penetration and proliferation of endothelial cells.* Acta Biomaterialia, 2008. **4**(3): p. 477-489.
104. Zisch, A.H., et al., *Cell-demanded release of VEGF from synthetic, biointeractive cell-ingrowth matrices for vascularized tissue growth.* Faseb Journal, 2003. **17**(13): p. 2260-+.
105. Baldwin, S.P. and W. Mark Saltzman, *Materials for protein delivery in tissue engineering.* Advanced Drug Delivery Reviews, 1998. **33**(1–2): p. 71-86.
106. Biondi, M., et al., *Controlled drug delivery in tissue engineering.* Advanced Drug Delivery Reviews, 2008. **60**(2): p. 229-242.
107. Edelman, E.R., et al., *Controlled and modulated release of basic fibroblast growth factor.* Biomaterials, 1991. **12**(7): p. 619-626.

108. Holland, T.A., Y. Tabata, and A.G. Mikos, *Dual growth factor delivery from degradable oligo(poly(ethylene glycol) fumarate) hydrogel scaffolds for cartilage tissue engineering.* Journal of Controlled Release, 2005. **101**(1–3): p. 111-125.
109. Taipale, J. and J. Keski-Oja, *Growth factors in the extracellular matrix.* The FASEB Journal, 1997. **11**(1): p. 51-59.
110. Ding, S.S., et al., *Heparin for Growth Factor Delivery Systems.* Progress in Chemistry, 2008. **20**(12): p. 1998-2011.
111. Pike, D.B., et al., *Heparin-regulated release of growth factors in vitro and angiogenic response in vivo to implanted hyaluronan hydrogels containing VEGF and bFGF.* Biomaterials, 2006. **27**(30): p. 5242-5251.
112. Sakiyama, S.E., J.C. Schense, and J.A. Hubbell, *Incorporation of heparin-binding peptides into fibrin gels enhances neurite extension: an example of designer matrices in tissue engineering.* Faseb Journal, 1999. **13**(15): p. 2214-2224.
113. Ishihara, M., et al., *Heparin-carrying polystyrene (HCPS)-bound collagen substratum to immobilize heparin-binding growth factors and to enhance cellular growth.* Journal of Biomedical Materials Research, 2001. **56**(4): p. 536-544.
114. Tanihara, M., et al., *Sustained release of basic fibroblast growth factor and angiogenesis in a novel covalently crosslinked gel of heparin and alginate.* Journal of Biomedical Materials Research, 2001. **56**(2): p. 216-221.
115. Cai, S.S., et al., *Injectable glycosaminoglycan hydrogels for controlled release of human basic fibroblast growth factor.* Biomaterials, 2005. **26**(30): p. 6054-6067.
116. Gilmore, L., S. MacNeil, and S. Rimmer, *Phosphate Functional Core-Shell Polymer Nanoparticles for the Release of Vascular Endothelial Growth Factor.* Chembiochem, 2009. **10**(13): p. 2165-2170.
117. Oliviero, O., M. Ventre, and P.A. Netti, *Functional porous hydrogels to study angiogenesis under the effect of controlled release of vascular endothelial growth factor.* Acta Biomaterialia, 2012. **8**(9): p. 3294-3301.
118. Chapanian, R., et al., *Osmotic release of bioactive VEGF from biodegradable elastomer monoliths is the same in vivo as in vitro.* Journal of Pharmaceutical Sciences, 2012. **101**(2): p. 588-597.
119. Daugherty, A.L., et al., *Sustained release formulations of rhVEGF(165) produce a durable response in a murine model of peripheral angiogenesis.* European Journal of Pharmaceutics and Biopharmaceutics, 2011. **78**(2): p. 289-297.
120. Jia, X.L., et al., *Sustained Release of VEGF by Coaxial Electrospun Dextran/PLGA Fibrous Membranes in Vascular Tissue Engineering.* Journal of Biomaterials Science-Polymer Edition, 2011. **22**(13): p. 1811-1827.
121. Karal-Yilmaz, O., et al., *Preparation and in vitro characterization of vascular endothelial growth factor (VEGF)-loaded poly(D,L-lactic-co-glycolic acid) microspheres using a double emulsion/solvent evaporation technique.* Journal of Microencapsulation, 2011. **28**(1): p. 46-54.
122. Briganti, E., et al., *A composite fibrin-based scaffold for controlled delivery of bioactive pro-angiogenetic growth factors.* Journal of Controlled Release, 2010. **142**(1): p. 14-21.
123. Oredein-McCoy, O., et al., *Novel factor-loaded polyphosphazene matrices: Potential for driving angiogenesis.* Journal of Microencapsulation, 2009. **26**(6): p. 544-555.

124. Patel, Z.S., et al., *In vitro and in vivo release of vascular endothelial growth factor from gelatin microparticles and biodegradable composite scaffolds.* Pharmaceutical Research, 2008. **25**(10): p. 2370-2378.
125. Kanczler, J.M., et al., *Supercritical carbon dioxide generated vascular endothelial growth factor encapsulated poly(DL-lactic acid) scaffolds induce angiogenesis in vitro.* Biochemical and Biophysical Research Communications, 2007. **352**(1): p. 135-141.
126. Davda, J. and V. Labhasetwar, *Sustained Proangiogenic Activity of Vascular Endothelial Growth Factor Following Encapsulation in Nanoparticles.* Journal of Biomedical Nanotechnology, 2005. **1**(1): p. 74-82.
127. Faranesh, A.Z., et al., *In vitro release of vascular endothelial growth factor from gadolinium-doped biodegradable microspheres.* Magnetic Resonance in Medicine, 2004. **51**(6): p. 1265-1271.
128. Delgado, J.J., et al., *A platelet derived growth factor delivery system for bone regeneration.* Journal of Materials Science-Materials in Medicine, 2012. **23**(8): p. 1903-1912.
129. Tengood, J.E., et al., *Sequential Delivery of Basic Fibroblast Growth Factor and Platelet-Derived Growth Factor for Angiogenesis.* Tissue Engineering Part A, 2011. **17**(9-10): p. 1181-1189.
130. Sun, Q.H., et al., *Sustained Release of Multiple Growth Factors from Injectable Polymeric System as a Novel Therapeutic Approach Towards Angiogenesis.* Pharmaceutical Research, 2010. **27**(2): p. 264-271.
131. Li, B., J.M. Davidson, and S.A. Guelcher, *The effect of the local delivery of platelet-derived growth factor from reactive two-component polyurethane scaffolds on the healing in rat skin excisional wounds.* Biomaterials, 2009. **30**(20): p. 3486-3494.
132. Santo, V.E., et al., *Carrageenan-Based Hydrogels for the Controlled Delivery of PDGF-BB in Bone Tissue Engineering Applications.* Biomacromolecules, 2009. **10**(6): p. 1392-1401.
133. Wei, G.B., et al., *Nano-fibrous scaffold for controlled delivery of recombinant human PDGF-BB.* Journal of Controlled Release, 2006. **112**(1): p. 103-110.
134. Desire, L., et al., *Sustained delivery of growth factors from methylidene malonate 2.1.2-based polymers.* Biomaterials, 2006. **27**(12): p. 2609-2620.
135. Im, S.Y., et al., *Growth factor releasing porous poly (epsilon-caprolactone)-chitosan matrices for enhanced bone regenerative therapy.* Archives of Pharmacal Research, 2003. **26**(1): p. 76-82.
136. Park, Y.J., et al., *Controlled release of platelet-derived growth factor-BB from chondroitin sulfate-chitosan sponge for guided bone regeneration.* Journal of Controlled Release, 2000. **67**(2-3): p. 385-394.
137. Walsh, W.R., et al., *Controlled release of platelet-derived growth factor using ethylene-vinyl acetate copolymer (EVAC) coated on stainless steel wires.* Biomaterials, 1995. **16**(17): p. 1319-1325.
138. Norrby, K., *In vivo models of angiogenesis.* Journal of Cellular and Molecular Medicine, 2006. **10**(3): p. 588-612.
139. Carolyn A. Staton, M.W.R.R.a.N.J.B., *A critical analysis of current in vitro and in vivo angiogenesis assays.* International Journal of Experimental Pathology, 2009(90): p. 195-221.
140. Auerbach, R., et al., *Angiogenesis assays: A critical overview.* Clinical Chemistry, 2003. **49**(1): p. 32-40.

141. Egginton, S. and M. Gerritsen, *Lumen formation - In vivo versus in vitro observations.* Microcirculation, 2003. **10**(1): p. 45-61.
142. Gomez, D. and N.C. Reich, *Stimulation of primary human endothelial cell proliferation by IFN.* Journal of Immunology, 2003. **170**(11): p. 5373-5381.
143. Hemalatha, T., et al., *Platelet-derived endothelial cell growth factor mediates angiogenesis and antiapoptosis in rat aortic endothelial cells.* Biochemistry and Cell Biology-Biochimie Et Biologie Cellulaire, 2009. **87**(6): p. 883-893.
144. Detoraki, A., et al., *Vascular endothelial growth factors synthesized by human lung mast cells exert angiogenic effects.* Journal of Allergy and Clinical Immunology, 2009. **123**(5): p. 1142-1149.
145. Mastyugin, V., et al., *A quantitative high-throughput endothelial cell migration assay.* Journal of Biomolecular Screening, 2004. **9**(8): p. 712-718.
146. Albini, A., et al., *The "chemoinvasion assay": a tool to study tumor and endothelial cell invasion of basement membranes.* International Journal of Developmental Biology, 2004. **48**(5-6): p. 563-571.
147. Ariano, P., et al., *A simple method to study cellular migration.* Journal of Neuroscience Methods, 2005. **141**(2): p. 271-276.
148. Donovan, D., et al., *Comparison of three in vitro human 'angiogenesis' assays with capillaries formed in vivo.* Angiogenesis, 2001. **4**(2): p. 113-121.
149. Ucuzian, A.A., et al., *Angiogenic endothelial cell invasion into fibrin is stimulated by proliferating smooth muscle cells.* Microvascular Research, 2013. **90**: p. 40-47.
150. Arnaoutova, I., et al., *The endothelial cell tube formation assay on basement membrane turns 20: state of the science and the art.* Angiogenesis, 2009. **12**(3): p. 267-274.
151. Arnaoutova, I. and H.K. Kleinman, *In vitro angiogenesis: endothelial cell tube formation on gelled basement membrane extract.* Nature Protocols, 2010. **5**(4): p. 628-635.
152. Wolfe, A., et al., *Pharmacologic Characterization of a Kinetic In Vitro Human Co-Culture Angiogenesis Model Using Clinically Relevant Compounds.* Journal of Biomolecular Screening, 2013. **18**(10): p. 1234-1245.
153. Thommen, R., et al., *PDGF-BB increases endothelial migration and cord movements during angiogenesis in vitro.* Journal of Cellular Biochemistry, 1997. **64**(3): p. 403-413.
154. Shimo, T., et al., *Connective tissue growth factor induces the proliferation, migration, and tube formation of vascular endothelial cells in vitro, and angiogenesis in vivo.* Journal of Biochemistry, 1999. **126**(1): p. 137-145.
155. Stellos, K., et al., *Junctional Adhesion Molecule A Expressed on Human CD34(+) Cells Promotes Adhesion on Vascular Wall and Differentiation Into Endothelial Progenitor Cells.* Arteriosclerosis Thrombosis and Vascular Biology, 2010. **30**(6): p. 1127-U114.
156. Dietrich, F. and P.I. Lelkes, *Fine-tuning of a three-dimensional microcarrier-based angiogenesis assay for the analysis of endothelial-mesenchymal cell co-cultures in fibrin and collagen gels.* Angiogenesis, 2006. **9**(3): p. 111-125.
157. Stiffey-Wilusz, J., et al., *An ex vivo angiogenesis assay utilizing commercial porcine carotid artery: Modification of the rat aortic ring assay.* Angiogenesis, 2001. **4**(1): p. 3-9.
158. Baker, M., et al., *Use of the mouse aortic ring assay to study angiogenesis.* Nature Protocols, 2012. **7**(1): p. 89-104.

159. Blacher, S., et al., *Improved quantification of angiogenesis in the rat aortic ring assay.* Angiogenesis, 2001. **4**(2): p. 133-142.
160. Akhtar, N., E.B. Dickerson, and R. Auerbach, *The sponge/Matrigel angiogenesis assay.* Angiogenesis, 2002. **5**(1-2): p. 75-80.
161. Nicosia, R.F., et al., *A new ex vivo model to study venous angiogenesis and arterio-venous anastomosis formation.* Journal of Vascular Research, 2005. **42**(2): p. 111-119.
162. Liu, X., et al., *In vivo studies on angiogenic activity of two designer self-assembling peptide scaffold hydrogels in the chicken embryo chorioallantoic membrane.* Nanoscale, 2012. **4**(8): p. 2720-2727.
163. Chow, L.W., et al., *A bioactive self-assembled membrane to promote angiogenesis.* Biomaterials, 2011. **32**(6): p. 1574-1582.
164. Murray, B. and D.J. Wilson, *A study of metabolites as intermediate effectors in angiogenesis.* Angiogenesis, 2001. **4**(1): p. 71-77.
165. Arnold, S.A., et al., *Lab on a chick: a novel in vivo angiogenesis assay.* Clinical & Experimental Metastasis, 2011. **28**(2): p. 243-243.
166. Niiyama, H., et al., *Murine model of hindlimb ischemia.* J Vis Exp, 2009(23).
167. Hardy, B., et al., *Therapeutic angiogenesis of mouse hind limb ischemia by novel peptide activating GRP78 receptor on endothelial cells.* Biochemical Pharmacology, 2008. **75**(4): p. 891-899.
168. Silva, E.A. and D.J. Mooney, *Effects of VEGF temporal and spatial presentation on angiogenesis.* Biomaterials, 2010. **31**(6): p. 1235-1241.
169. Jo, J., et al., *Preparation of Polymer-Based Magnetic Resonance Imaging Contrast Agent to Visualize Therapeutic Angiogenesis.* Tissue Engineering Part A, 2013. **19**(1-2): p. 30-39.
170. Chen, D.Y., et al., *Three-dimensional cell aggregates composed of HUVECs and cbMSCs for therapeutic neovascularization in a mouse model of hindlimb ischemia.* Biomaterials, 2013. **34**(8): p. 1995-2004.
171. Huang, C.C., et al., *Hypoxia-induced therapeutic neovascularization in a mouse model of an ischemic limb using cell aggregates composed of HUVECs and cbMSCs.* Biomaterials, 2013. **34**(37): p. 9441-9450.
172. Kim, S.J., et al., *Rapid Transfer of Endothelial Cell Sheet Using a Thermosensitive Hydrogel and Its Effect on Therapeutic Angiogenesis.* Biomacromolecules, 2013. **14**(12): p. 4309-4319.
173. Reis, P.E.O., et al., *Impact of Angiogenic Therapy in the Treatment of Critical Lower Limb Ischemia in an Animal Model.* Vascular and Endovascular Surgery, 2014. **48**(3): p. 207-216.
174. Won, Y.W., et al., *Synergistically Combined Gene Delivery for Enhanced VEGF Secretion and Antiapoptosis.* Molecular Pharmaceutics, 2013. **10**(10): p. 3676-3683.
175. Su, G.H., et al., *Hepatocyte Growth Factor Gene-modified Bone Marrow-derived Mesenchymal Stem Cells Transplantation Promotes Angiogenesis in a Rat Model of Hindlimb Ischemia.* Journal of Huazhong University of Science and Technology-Medical Sciences, 2013. **33**(4): p. 511-519.
176. Fournier, G.A., et al., *A CORNEAL MICROPOCKET ASSAY FOR ANGIOGENESIS IN THE RAT EYE.* Investigative Ophthalmology & Visual Science, 1981. **21**(2): p. 351-354.

177. Tong, S. and F. Yuan, *Dose response of angiogenesis to basic fibroblast growth factor in rat corneal pocket assay: I. Experimental characterizations.* Microvascular Research, 2008. **75**(1): p. 10-15.
178. Ho, T.C., et al., *PEDF Promotes Self-Renewal of Limbal Stem Cell and Accelerates Corneal Epithelial Wound Healing.* Stem Cells, 2013. **31**(9): p. 1775-1784.
179. Amoh, Y., K. Katsuoka, and R.M. Hoffman, *Color-Coded Fluorescent Protein Imaging of Angiogenesis: The AngioMouse (R) Models.* Current Pharmaceutical Design, 2008. **14**(36): p. 3810-3819.
180. Lichtenberg, J., et al., *The rat subcutaneous air sac model: A new and simple method for in vivo screening of antiangiogenesis.* Pharmacology & Toxicology, 1997. **81**(6): p. 280-284.
181. Lichtenberg, J., et al., *The rat subcutaneous air sac model: A quantitative assay of antiangiogenesis in induced vessels.* Pharmacology & Toxicology, 1999. **84**(1): p. 34-40.
182. Edwards, J.C.W., A.D. Sedgwick, and D.A. Willoughby, *THE FORMATION OF A STRUCTURE WITH THE FEATURES OF SYNOVIAL LINING BY SUBCUTANEOUS INJECTION OF AIR - AN INVIVO TISSUE-CULTURE SYSTEM.* Journal of Pathology, 1981. **134**(2): p. 147-156.
183. Serbedzija, G., E. Flynn, and C. Willett, *Zebrafish angiogenesis: A new model for drug screening.* Angiogenesis, 1999. **3**(4): p. 353-359.
184. Ny, A., M. Autiero, and P. Carmeliet, *Zebrafish and Xenopus tadpoles: Small animal models to study angiogenesis and lymphangiogenesis.* Experimental Cell Research, 2006. **312**(5): p. 684-693.
185. Weinstein, K.R.K.a.B.M., *Fishing for novel angiogenic therapies.* British Journal of Pharmacology, 2003(140): p. 585-594.
186. Stainier, D.Y.R., et al., *Mutations affecting the formation and function of the cardiovascular system in the zebrafish embryo.* Development, 1996. **123**: p. 285-292.
187. Weinstein, B.M., *Plumbing the mysteries of vascular development using the zebrafish.* Seminars in Cell & Developmental Biology, 2002. **13**(6): p. 515-522.
188. Nicoli, S., G. De Sena, and M. Presta, *Fibroblast growth factor 2-induced angiogenesis in zebrafish: the zebrafish yolk membrane (ZFYM) angiogenesis assay.* Journal of Cellular and Molecular Medicine, 2009. **13**(8B): p. 2061-2068.
189. Lawson, N.D. and B.M. Weinstein, *In vivo imaging of embryonic vascular development using transgenic zebrafish.* Developmental Biology, 2002. **248**(2): p. 307-318.
190. Chan, J., et al., *Dissection of angiogenic signaling in zebrafish using a chemical genetic approach.* Cancer Cell, 2002. **1**(3): p. 257-267.
191. Cheng, S.H., P.K. Chan, and R.S.S. Wu, *The use of microangiography in detecting aberrant vasculature in zebrafish embryos exposed to cadmium.* Aquatic Toxicology, 2001. **52**(1): p. 61-71.
192. Gupta, K.C. and M. Kumar, *Drug release behavior of beads and microgranules of chitosan.* Biomaterials, 2000. **21**(11): p. 1115-1119.
193. Nadrah, P., et al., *Hindered Disulfide Bonds to Regulate Release Rate of Model Drug from Mesoporous Silica.* Acs Applied Materials & Interfaces, 2013. **5**(9): p. 3908-3915.

194. Peng, K., et al., *Cyclodextrin/dextran based drug carriers for a controlled release of hydrophobic drugs in zebrafish embryos.* Soft Matter, 2010. **6**(16): p. 3778-3783.
195. Finne-Wistrand, A. and A.C. Albertsson, *The use of polymer design in resorbable colloids*, in *Annual Review of Materials Research*. 2006, Annual Reviews: Palo Alto. p. 369-395.
196. Odian, G., *Principles of Polymerization*. 4th ed. 2004, New Jersey: John Wiley & Sons. 812.
197. Chen, L.J., et al., *Critical micelle concentration of mixed surfactant SDS/NP(EO)(40) and its role in emulsion polymerization.* Colloids and Surfaces a-Physicochemical and Engineering Aspects, 1997. **122**(1-3): p. 161-168.
198. Dong, Y. and D.C. Sundberg, *Radical Entry in Emulsion Polymerization: Estimation of the Critical Length of Entry Radicals via a Simple Lattice Model.* Macromolecules, 2002. **35**(21): p. 8185-8190.
199. De Bruyn, H., et al., *Emulsion Polymerization of Vinyl neo-Decanoate, a "Water-Insoluble" Monomer.* Macromolecules, 2002. **35**(22): p. 8371-8377.
200. Kataoka, K., A. Harada, and Y. Nagasaki, *Block copolymer micelles for drug delivery: design, characterization and biological significance.* Advanced Drug Delivery Reviews, 2001. **47**(1): p. 113-131.
201. Ramli, R.A., W.A. Laftah, and S. Hashim, *Core-shell polymers: a review.* Rsc Advances, 2013. **3**(36): p. 15543-15565.
202. Bouvier-Fontes, L., et al., *Seeded Semicontinuous Emulsion Copolymerization of Butyl Acrylate with Cross-Linkers†.* Macromolecules, 2005. **38**(4): p. 1164-1171.
203. Hendrickson, G.R., et al., *Design of Multiresponsive Hydrogel Particles and Assemblies.* Advanced Functional Materials, 2010. **20**(11): p. 1697-1712.
204. Hoffman, A.S., *Hydrogels for biomedical applications.* Advanced Drug Delivery Reviews, 2002. **54**(1): p. 3-12.
205. Dingenouts, N., C. Norhausen, and M. Ballauff, *Observation of the volume transition in thermosensitive core-shell latex particles by small-angle X-ray scattering.* Macromolecules, 1998. **31**(25): p. 8912-8917.
206. Gan, D.J. and L.A. Lyon, *Fluorescence nonradiative energy transfer analysis of crosslinker heterogeneity in core-shell hydrogel nanoparticles.* Analytica Chimica Acta, 2003. **496**(1-2): p. 53-63.
207. Li, Y.X., et al., *A facile strategy for synthesis of multilayer and conductive organo-silica/polystyrene/polyaniline composite particles.* Journal of Colloid and Interface Science, 2011. **355**(2): p. 269-273.
208. Li, X., et al., *Preparation and Characterization of Narrowly Distributed Nanogels with Temperature-Responsive Core and pH-Responsive Shell.* Macromolecules, 2004. **37**(26): p. 10042-10046.
209. Xiao, X.C., et al., *Positively Thermo-Sensitive Monodisperse Core–Shell Microspheres.* Advanced Functional Materials, 2003. **13**(11): p. 847-852.
210. Ballauff, M. and Y. Lu, *"Smart" nanoparticles: Preparation, characterization and applications.* Polymer, 2007. **48**(7): p. 1815-1823.
211. Chern, C.S., *Emulsion polymerization mechanisms and kinetics.* Progress in Polymer Science, 2006. **31**(5): p. 443-486.
212. Lewis, P.C., et al., *Continuous Synthesis of Copolymer Particles in Microfluidic Reactors.* Macromolecules, 2005. **38**(10): p. 4536-4538.

213. !!! INVALID CITATION !!!
214. Carter, S., S.Y. Lu, and S. Rimmer, *Core-shell molecular imprinted polymer colloids.* Supramolecular Chemistry, 2003. **15**(3): p. 213-220.
215. Carter, S.R. and S. Rimmer, *Surface molecular imprinting in aqueous medium on polymer core-shell particles.* Abstracts of Papers of the American Chemical Society, 2002. **224**: p. U453-U453.
216. Carter, S.R. and S. Rimmer, *Molecular recognition of caffeine by shell molecular imprinted core-shell polymer particles in aqueous media.* Advanced Materials, 2002. **14**(9): p. 667-670.
217. Murata, M., et al., *Template-dependent selectivity in metal adsorption on phosphoric diester-carrying resins prepared by surface template polymerization technique.* Bulletin of the Chemical Society of Japan, 1996. **69**(3): p. 637-642.
218. Liekens, S., et al., *The sulfonic acid polymers PAMPS poly(2-acrylamido-2-methyl-1-propanesulfonic acid) and related analogues are highly potent inhibitors of angiogenesis.* Oncology Research, 1997. **9**(4): p. 173-181.
219. Garcia-Fernandez, L., et al., *Anti-angiogenic activity of heparin-like polysulfonated polymeric drugs in 3D human cell culture.* Biomaterials, 2010. **31**(31): p. 7863-7872.
220. Chiefari, J., et al., *Living Free-Radical Polymerization by Reversible Addition–Fragmentation Chain Transfer: The RAFT Process.* Macromolecules, 1998. **31**(16): p. 5559-5562.
221. Platt, L., L. Kelly, and S. Rimmer, *Controlled delivery of cytokine growth factors mediated by core-shell particles with poly(acrylamidomethylpropane sulphonate) shells.* Journal of Materials Chemistry B, 2014. **2**(5): p. 494-501.
222. England, R.M. and S. Rimmer, *Hyper/highly-branched polymers by radical polymerisations.* Polymer Chemistry, 2010. **1**(10): p. 1533-1544.
223. Wang, X.G., et al., *Ab Initio Batch Emulsion RAFT Polymerization of Styrene Mediated by Poly(acrylic acid-b-styrene) Trithicicarbonate.* Macromolecules, 2009. **42**(17): p. 6414-6421.
224. Favier, A. and M.T. Charreyre, *Experimental requirements for an efficient control of free-radical polymerizations via the reversible addition-fragmentation chain transfer (RAFT) process.* Macromolecular Rapid Communications, 2006. **27**(9): p. 653-692.
225. Sakai, T., *Surfactant-free emulsions.* Current Opinion in Colloid & Interface Science, 2008. **13**(4): p. 228-235.
226. Ferguson, C.J., et al., *Ab Initio Emulsion Polymerization by RAFT-Controlled Self-Assembly§.* Macromolecules, 2005. **38**(6): p. 2191-2204.
227. Rieger, J., et al., *Surfactant-Free Controlled/Living Radical Emulsion (Co)polymerization of n-Butyl Acrylate and Methyl Methacrylate via RAFT Using Amphiphilic Poly(ethylene oxide)-Based Trithiocarbonate Chain Transfer Agents.* Macromolecules, 2009. **42**(15): p. 5518-5525.
228. Manguian, M., M. Save, and B. Charleux, *Batch Emulsion Polymerization of Styrene Stabilized by a Hydrophilic Macro-RAFT Agent.* Macromolecular Rapid Communications, 2006. **27**(6): p. 399-404.
229. Yeole, N., D. Hundiwale, and T. Jana, *Synthesis of core–shell polystyrene nanoparticles by surfactant free emulsion polymerization using macro-RAFT agent.* Journal of Colloid and Interface Science, 2011. **354**(2): p. 506-510.

230. Zhang, Y. and J. Yang, *Design strategies for fluorescent biodegradable polymeric biomaterials.* Journal of Materials Chemistry B, 2013. **1**(2): p. 132-148.
231. Breul, A.M., M.D. Hager, and U.S. Schubert, *Fluorescent monomers as building blocks for dye labeled polymers: synthesis and application in energy conversion, biolabeling and sensors.* Chemical Society Reviews, 2013. **42**(12): p. 5366-5407.
232. Mailänder, V. and K. Landfester, *Interaction of Nanoparticles with Cells.* Biomacromolecules, 2009. **10**(9): p. 2379-2400.
233. Tronc, F., et al., *Fluorescent polymer particles by emulsion and miniemulsion polymerization.* Journal of Polymer Science Part A: Polymer Chemistry, 2003. **41**(6): p. 766-778.
234. Oh, J.K., et al., *Emulsion copolymerization of vinyl acetate and butyl acrylate in the presence of fluorescent dyes.* Journal of Polymer Science Part a-Polymer Chemistry, 2002. **40**(10): p. 1594-1607.
235. Drury, J.L. and D.J. Mooney, *Hydrogels for tissue engineering: scaffold design variables and applications.* Biomaterials, 2003. **24**(24): p. 4337-4351.
236. Slaughter, B.V., et al., *Hydrogels in Regenerative Medicine.* Advanced Materials, 2009. **21**(32-33): p. 3307-3329.
237. Dumitriu, R.P., et al., *Biocompatible and Biodegradable Alginate/Poly(N-isopropylacrylamide) Hydrogels for Sustained Theophylline Release.* Journal of Applied Polymer Science, 2014. **131**(17).
238. Qiu, Y. and K. Park, *Environment-sensitive hydrogels for drug delivery.* Advanced Drug Delivery Reviews, 2001. **53**(3): p. 321-339.
239. Veiga, A.S. and J.P. Schneider, *Antimicrobial Hydrogels for the Treatment of Infection.* Biopolymers, 2013. **100**(6): p. 637-644.
240. Langer, R. and D.A. Tirrell, *Designing materials for biology and medicine.* Nature, 2004. **428**(6982): p. 487-492.
241. Powers, J.G., L.M. Morton, and T.J. Phillips, *Dressings for chronic wounds.* Dermatologic Therapy, 2013. **26**(3): p. 197-206.
242. Moody, A., *Use of a hydrogel dressing for management of a painful leg ulcer.* British journal of community nursing, 2006. **11**(6): p. S12, S14, S16-7.
243. Morgan, D., *Wounds - what should a dressings formulary include?* Hospital Pharmacist, 2009. **9**: p. 261.
244. Layman, H., et al., *The effect of the controlled release of basic fibroblast growth factor from ionic gelatin-based hydrogels on angiogenesis in a murine critical limb ischemic model.* Biomaterials, 2007. **28**(16): p. 2646-2654.
245. Saik, J.E., et al., *Biomimetic Hydrogels with Immobilized EphrinA1 for Therapeutic Angiogenesis.* Biomacromolecules, 2011. **12**(7): p. 2715-2722.
246. Silva, E.A. and D.J. Mooney, *Spatiotemporal control of vascular endothelial growth factor delivery from injectable hydrogels enhances angiogenesis.* Journal of Thrombosis and Haemostasis, 2007. **5**(3): p. 590-598.
247. Elia, R., et al., *Stimulation of in vivo angiogenesis by in situ crosslinked, dual growth factor-loaded, glycosaminoglycan hydrogels.* Biomaterials, 2010. **31**(17): p. 4630-4638.
248. Gilmore, L., et al., *Arginine functionalization of hydrogels for heparin bindingua supramolecular approach to developing a pro-angiogenic biomaterial.* Biotechnology and Bioengineering, 2013. **110**(1): p. 296-317.

249. Lopes, C.M.A. and M.I. Felisberti, *Mechanical behaviour and biocompatibility of poly(1-vinyl-2-pyrrolidinone)-gelatin IPN hydrogels.* Biomaterials, 2003. **24**(7): p. 1279-1284.
250. D'Erricot, G., et al., *Structural and mechanical properties of UV-photo-cross-linked poly(N-vinyl-2-pyrrolidone) hydrogels.* Biomacromolecules, 2008. **9**(1): p. 231-240.
251. Lopergolo, L.C., A.B. Lugao, and L.H. Catalaini, *Development of a poly(N-vinyl-2-pyrrolidone)/poly (ethylene glycol) hydrogel membrane reinforced with methyl methacrylate-grafted polypropylene fibers for possible use as wound dressing.* Journal of Applied Polymer Science, 2002. **86**(3): p. 662-666.
252. Kao, F.J., G. Manivannan, and S.P. Sawan, *UV curable bioadhesives: Copolymers of N-vinyl pyrrolidone.* Journal of Biomedical Materials Research, 1997. **38**(3): p. 191-196.
253. Fogaca, R. and L.H. Catalani, *PVP Hydrogel Membranes Produced by Electrospinning for Protein Release Devices.* Soft Materials, 2013. **11**(1): p. 61-68.
254. Eid, M., et al., *Radiation synthesis and characterization of poly(vinyl alcohol)/poly(N-vinyl-2-pyrrolidone) based hydrogels containing silver nanoparticles.* Journal of Polymer Research, 2012. **19**(3).
255. Rosiak, J.M. and P. Ulanski, *Synthesis of hydrogels by irradiation of polymers in aqueous solution.* Radiation Physics and Chemistry, 1999. **55**(2): p. 139-151.
256. Sen, M. and E.N. Avci, *Radiation synthesis of poly(N-vinyl-2-pyrrolidone)-kappa-carrageenan hydrogels and their use in wound dressing applications. I. Preliminary laboratory tests.* Journal of Biomedical Materials Research Part A, 2005. **74A**(2): p. 187-196.
257. Singh, B. and L. Pal, *Radiation crosslinking polymerization of sterculia polysaccharide-PVA-PVP for making hydrogel wound dressings.* International Journal of Biological Macromolecules, 2011. **48**(3): p. 501-510.
258. Yu, H.J., et al., *Medicated wound dressings based on poly(vinyl alcohol)/poly(N-vinyl pyrrolidone)/chitosan hydrogels.* Journal of Applied Polymer Science, 2006. **101**(4): p. 2453-2463.
259. Nedelkov, D., *Mass spectrometry-based immunoassays for the next phase of clinical applications.* Expert Review of Proteomics, 2006. **3**(6): p. 631-640.
260. Guerrera, I.C. and O. Kleiner, *Application of mass spectrometry in proteomics.* Bioscience Reports, 2005. **25**(1-2): p. 71-93.
261. Qiao, J.L., T. Hamaya, and T. Okada, *New highly proton-conducting membrane poly(vinylpyrrolidone)(PVP) modified poly(vinyl alcohol)/2-acrylamido-2-methyl-1-propanesulfonic acid (PVA-PAMPS) for low temperature direct methanol fuel cells (DMFCs).* Polymer, 2005. **46**(24): p. 10809-10816.
262. Bravo-Osuna, I., G. Ponchel, and C. Vauthier, *Tuning of shell and core characteristics of chitosan-decorated acrylic nanoparticles.* European Journal of Pharmaceutical Sciences, 2007. **30**(2): p. 143-154.
263. Szabo, A., et al., *Structural elucidation of hyaluronic acid gels after heat sterilisation.* Polymer Testing, 2013. **32**(8): p. 1322-1325.
264. Huebsch, N., M. Gilbert, and K.E. Healy, *Analysis of sterilization protocols for peptide-modified hydrogels.* Journal of Biomedical Materials Research Part B-Applied Biomaterials, 2005. **74B**(1): p. 440-447.

265. Wang, M., et al., *Radiation synthesis of PVP/CMC hydrogels as wound dressing.* Nuclear Instruments & Methods in Physics Research Section B-Beam Interactions with Materials and Atoms, 2007. **265**(1): p. 385-389.
266. Matsuda, M., T. Yakushiji, and K. Sakai, *Effect of gamma irradiation on the surface properties of wet polysulfone films containing poly(vinylpyrrolidone).* Surface and Interface Analysis, 2011. **43**(6): p. 976-983.
267. Marquez, B.V., et al., *Development of a Radio labeled Irreversible Peptide Ligand for PET Imaging of Vascular Endothelial Growth Factor.* Journal of Nuclear Medicine, 2014. **55**(6): p. 1029-1034.
268. Liu, S.Q., et al., *Degradation of dye rhodamine B under visible irradiation with Prussian blue as a photo-Fenton reagent.* Environmental Chemistry Letters, 2011. **9**(1): p. 31-35.
269. Smithmyer, M.E., L.A. Sawicki, and A.M. Kloxin, *Hydrogel scaffolds as in vitro models to study fibroblast activation in wound healing and disease.* Biomaterials Science, 2014. **2**(5): p. 634-650.
270. Ansell, D.M., K.A. Holden, and M.J. Hardman, *Animal models of wound repair: Are they cutting it?* Experimental Dermatology, 2012. **21**(8): p. 581-585.